REVUE ROUMAINE DE CHIMIE (ROUMANIAN JOURNAL OF CHEMISTRY)

Tome 57, N° 3 **Mars 2012**

PAPERS

Eugenia Dumitra TEODOR, Georgiana TRUICĂ and Gabriel Lucian RADU

Hyaluronic acid detection from natural extract by diode array-capillary electrophoresis methods

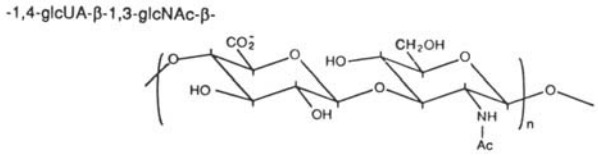

Rev. Roum. Chim., **2012**, *57*(3), 223-227

Key words: hyaluronic acid, natural extracts, capillary electrophoresis, diode array detection.

Corina CHEPTEA, Valeriu SUNEL, Cristina STAN and Dana Ortansa DOROHOI

New derivatives of 5-nitroindazole with potential antitumor activity

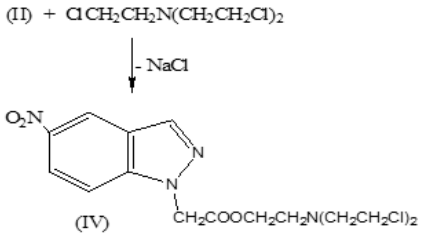

Rev. Roum. Chim., **2012**, *57*(3), 229-234

Key words: synthesis of 5-nitroindazole derivatives, ^{1}H-NMR and FT-IR analysis, cytostatic action.

ACADEMIA ROMÂNĂ
Revue Roumaine de Chimie
http://web.icf.ro/rrch/

Rev. Roum. Chim.,
2012, *57*(3), 163-168

ENTRAPMENT OF MICROBIAL AMYLASES AND CELLULASES IN SILICA-GELS

Monica DRAGOMIRESCU,[a] Teodor VINTILĂ[a] and Gabriela PREDA[b*]

[a]Banat University of Agricultural Science and Veterinary Medicine from Timişoara, Faculty of Animal Sciences and Biotechnologies, 119 Calea Aradului, 300645-Timişoara, Roumania
[b]West University of Timişoara, Faculty of Chemistry-Biology-Geography, 16 Pestalozzi, 300115-Timişoara, Roumania

Received June 2, 2010

Amylases and cellulases are very useful hydrolases with extensive biotechnological applications. Effective bioconversion catalyzed by enzymes claims different kinds of stable and reusable biocatalysts. A good strategy to improve the stability of free enzymatic preparations could be immobilization in porous supports. The sol-gel process is a well-known method to obtain hybrid organic-inorganic biocompatible ceramic mesoporous materials under mild conditions. The aim of this study was to immobilize two enzymatic preparations from *Bacillus amyloliquefaciens* and *Trichoderma viride* with amylase and cellulase activity respectively, by entrapment in silica gel. The silica gels were obtained by using an organoalkoxisilane precursor tetrakis (2-hydroxiethyl) orthosilicate (THEOS). The activity and stability of native and entrapped enzymatic preparations were studied comparatively, as well as their kinetic behavior.

INTRODUCTION

Enzymes catalyze biochemical reactions being involved in the metabolism of all living organisms, and in the same time are useful biocatalysts with great specificity for industrial biocatalytic conversions.

Enzymatic bioconversion of starch and cellulose and also of their derivatives (for instance carboxymethyl cellulose (CMC)), to monomeric sugars, with significant commercial interest, has been intensively studied in the recent years to produce bioethanol and bio-based products, food and animal feeds, many valuable chemicals, pharmaceuticals and biosensors.[1-3]

Effective conversion of starch and cellulose to fermentable sugars requires enzymatic preparations with great stability for specific processes and high catalytic efficiency.[4] A good strategy to improve the low stability of free enzymatic preparations with amylase and cellulase activity could be immobilization in hybrid organic-inorganic porous supports, with high surface area and high pores volume.[5,1]

The sol-gel process is a well-known method to obtain biocompatible mesoporous materials under mild conditions. Bioimmobilization by entrapment in silica gels has been shown to improve enzyme activity and stability in aqueous and organic-aqueous media.[6-9]

Tetrakis (2-hydroxiethyl) orthosilicate (THEOS) is a completely water-soluble precursor that forms porous three dimensional networks in aqueous solution in the absence of added alcohol.[10] The alcohol needed by the poor-water soluble common tetraalcoxysilane precursors (tetramethoxysilane, TMOS and tetraethoxysilane, TEOS) can lead to partial denaturation of enzyme molecules. During the gelification process the enzyme is entrapped in silica materials without covalent binding to the matrix.[11-13]

RESULTS

Enzymatic preparations with amylase and cellulase activities were obtained by fermentation of a series of *Bacillus* and *Trichoderma* microbial

* Corresponding author: gpreda@cbg.uvt.ro

cells, in order to select the strains producing the best enzymatic activity. Amylase production by five *Bacillus* strains and cellulase production by two *Trichoderma* strains are shown in Table 1 and Table 2 respectively.

In our immobilization work two microbial strains were used, an amylase producing bacterial *Bacillus amyloliquefaciens* DSM 7 strain and a cellulase (CMCase and cellobiase) producing fungal *Trichoderma viride* CMGB 1 strain. These enzymatic preparations were subsequently immobilized by entrapment in silica gel obtained using tetrakis (2-hydroxiethyl) orthosilicate (THEOS) as organoalkoxisilane precursor by sol-gel method. Enzyme activity and protein content of free and immobilized enzymes are given in Table 3.

Table 1

Selection of amylase producing *Bacillus* strains

Bacterial strain	pH	Fermentation time h	Amylase activity $\mu mol \cdot min^{-1} \cdot mL^{-1}$	Protein content $mg_{BSA} \cdot mL^{-1}$
Bacillus subtilis 222	8.00	72.00	0.92±0.18	1.89±0.16
Bacillus subtilis SML amy+	8.00	72.00	0.94±0.21	2.28±0.19
Bacillus subtilis 3218	8.00	72.00	2.03±0.28	2.34±0.22
Bacillus globigi CMIT 1.44	8.00	72.00	2.36±0.30	2.46±0.23
***Bacillus amyloliquefaciens* DSM 7**	**8.00**	**24.00**	**10.54**±1.32	**3.38**±0.29

Table 2

Selection of cellulase (CMCase and cellobiase) producing *Trichoderma* strains

Strain	pH	CMCase activity $mmol \cdot min^{-1} \cdot mL^{-1}$	Cellobiase activity $mmol \cdot min^{-1} \cdot mL^{-1}$	Protein content $mg_{BSA} \cdot mL^{-1}$
***Trichoderma viride* CMGB 1**	**4.50**	1.79±0.16	0.72±0.11	**3.30**±0.27
Trichoderma longibrachiatum DSM 769	5.00	0.24±0.08	0.32±0.09	2.28±0.10

Table 3

Protein content and enzyme activity of free and immobilized preparations

***Bacillus amyloliquefaciens* DSM 7 amylase**

	Protein content $mg_{BSA} \cdot mL^{-1}$ $mg_{BSA} \cdot g^{-1}$	Amylase activity $\mu mol \cdot min^{-1} \cdot mL^{-1}$ $\mu mol \cdot min^{-1} \cdot g^{-1}$	Immobilization yield[c] %
Native			
Fermentation medium[a]	3.38±0.29	10.54±1.32	-
Lyophilized enzymatic preparation[b]	278.36±23.36	1196.00±10.87	-
Immobilized[b]			
Entrapment THEOS	3.56±0.28	7.34±1.21	45.08±5.13

***Trichoderma viride* CMGB 1 cellulase**

	Protein content $mg_{BSA} \cdot mL^{-1}$ $mg_{BSA} \cdot g^{-1}$	CMCase activity $mmoli \cdot min^{-1} \cdot mL^{-1}$ $mmoli \cdot min^{-1} \cdot g^{-1}$	Immobilization yield[c] %
Native			
Fermentation medium[a]	3.30±0.27	1.79±0.16	-
Lyophilized enzyme[b]	19.28±2.05	66.15±3.38	-
Immobilized[b]			
Entrapment THEOS	14.62±1.31	2.03±0.30	8.98±1.12
	Cellobiase activity $mmoli \cdot min^{-1} \cdot mL^{-1}$ $mmoli \cdot min^{-1} \cdot g^{-1}$	**Specific activity** $U\ mg_{BSA}^{-1}$	**Immobilization yield[c] %**
Native			
Fermentation medium[a]	0.72±0.11	0.22±0.04	-
Lyophilized enzyme[b]	23.65±2.79	1.23±0.09	-
Immobilized[b]			
Entrapment THEOS	2.26±0.33	0.16±0.02	5.87±1.04

[a]liquid, [b]solid, [c]Immobilization yield (%) = $100.U_{tot(im)}/U_{tot(i)}$, where $U_{tot(im)}$ = activity of immobilized enzyme (U/mg)·total weight of immobilized enzyme (mg), $U_{tot(i)}$ = activity of native enzyme (U/mL)·total volume of native enzyme used for immobilization (mL)

The influence of the ionic microenvironment and the heat energy around amylase and cellulase molecule, on the free and entrapped enzymatic preparation activity, was studied comparatively. The enzymes activities (amylase and CMCase activity) were determined in buffered solutions of pH range 2.2 – 8.0 (citric acid/Na_2HPO_4 buffer solution) and at temperatures ranging from 20 to 95ºC (as shown in Figs. 1 and 2).

The stability of entrapped enzymatic preparations with amylase and CMCase activity was tested for an hour in aqueous medium, at pH 2.6 and 37ºC. The residual activity vs. time dependence of the entrapped amylase and CMCase are shown in Fig. 3.

The enzyme-substrate affinity modification was investigated based on the kinetics of native and immobilized enzymes respectively, in the hydrolysis of starch in case of amylase, and in the hydrolysis of CMC in case of CMCase. The kinetic parameters of free and entrapped *Bacillus amyloliquefaciens* DSM 7 amylase and *Trichoderma viride* CMGB 1 cellulase obtained in the hydrolysis of starch and CMC-cellulose respectively are given in Table 4.

Enzymes stability was analyzed as well after two months of storage at 4ºC. The immobilized enzymatic preparations were kept at 4ºC and the stability was monitored in time. The enzymes activity was determined periodically. The residual amylase and CMCase activity of the immobilized enzymes in the absence of any preservation agent is shown in Table 5.

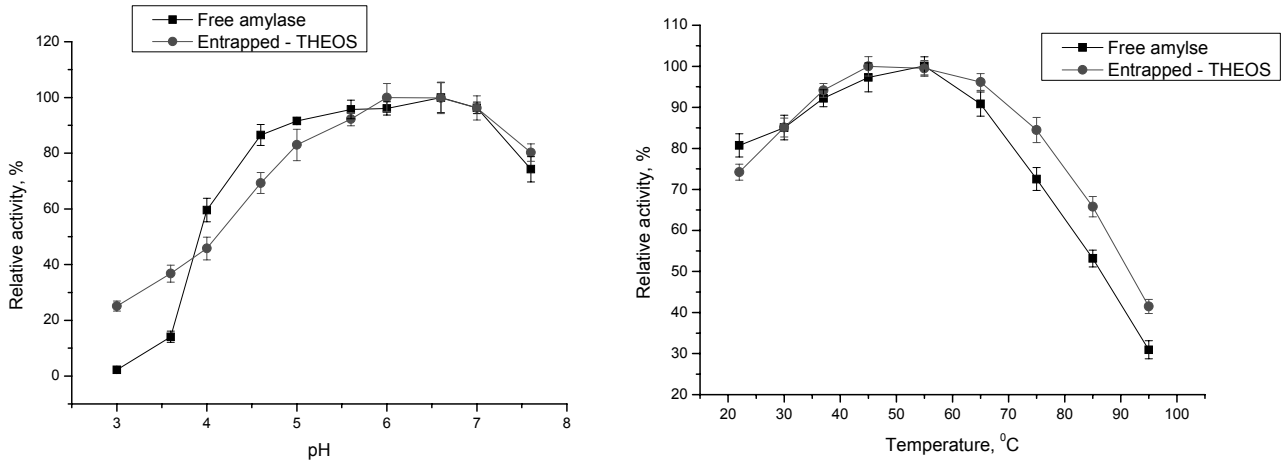

Fig. 1 – The effect of pH and temperature on the activity of immobilized and native amylase.

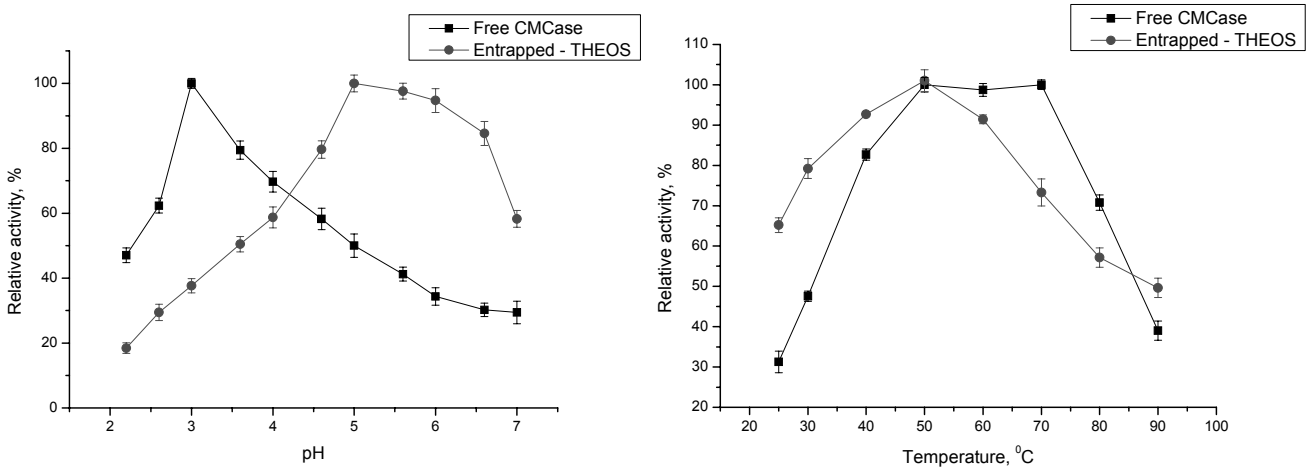

Fig. 2 – The effect of pH and temperature on the activity of immobilized and native cellulase (CMCase activity).

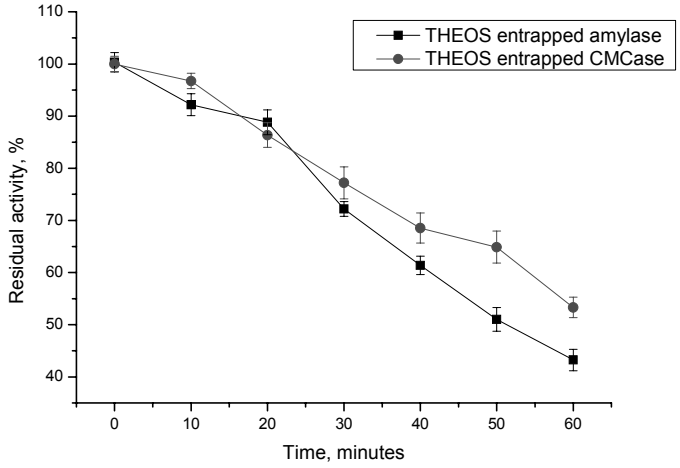

Fig. 3 – Stability of the immobilized enzymatic preparation at pH 3.0 and 37ºC.

Table 4

The kinetic parameters obtained from the Lineweaver – Burk linearization

Lineweaver – Burk linearization		***Bacillus amyloliquefaciens* DSM 7 amylase**	
Kinetics parameters	**K_m mg_{starch}/mL**	**V_{max} $\mu mol_{maltose}$/mL·min**	**$V_{max}.10^3/K_m$ $\mu mol_{maltose}$/mg·min**
Free amylase	12.28±1.11	0.82±0.09	66.86±5.83
Entrapped (THEOS) - amylase	20.94±2.38	0.99±0.12	47.28±4.86
Lineweaver – Burk linearization		***Trichoderma viride* CMGB 1 cellulase**	
Kinetics parameters	**K_m mg_{CMC}/mL**	**V_{max} $mmol_{glucose}$/mL·min**	**$V_{max}.10^3/K_m$ $\mu mol_{glucose}$/mg·min**
Free CMCase	6.10±0.55	0.95±0.09	155.73±16.21
Entrapped (THEOS) - CMCase	7.85±0.62	0.89±0.07	113.38±10.44

Table 5

Preservation stability of immobilized enzyme

Immobilized enzymes	**Residual enzymes activity %**		
	initial	**one month**	**two months**
Entrapped (THEOS) amylase	100.00	83.25±6.41	67.32±4.82
Entrapped (THEOS) CMCase	100.00	105.78±8.74	89.64±6.77

DISCUSSION

An important objective of any enzymes stabilization work should be to minimize costs. The enzyme could represent one of the main cost components and following this point of view we tested a series of microbial strains to produce the immobilized enzymatic preparations as cheap as possible. The best enzyme activities were obtained in case of *Bacillus amyloliquefaciens* DSM 7 strain (submerse mineral medium, stirred flasks) and *Trichoderma viride* CMGB 1 strain (solid state fermentation). The aqueous enzymatic preparations were concentrated from fermentation medium by liophylization and then the enzymes were entrapped in silica gel.

Our results show that both enzymes, but especially amylase, were successfully entrapped in THEOS based silica matrices. The mild condition required by the sol-gel synthesis allowed immobilization at a slightly lower pH and low temperature needed by enzymes to retain their biocatalitic activity. The good enzyme activities measured after entrapment could be explained by a minimal modification in conformational structure of enzyme. The entrapped amylase was obtained with an immobilization yield of 45%. In case of CMCase and cellobiase, the immobilization yield

was 8.44%, at a lower initial enzyme loading of silica matrix than in case of amylase because of lower free enzyme activity (66.15 CMCase units/g lyophilized powder, 1196 amylase units/g lyophilized powder).

Optimum temperature and pH for the activity of free and entrapped amylase and CMCase were determined comparatively. The optimum pH of the free enzymatic preparation with amylase activity was 6.6, and at pH range 5 to 7 the enzyme retained more than 90% of its maximum activity. The highest entrapped amylase activity was achieved when the pH values of the environment were 6-7. The relative activity obtained for immobilized amylase at pH 2.6 was 10% higher than in case of free one. The enzymatic activity as a function of temperature had almost the same profile for free and immobilized amylase. Both of them preserved more than 90% of the maximum activity in 37-65ºC temperature range. At temperatures above 70ºC the activity of free and entrapped amylase decreased slowly.

Entrapment in silica matrix of cellulase changed the optimum pH of CMCase from 3 to 5 and more than 85% of the peak activity was displayed in the pH range 5-7. The maximum CMCase activity of free enzymatic preparation was found at a temperature range of 60-70°C. Entrapment revealed a changing of optimal temperature to 50°C. The immobilized enzyme showed 65% and 50% of maximum activity at 25°C and 90°C, respectively.

A good enzyme stability at low pH values (pH 2-3) and below 40°C is very important from the viewpoint of application as feed additive. The enzymes performed a good stability at pH 2.6 and retained more than 40% and 50% of maximum amylase and CMCase activity respectively, after one hour of incubation at 37°C.

The kinetic constants of immobilized enzymes are usually different from those of the native form, as conformational changes, steric hindrances and partition and diffusion effects may occur simultaneously or separately on enzyme immobilization. The conformational effects may also change the affinity between enzyme and substrate.

The kinetic study revealed that both free and immobilized amylase and CMCase, follow a Michaelis–Menten type kinetics. In the case of the immobilized enzymes, the *apparent Michaelis constant*, K_m, was greater than that of the native one, as it was expected. K_m increased 1.7 times for the THEOS entrapped amylase and 1.3 times for the immobilized CMCase (Table 4). For the immobilized enzymes, V_{max}/K_m ratio indicated that immobilization decreased the catalytic efficiency by 1.4 times, for both enzymes. The maximum velocity changed insignificantly after immobilization.

Preservation stability is very important in industrial application of immobilized enzymes. Both amylase and cellulase present a good stability in time. The highest stability was obtained for *Trichoderma viride* CMGB 1 CMCase. After two months of storage at 4°C, entrapped CMCase has lost only 10% of initial enzyme activity. The slight increase in CMCase activity after one month could be explained by the slow drying of silica gel matrix containing the enzyme entrapped. The residual activity of *Bacillus amyloliquefaciens* DSM 7 amylase is 67% from initial enzyme activity. The high preservation stability of THEOS entrapped enzymes makes them to be appropriate preparations with amylase and cellulase activity in different applications.

EXPERIMENTAL

Soluble potatoes starch, maltose, carboxymethyl cellulose (CMC), cellobiose, glucose, Folin-Ciocalteu's phenol reagent and bovine serum albumin (BSA) were purchased from Merck, 3,5-dinitrosalicylic acid (DNS) and tetrakis (2-hydroxiethyl) orthosilicate (THEOS) were obtained from Fluka. All the other chemicals were obtained from local suppliers or were commercially available reagent grade products and were used without further purification.

The *Bacillus amyloliquefaciens* DSM 7 strain was purchased from DSMZ Germany. Microbial cells of *Bacillus amyloliquefaciens* were cultured under aerobic conditions (rotary shaker, 175 rpm), for 24 hours, at 37ºC, in Erlenmeyer flasks containing 50 mL mineral medium.[14] The purity, pH, amylase activity and protein content were monitored continuously. The enzymatic preparation with amylase activity was liophylized from fermentation medium for 24 hours, at -56ºC and 26 mTorr (iLShin Europe Dry Freezer).

The protein content was assayed according to the Lowry method, using the Folin-Ciocalteu's phenol reagent and bovine serum albumin (BSA) as standard.[15] The amylase activity was measured by UV-VIS spectrometry, according to the Sumner method, using DNS as reagent.[16] One unit of activity is defined as the amount of enzyme that hydrolyzes starch liberating 1 $\mu mol_{maltose} \cdot mL^{-1} \cdot min^{-1}$, at 25ºC.[17]

The *Trichoderma viride* CMGB 1 strain is preserved in the collection of industrial microorganisms of the Industrial Microbiology Laboratory of USAMVB Timisoara. Microbial cells of *Trichoderma* were cultured in solid state fermentation, for 168 hours, at 37ºC using wheat bran as carbon source.[11] The extraction of enzymatic preparation was done in distilled water (1:7) under magnetic stirring (75 minutes, 28°C, 150 rpm). The extraction medium was initially filtered through gauze and filter paper and finally centrifuged (10 minutes, 4ºC, 10000 rpm). The enzymatic preparation with CMCase and cellobiase activity was lyophilized from extraction medium (24 hours, -56ºC, 26 mTorr (iLShin Europe Dry Freezer).

The CMCase and cellobiase activities were measured by UV-VIS spectrometry, according to the Petterson and Porath

method, using CMC (CMCase activity) and cellobiose (cellobiase activity) as substrates and DNS as reagent.[18]

A sol-gel entrapment method was performed using a one step procedure by magnetically stirring of tetrakis (2-hydroxiethyl) orthosilicate (THEOS) with a buffered enzymatic solution (1:1.1, v/v). In all cases the gelation occurred in a few seconds. The gels were left overnight for aging (4°C), washed with n-hexane and then assayed.[19] A buffered enzymatic solution contained 28.7 amylase units/1 mL THEOS from lyophilized *B. amyloliquefaciens* enzymatic preparation and 13.5 CMCase units/1 mL THEOS and 9.86 cellobiase units/1 mL THEOS from lyophilized *T. viride* enzymatic preparation, respectively in 0.1 M citric acid – 0.2 M Na_2HPO_4 buffer, pH 4.6.

The effect of temperature and pH on the activity of native and immobilized enzymes was investigated by DNS assay, measuring the glucose concentration at various temperatures (20-95ºC) and in the presence of 0.1 M citric acid – 0.2 M Na_2HPO_4 buffer ranged from 2.2 to 8 respectively, at room temperature.

Stability test – the immobilized enzymes (300 mg immobilized enzyme from *B. amyloliquefaciens* and *T. viride*, respectively) in 0.1 M citric acid – 0.2 M Na_2HPO_4 buffer, pH 2.6 (5 mL) were incubated at 37ºC for one hour. Samples were withdrawn at every 10 minutes and amylase and CMCase activities were assayed. Enzymes stability was analyzed as well, after two months of storage at 4ºC.

The kinetic study was carried out on the native enzymes and on the enzymes entrapped in silica gels obtained using THEOS as precursor. The substrates used were soluble starch, in case of amylase and carboximethyl cellulose in case of CMCase.

To determine the kinetic parameters, the substrate hydrolysis by amylase was performed for 20 minutes, at 25ºC, by varying the concentration of starch solution (2-8 mg/mL), with native (1 mL lyophilized enzymatic solution, 1mg/mL) and immobilized (100 mg) enzymes in 0.1 M citric acid – 0.2 M Na_2HPO_4 buffer solution, pH 4.6. Samples were taken at every 2 minutes; the absorbance was measured at 540 nm (reducing sugar assay with Sumner method) in a UV-VIS spectrophotometer (PG Instrument T60U Spectrophotometer, 37°C) comparatively with a control. The product concentration (glucose) was obtained from the calibration curve. The initial reaction rates were calculated from the d[glucose]/dt slope at all initial starch concentrations for the native and entrapped amylase. The data were fitted using the Lineweaver-Burk equation (linear regression).

In case of enzymatic preparations with CMCase activity the kinetic studies were performed following the same steps. The kinetic parameters were determined at 50ºC; the concentration of carboximethyl cellulose varied from 0.46 to 4.60 mg/mL, for both native (2 mL lyophilized enzymatic solution, 5 mg/mL) and entrapped (200 mg) enzymes in 0.1 M citric acid – 0.2 M Na_2HPO_4 buffer solution pH 4.6. The data were fitted using the Lineweaver-Burk equation (linear regression).

CONCLUSIONS

Tetrakis (2-hydroxiethyl) orthosilicate (THEOS) and sol-gel method have made possible the generation of hybrid organic-inorganic mesoporous tridimensional networks suited for entrapment of enzymes. The successful immobilization indicates that silica gels minimally affect the enzymes biocatalytic active centers. The kinetic parameters indicate that the immobilized enzymatic preparation shows less affinity for substrate, K_m being 1.7 and 1.4 times higher than that of the native enzyme.

The exogenous immobilized microbial enzymatic preparations with amylase and CMCase activity can act on available substrates at low pH in animal stomach and can be used as feed additives. They are stable for a time sufficiently long to act in proximal segment of digestive tract. The entrapped enzymatic preparations present an enhanced stability in time that makes them suitable for a lot of industrial applications.

Acknowledgements: This work was supported by CNCSIS – UEFISCSU, project number 426/01.10.2007 PNII – IDEI code 1134/2007. The financial support provided by the grant POSDRU /21/1.5/G/38347 is also acknowledged.

RERERENCES

1. A. Takimoto, T. Shiomi, K. Ino, T. Tsunoda, A. Kawai, F. Mizukami and K. Sakaguchi, *Micropor. Mesopor. Mater.*, **2008**, *116*, 601-606.
2. M.G. Adsul, K.B. Bastawde, A.J. Varma and D.V. Gokhale, *Bioresource Technol.*, **2007**, *98*, 1467-1473.
3. C. Diguta, S. Jurcoane, F. Israel-Roming, M. Brule, M. Mukengele, A. Lemmer and H. Oechsner, *Rom. Biotechnol. Lett*., **2007**, *12*, 3203-3207.
4. Y.-H. P. Zhang, M.E. Himmel and J.R. Mielenz, *Biotechnol.Adv.*, **2006**, *24*, 452-481.
5. M. Paljevac, M. Primožič, M. Habulin, Z. Novak and Z. Knez, *J. Supercritical Fluids*, **2007**, *43*, 74-80.
6. J. Livage, T. Coradin and C. Roux, *J. Phys.: Condens. Matter*., **2001**, *13*, 673-691.
7. J. Kim, J.W. Grate and P. Wang, *Chem. Eng. Sci*., **2006**, *61*, 1017-1026.
8. K. Sangeetha, V.B. Morris and T.E. Abraham, *Appl. Catalysis A: General*, **2008**, *341*, 168-173.
9. P.V. Iyer and L. Ananthanarayan, *Process Biochem.*, **2008**, *43*, 1019-1032.
10. Y.A. Schipunov, T.Y. Karpenko, I.Y. Bakunina, Y.V. Burtseva and T.N. Zvyagintseva, *J. Biochem. Biophys. Methods*, **2004**, *58*, 25-38.
11. T. Vintilă, M. Dragomirescu, S. Jurcoane, D. Vintila, R. Caprita and M. Maniu, *Rom. Biotechnol. Lett.*, **2009**, *14*(2), 4275-4281.
12. B. Vlad-Oros, Z. Dudas, G. Preda, M. Dragomirescu and A. Chiriac, *Rev. Chim*. (Bucureşti), **2009**, *7*, 794-796.
13. I. Gill and A. Ballesteros, *Trends Biotechnol*., **2000**, *18*, 282-296.
14. M. Dragomirescu, T. Vintilă and G. Preda, *Lucr. Şt. Zoot. Biot.*, **2009**, *42*, 35-39.
15. O.H. Lowry, N.J. Rozbrough, L.A. Pan and R.J. Randall, *J. Biol. Chem*., **1951**, 193; *Chem Abstr.,* **1959**, *42*, 75843.
16. J. B. Sumner and V. A. Graham, *J. Biol.Chem.*, **1921**, *47*, 5-9.
17. ***, BDH Enzyme Catalog, 1981.
18. D. Iordachescu and I. F. Dumitru, "Biochimie practică", Tipografia Universităţii din Bucureşti, Bucureşti, 1980, p. 138-141.
19. M.T. Reetz, A. Zonta and J. Simpelkamp, *Biotechnol. Bioeng*., **1996**, *49*, 527-534.

ACADEMIA ROMÂNĂ
Revue Roumaine de Chimie
http://web.icf.ro/rrch/

Rev. Roum. Chim.,
2012, *57*(3), 169-175

BEHAVIOR OF EUROPIUM, STRONTIUM AND CESIUM ON ION EXCHANGERS PREAPARED FROM POLYVINYL ALCOHOL GRAFTED WITH SUCCINIC OR CITRIC ACID USING GAMMA RADIATION

Oussama Alhassanieh[a*] and Zaki Ajji[b]

[a]Nuclear and Radiochemistry Division, Chemistry Department
[b]Polymer Technology Division, Radiation Technology Department,
Atomic Energy Commission of Syria, Damascus P.O. Box 6091, Syria

Received December 20, 2010

The behavior of europium, strontium and cesium on ion exchange resins prepared from polyvinyl alcohol grafted with citric or succinic acid was investigated using gamma spectroscopy in three different media (HNO_3, HCl, and H_2SO_4). The investigation shows that adsorption of the studied elements depends on the concentration of grafted succinic or citric acid and the concentration of the used acidic media. The time needed to reach the adsorption equilibrium is relatively short. The resins were prepared by irradiation of ternary mixtures of PVA / citric or succinic acid / water by gamma irradiation dose of 25 kGy in air and at ambient temperature. The maximum swelling and gel fraction of the prepared resins were investigated. Swelling and gelation decrease with increasing the concentration of citric acid. The decrease in the maximum swelling is due to increased hydrogen bonding between the carboxyl groups of the bonded/trapped citric or succinic molecules and the hydroxyl groups of the polymer. The decrease in the gel fraction can be explained by the presence of the acid that leads to other reactions in the mixture and not preferably to building cross links between the polymer chains.

INTRODUCTION

Ion-exchange resins are widely used chemicals in separation, purification, and decontamination processes: water softening, removal of toxic metals from water in the environment, wastewater treatment, hydrometallurgy, sensors, chromatography, and bimolecular separations.[1-4] Ion-exchange resins are divided in two groups: organic and inorganic resins. Some organic ion exchange resins consist usually of polymers with a carboxyl function group for cation exchange resins. The required active groups can be introduced after polymerization, or substituted monomers can be used. Radiation synthesis of membranes, hydrogels and adsorbents for various purposes is a wide field of important applications of the radiation technology.

Radiation processing techniques have been widely applied for the synthesis of new materials with specific functional features for various applications such as: hydrogel dressings,[5-8] and membranes for separation.[9-11]

There are a number of works in literature about modification of PVA by means of radiation-induced graft copolymerization of monomers.[12-22] In all this works, with the exception of the work of Yan 2003, only the uptake capacity of the resin for various elements was determined. In this work the behavior of europium, cesium and strontium on ion exchange resin, prepared from polyvinyl alcohol, grafted with citric or succinic acid, was studied. The effect on the sorption of the concentration and nature of acidic external solutions and the effect of contact time were investigated.

* Corresponding author: cscientific@aec.org.sy

EXPERIMENTAL

1. Preparation of the resin

Polyvinyl alcohol was used for the preparation of the cross-linked resin. 10 g PVA (Merck, MW = 72000) was dissolved in 90 mL distilled water and heated. Then different amounts of grafting acid (0.8 – 15 g) were dissolved in the 10% (w/w) PVA solutions, heated and placed into PVC straws. Before irradiation they were degassed in an ultrasonic bath. They were irradiated in air at ambient temperature in a Co-60 Gamma cell at a dose rate of 3.5 kGy/h, to a dose of 25 kGy. The long cylindrical hydrogels obtained were cut into pieces of 2-3 mm in length and dried in air, and then in a vacuum oven (W_o).

2. Gel fraction

The samples were dried after irradiation (W_o), and then soaked in distilled water for 3 days at room temperature, to achieve the equilibrium of swelling W_S in order to remove the soluble and unreacted species. The gels were then dried again in air and in a vacuum oven (W_E) at 50 ^oC until constant weight. The gel fraction was calculated according to the following equation:

$$gel - fraction\ [\%] = \frac{W_E}{W_o} \times 100 \qquad (1)$$

where W_o is the weight of dried gel after irradiation, and W_E is the dried weight of the sample after extraction of soluble and unreacted species.

3. Maximum swelling

After the soaking and washing procedures, maximum swelling (S_{max}%) was calculated using the following equation:

$$S_{max}\% = \frac{W_S - W_o}{W_o} \times 100 \qquad (2)$$

where W_S is the weight of gel at swelling equilibrium (after three days of soaking in water), and W_o is the weight of dried gel after irradiation.

4. Sorption of the investigated elements on the resin

To study the sorption behavior of the elements from different acidic media (HNO_3, HCl, and H_2SO_4) on the prepared resins a certain activity of the isotopes (^{152}Eu, ^{137}Cs, ^{85}Sr) is injected in solutions of various acids with various concentrations (0.001, 0.01, 0.1, 1, 3, and 5 mol/L). These liquid phases were brought in contact with the resins. After a certain time, the phases were separated and measured using γ-spectrometry. An experiment series was done to determine the equilibrium time. Because of the short equilibrium time (less than 3 hours in all cases) a contact time of 24 hours was taken in all following experiments. The weight of the solid phase was 0.2 g, the volume of the liquid 5 mL, and the concentration of the investigated elements 0.1 mol/L in all experiments.

The prepared resin was used in a first experiment series without any conditioning. It was only washed with distilled water for 48 hours to reach the maximal possible swelling. The results show that the adsorption of all three elements is less than 5%.

The reported results in this work were obtained after socking the resin in distilled water for 48 hours to reach the maximum possible swelling. The resin was then washed with various concentrations of hydrochloric acid for 24 hours, and finally with distilled water.

As mentioned before, the element ratios of Eu, Sr, and Cs were determined using γ-spectrometry (HPGe-Detector, 60% Eff., FWHM=0.998 at 122 keV and 1.88 at 1332 keV, Canberra 35 plus). The uncertainties of all γ-measurements were estimated of about 5%. ^{137}Cs was taken from an IAEA-standard. ^{152}Eu and ^{85}Sr were produced in the Syrian MNSR-reactor by irradiation of their nitrates with a neutron flux of 10^{11} cm^{-2} s^{-1}.

The element fraction in the aqueous phase was calculated according to the following equations:

$$F_w = \{[C_W]/[C_o]\} * 100 = A_w/A_0 * 100 \qquad (3)$$

where F_w is the element fraction in the aqueous phase, $[C_w]$ is the element concentration in the aqueous phase after phase separation, $[C_o]$ is the initial element concentration, A_w is the activity of the aqueous phase after phase separation, and A_0 is the initial activity.

RESULTS AND DISCUSSION

1. Gel fraction

When polymer solutions are irradiated with high-energy radiations, macroradicals are generally produced as a result of indirect effect of radiation. These macroradicals disappear later either through the formation of crosslinks between the polymer chains, or stabilize themselves by intramolecular linking or by chain scission.

Fig. 1 represents the gel fraction of PVA with respect to the amounts of citric or succinic acid, whereas the samples were exposed to a constant irradiation dose of 25 kGy. It can be observed that the gel fraction becomes lower as the acid concentration increases. One explanation for this behavior might be that the formed macromolecule radicals would react with the acid molecules; therefore, the polymer backbone becomes busy at these positions for crosslinking reactions. Another explanation could be that the formed acid radicals would react with the polymer radicals. In this case the polymer backbone will be blocked at these locations for crosslinking reactions.

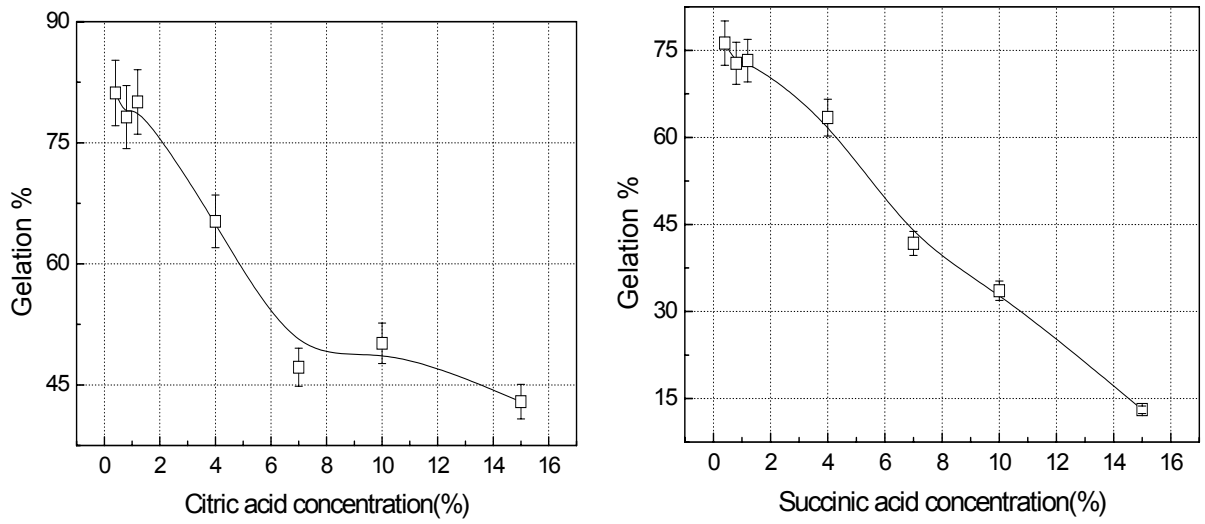

Fig. 1 – Gel fraction of PVA grafted with different citric and succinic acid concentrations.

2. Maximal swelling

The swelling of non-ionic hydrogels depends on the hydrophilicity of the base monomer or polymer, and the density of the intermolecular cross-links.[23] Fig. 2 shows the maximum swelling of the prepared resins versus the amounts of citric or succinic acid. It can be seen that the maximum swelling decreases with increasing the acid concentration. This behavior can be explained with increased hydrogen bonds due to the increased acid groups bonded to the polymer chains.

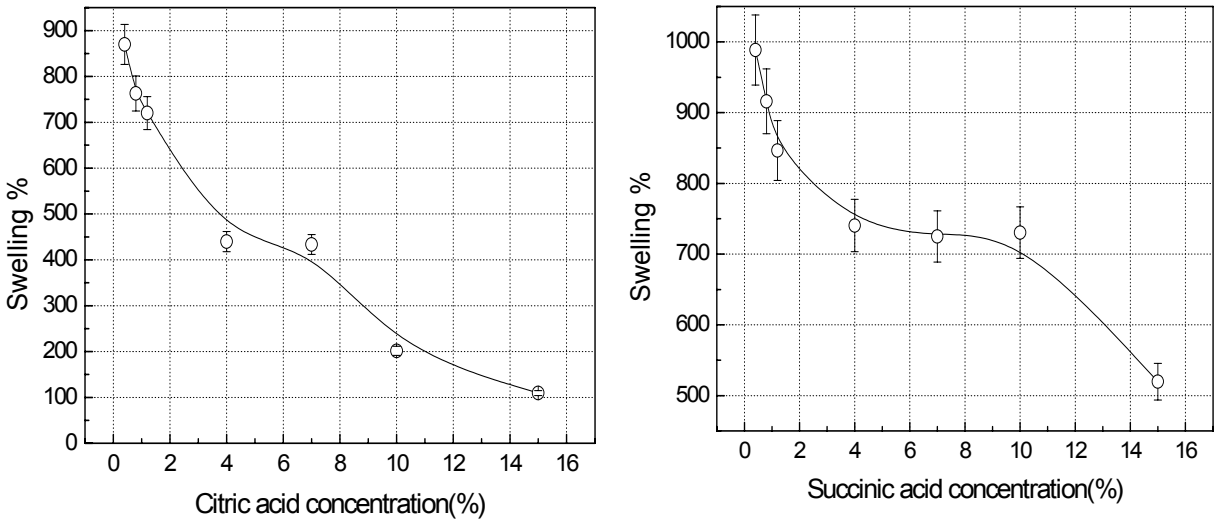

Fig. 2 – Maximal swelling of PVA grafted with different citric and succinic acid concentrations.

3. Sorption of the investigated Elements on the resin

Figs. 3, 4 and 5 show element ratios in the liquid phase in different acidic media for europium, cesium and strontium respectively (contact time of the phases 24 hours, weight of the solid phase 0.2 g, volume of the liquid phase 5 ml, initial concentration 0.1 mol/L). The left panel of the figures show the results for PVA grafted with citric acid and the right panel the results for PVA grafted with succinic acid. Every curve represents a different concentration of grafted acid.

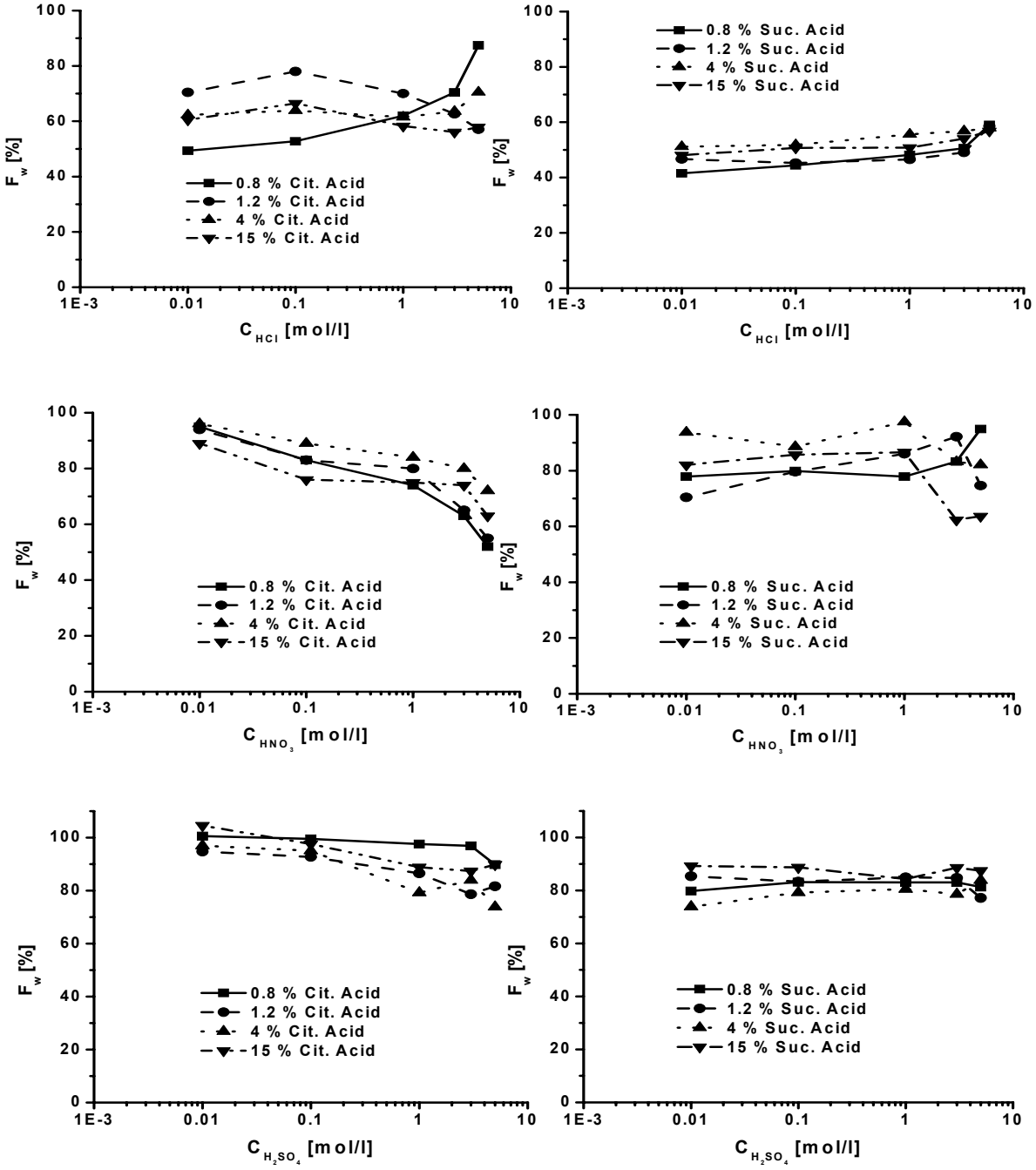

Fig. 3 – Europium ratios in the liquid phase in different acidic media
(t=24 h, weight of the solid phase 0.2 g, volume of the liquid phase 5 ml).

The adsorption of europium on both resins in all concentrations of H_2SO_4 is very weak (less than 4%) in all cases. Adsorption ratios of more than 60% are achieved in low HCl-concentration on the resin prepared in the presence of 0.8% succinic acid. The best adsorption ratio in HNO_3 is by the use of acid concentrations about 5 mol/L. By higher concentrations of HNO_3 the liquid phase became brown, which gives indication about resin degradation.

Fig. 4 shows cesium ratios in the liquid phase in different acidic media. In spite of europium, the best adsorption ratio can be achieved by the use of H_2SO_4 as a medium on the resin prepared in the presence of 10% succinic acid. Adsorption ratios of about 50% are achieved in 5 mol/L HCl on the resin prepared in the presence of 0.8% succinic

acid. The same ratio can also be achieved by the use of 5 mol/L HNO_3 on the resin prepared in the presence of 10% citric acid. By higher concentrations of HNO_3 and HCl the liquid phase became brown, which gives indication about resin degradation.

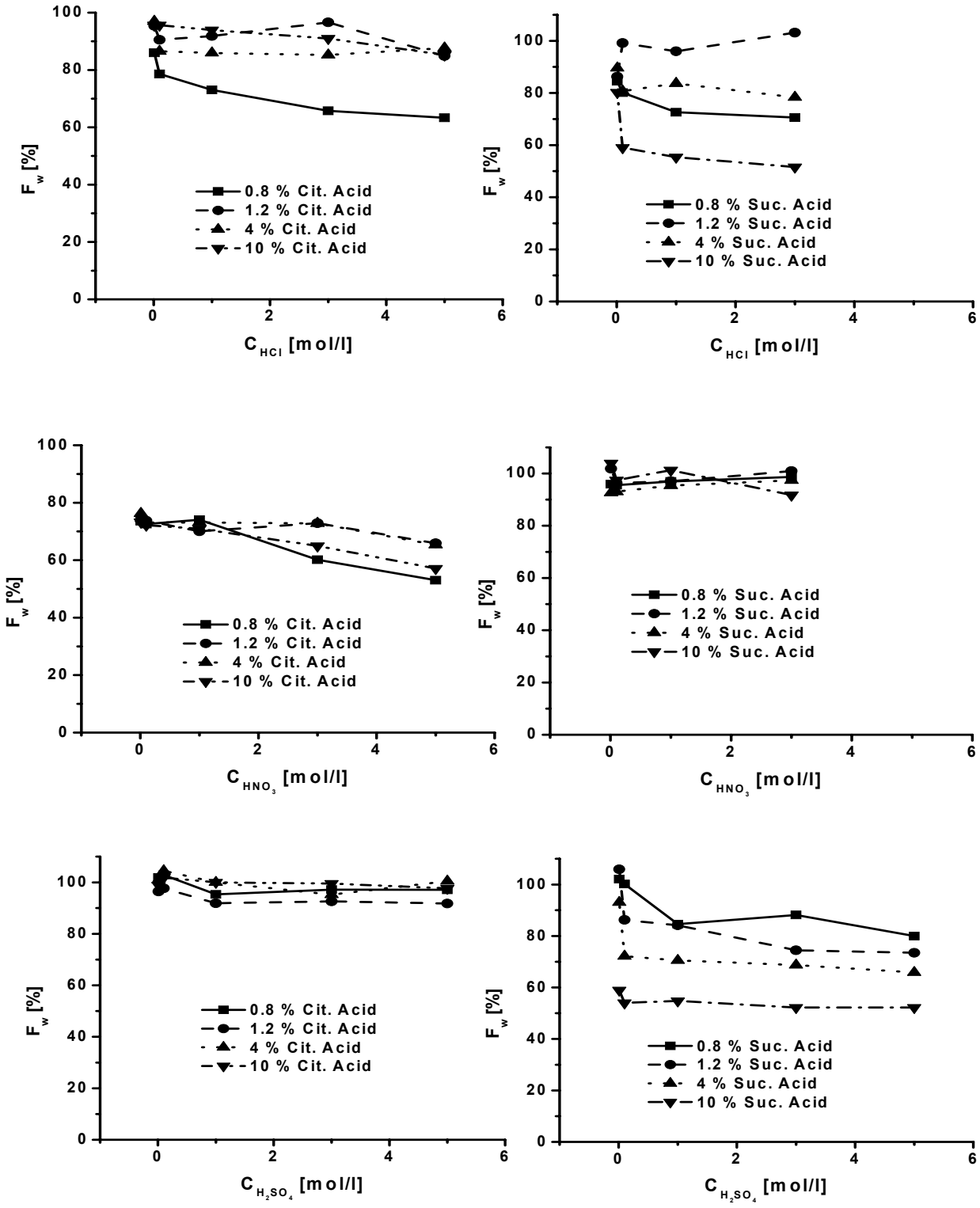

Fig. 4 – Cesium ratios in the liquid phase in different acidic media
(t=24 h, weight of the solid phase 0.2 g, volume of the liquid phase 5 ml).

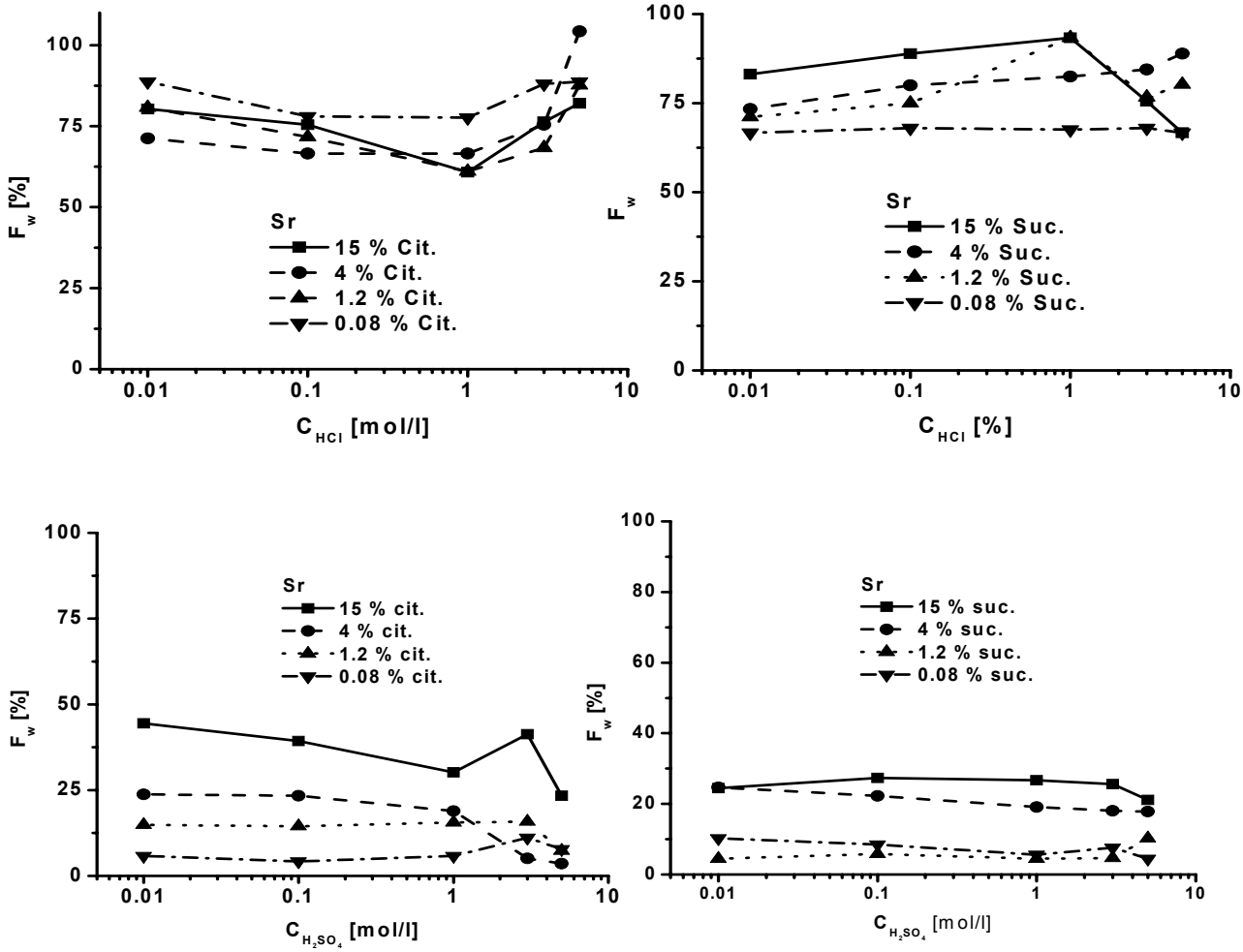

Fig. 5 – Strontium ratios in the liquid phase in different acidic media in equilibrium (t=24 h, weight of the solid phase 0.2 g, volume of the liquid phase 5 ml).

The strontium ratios in the liquid phase in HCl vary between 80 and 90 % and there are no special conditions or concentrations, which gives better results. Adsorption ratios more than 90% can be achieved on both resins in H_2SO_4 (Fig. 5).

The low adsorption ratios on the resins indicate that transport mechanism is another one than ion exchange. It could be electrolyte sorption on the resin.

CONCLUSION

Ion exchange resins have been prepared by grafting of polyvinyl alcohol with various concentrations of succinic and citric acid. The sorption of europium, cesium and strontium from different acidic media (HNO_3, HCl, H_2SO_4 with various concentrations) on the prepared weak acid ion exchangers containing carboxyl and hydroxyl functional groups was investigated. The low adsorption ratios on the prepared resins lead to the hypotheses that main mechanism of transport into the solid phase is electrolyte sorption instead of the ion exchange.

Acknowledgements: The authors would like to thank Prof. I. Othman (D. G. of AECS), Prof. T. Yassin and M. Albashir for their encouragement. Our thanks are extended to L. Stas, M. Swakeeh, A. Aquiel, S. Shashiet and H. Kousa for their efforts during the experiments.

REFERENCES

1. O.Alhassanieh, A. Abdul-Hadi, M. Ghafar, and A. Aba, *Appl. Radiat. and Isot*., **1999**, *51*, 493-498.
2. F. Helfferich, "Ion Exchange", Dover publication, New York, 1995.
3. M. Streat, "Applications of Ion Exchange in Hydrometallurgy, Hydrometallurgical Process Fundamentals"; Cambridge, 1984, p. 539-553.
4. J. B. Brower, R.L. Ryan, M. Pazirandeh, *Env. Sci. Tech*., **1997**, *31*, 2910-2914.

5. J.M. Rosiak, A. Rucinska-Reybas, W. Pekala, US Patent No. 4, 490, 871 Method of Manufacturing of Hydrogel Dressings, 1989.
6. M.T. Razzak, D. Darwis, S. Zainuddin, *Rad. Phys. Chem.*, **2001**, *62*, 107-113.
7. Z.Ajji, A.M. Ali, *Nucl. Inst. and Methods in Phys. Research* B, **2005**, *236*, 580-586.
8. Z. Ajji, G. Mirjalili, A. Alkhatab, H. Dada, *Rad. Phys. and Chem*., **2008**, *77*, 200-202.
9. IAEA 2005, Radiation synthesis of stimuli-responsive membranes, hydrogels and adsorbents for separation purposes, IAEA, Vienna, IAEA-TecDoc-1465, 2005.
10. E. A. Hegazy, H. A. Abd El-Rehim, H.Kamal, K. A. Kandeel, *Nucl. Inst. and Methods in Phy. Research B*, **2001**, *185*, 235-240.
11. A.M. Ali, Z. Ajji, *Rad. Phys. and Chem.,* **2009**, *78*, 927-932.
12. M.G. Katz, T. Wydeven, *J. Appl. Polym. Sci.*, **1981**, *26*, 2935-2943.
13. H.A. Abd El-Rehim, E.A. Hegazy, A.M. Ali, *J. Appl. Polym. Sci*., **1999**, *74*, 806-812.
14. H.A. Abd El-Rehim, E.A. Hegazy, A.M. Ali, *J. Appl. Polym. Sci.*, **2000**, *76*, 125-129.
15. K. Burczak, T. Fujisato, M. Hatada, Y. Ikada, *Proc. Jpn. Acad. B*, **1991**, *67*, 83-89.
16. V. Shantora, R.Y.M. Huang, *J. Appl. Polym. Sci.*, **1981**, *26*, 3223-3229.
17. Z. Ajji, A.M. Ali, *Nucl. Inst. and Methods in Phys. Research B*, **2007**, *265*, 362-365.
18. Z. Ajji, A.M. Ali, *J. of Hazardous Materials*, **2010**, *173*, 71-74.
19. Y. Zhanhai, R. Lei, X. Jun, DOI cnki:SCN:31-1258.0.**1997**-02-000.
20. Y. Zhanhai, R. Lei, X. Jun, *J. of Appl. Poyl. Sci*., **1992**, *198*, 683-687.
21. W. Yan, Z. Dong, T. Zhaoyi, L. Shunzhong, S. Zhenqing, Y. Anguo, F. Yijun, *Journal of The Chinese Rare Earth Society*, S1-007, DOI CNKI:SUN:XTXB.0.**2003**-S1-007.
22. N. Sahiner, N. Pekel, O. Güven, *Rad. Phys. Chem*., **1998**, *52*, 271-276.
23. O. Güven, M. Sen, E. Karadag, D. Saradin, *Rad. Phys. and Chem.* 56, **1998**, 381-386.

ACADEMIA ROMÂNĂ
Revue Roumaine de Chimie
http://web.icf.ro/rrch/

Rev. Roum. Chim.,
2012, *57*(3), 177-185

CHARACTERIZATION OF FUNCTIONALIZED POLYPYRROLE

Teodor SANDU,[a] Andrei SÂRBU,[b*] Floriana CONSTANTIN,[a] Cătălin Ilie SPĂTARU,[b]
Raluca Augusta GABOR,[b] Raluca ŞOMOGHI[b] and Horia IOVU[a]

[a]Department of Polymer Science and Technology, Faculty of Applied Chemistry and Materials Science, "Politehnica" University, 149 Calea Victoriei, Bucharest 010072, Roumania
[b]National R-D Institute of Chemical Research, 202-6 Splaiul Independentei, PO Box 174/35, Bucharest 060021, Roumania

Received March 2, 2011

Polypyrrole (PPY) was functionalized by reaction with glutardialdehyde using sulphuric acid as catalyst. The average size of polypyrrole powder particles was determined by Dynamic Light Scattering (DLS). The samples of functionalized polypyrrole were characterized by different techniques like thermo gravimetric analysis (TGA), differential scanning calorimetry (DSC), dynamic mechanical analysis (DMA), X-Ray Photoelectron Spectroscopy (XPS) and Fourier Transform Infrared Spectrometry (FTIR). The functionalization was not done during polymerization process as in other works, but after polymerization. The functionalization purpose was to create binding sites for enzyme immobilization at a distance from the polymer surface.

INTRODUCTION

Since polyacetylene was shown to exhibit high electrical conductivities when properly doped, π-polymers have been studied extensively.[1] During the last decades, conducting polymers (also called conjugated polymers or synthetic metals) such as polypyrrole (PPY) have been studied in great detail because of their rather straightforward preparation methods and reasonable stabilities in air and aqueous media. At the same time, they exhibit environmental stability, high mechanical strength and unique optical and electrical (switchable conductivity between insulator and metal) properties, leading to new possibilities for device fabrication. Polypyrrole and its derivatives, because of their long-term stability of its conductivity, are the leading materials among conducting polymers. Due to its surface properties such as wettability and because of potential applications in corrosion protection, conductive textiles, antistatic coatings, in the immobilization of biopolymers and growth control of living cells, interest has been recently increased in polypyrrole.[1-5] PPY and its derivatives can be easily synthesized either by chemical or electrochemical methods (electro polymerization). Electro polymerization usually gives higher polypyrrole conductivity than the chemical methods.[6] Chemical polymerization is carried out by reacting pyrrole monomer with an oxidant, such as ferric chloride or ammonium persulphate (which is faster than ferric chloride) in a suitable solvent. Electrochemical polymerization is done by oxidation of pyrrole monomer at a suitable anode upon application of a positive potential.[4, 7] The polymerization process in both cases involves the incorporation of certain charged anionic species into the polymer and may be simply described as follows:

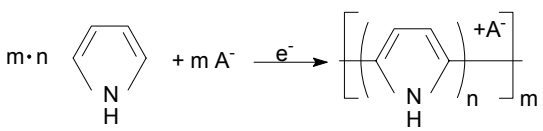

* Corresponding author: andr.sarbu@gmail.com

where A^- represents the counterion incorporated into the polymer to balance the charge, n is the number of pyrrole monomers per positive charge (usually 2~3), m is the number of the counterion incorporated into the polymer. Polypyrrole exhibits switching properties. After polymerization, polypyrroles exist in their oxidized states. By applying electrochemical stimulation polypyrrole is able of switching between its oxidized and reduced state.[4] Polypyrrole and its derivatives, *i.e.* pyrrolo [1,2-*a*] quinoline derivatives[8] and pyrrolo [1,2-*b*] pyridazine derivatives,[9] were also synthesized. Not only pyrrole derivatives can be synthesized, but also polypyrrole derivatives. Functionalized polypyrrole films have been obtained by electro polymerization in aqueous solution of pyrrole monomer in the presence of hydroquinone monosulfonate (HQS) as functional dopant in order to improve its electrical conductivity.[8] Also, in order to enhance the electroconductivity, single wall nanotubes functionalized with polypypyrrole films doped with poly (*m*-aminobenzene sulfonic acid) were synthesized.[9]

In our work, the functionalization was not done during the polymerization process as in the literature,[10, 11] but after polymerization. The functionalization was done using glutardialdehyde in order to create binding sites for enzyme immobilization at a distance from polymer surface.

RESULTS AND DISCUSSION

The average PPY particles diameter is about 2.5μm with a monomodal distribution as it can be noticed from Fig. 1.

In order to prove that PPY functionalization took place and to prove the reproducibility of the functionalization reaction, TGA tests for pure PPY and for three samples of functionalized PPY, prepared in identical conditions, were done. From Fig. 2 it can be observed that functionalized polypyrrole is more stable than pure polypyrrole. This is due to methylene-ammonium salt formation, which is a very stable compound. At the same time, the DTG curves (Fig. 3) confirm that functionalized polypyrrole is more stable than pure polypyrrole, because the temperature assigned to the maximum degradation speed is higher for all samples of functionalized polypyrrole. It can also be noticed that thermal degradation takes place with little differences between the three samples of functionalized polypyrrole, showing the reproducibility of the treatment process. The small differences in DTG of the functionalized samples are due to the concurrence between intramolecular and intermolecular crosslinking.

In order to better compare the thermal decomposition process for the four samples (pure polypyrrole and three samples of functionalized polypyrrole), the following parameters were measured for each sample: the temperature at which thermal degradation begins (T_{onset}) and it ends (T_{offset}), the weight loss, the temperature assigned to maximum degradation speed. These data are given in Table 1 and confirm that functionalized polypyrrole is more stable than pure polypyrrole because: for each sample of functionalized polypyrrole thermal degradation starts at a higher temperature than for pure polypyrrole and the weight loss is higher for pure polypyrrole than for functionalized polypyrrole.

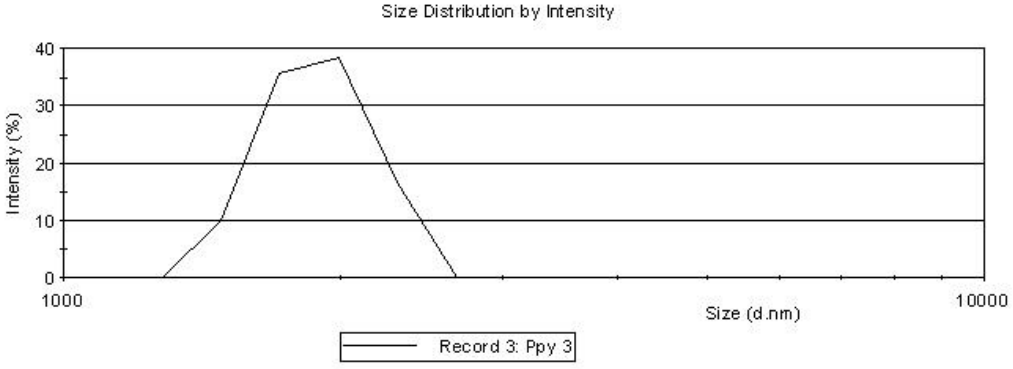

D=2469 nm

Fig. 1 – DLS analyses for polypyrrole powder particles.

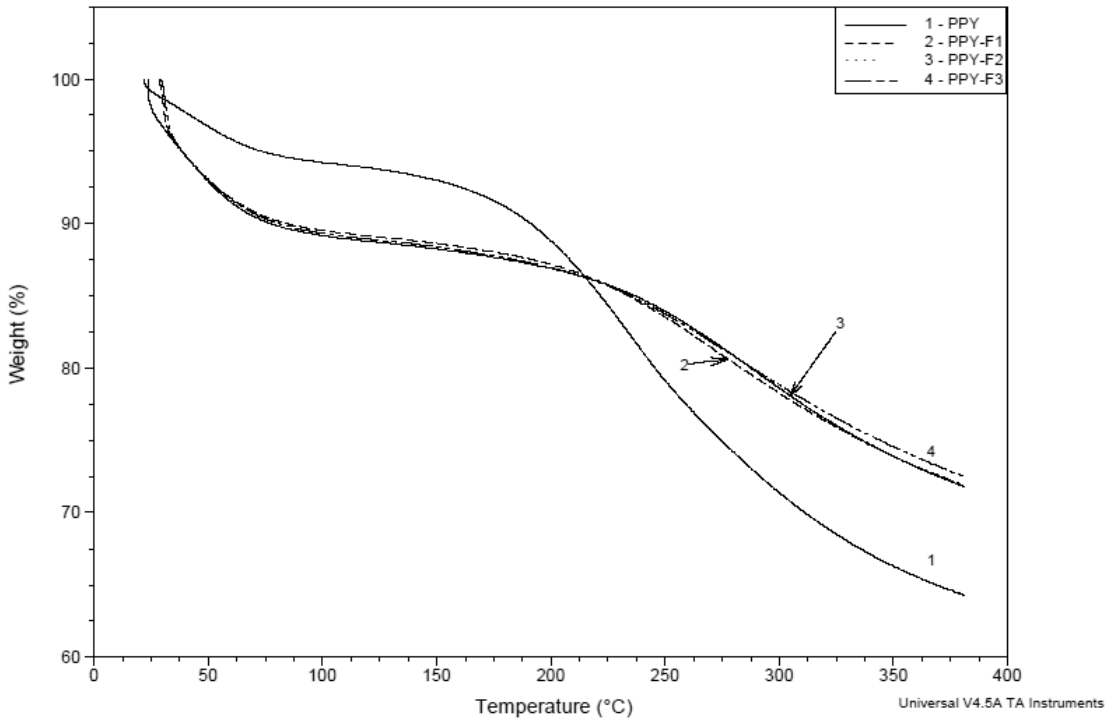

Fig. 2 – TGA curves for pure PPY (1) and three samples of functionalized polypyrrole prepared in identical conditions (2-4).

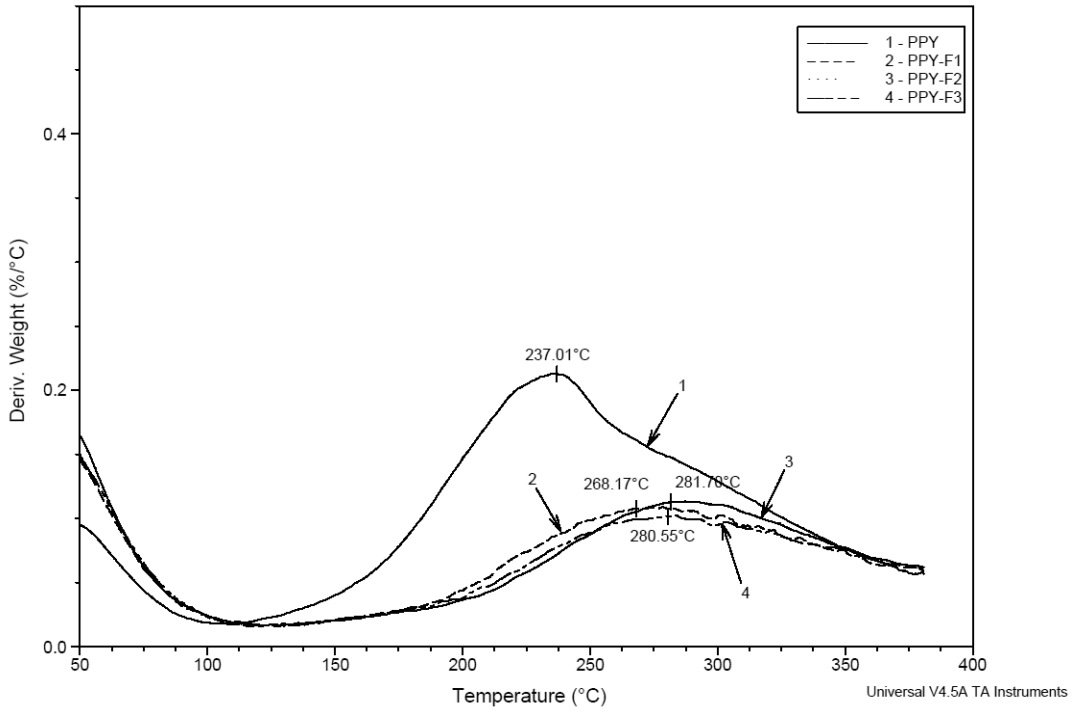

Fig. 3 – DTG curves for pure PPY (1) and three samples of functionalized polypyrrole prepared in identical conditions (2-4).

Table 1

Thermal decomposition data (main peak) for pure polypyrrole and functionalized polypyrrole

Sample	T_{onset} (°C)	T_{offset} (°C)	Weight loss (%)	T_{max} (°C)
PPY	102.40	379.37	29.85	235.51
PPY-F1	126.68	379.68	17.09	275.77
PPY-F2	154.97	380.60	16.35	291.45
PPY-F3	144.82	379.68	15.93	284.69

The reaction between CHO groups from glutaraldehyde and –NH groups from polypyrrole may be simply described as follows (Scheme 1):

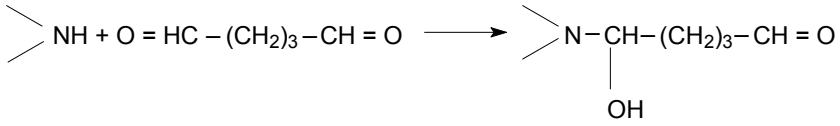

Scheme 1 – Functionalization reaction of polypyrrole with glutardialdehyde.

The second CHO group is able to react in the same way, leading to cyclization or crosslinking. Reaction conditions must be chosen in such a manner that enough unreacted CHO group remain for subsequent bonding of the enzyme. The immobilization reaction may be simply described as follows (Scheme 2):

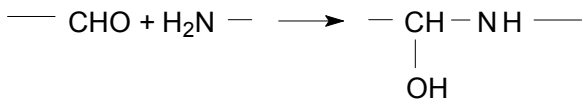

Scheme 2 – Enzyme immobilization reactions between free CHO groups from glutardialdehyde and H_2N groups from the enzyme.

The possibility of a physical glutaraldehyde immobilization was prevented, because the polymer obtained after functionalization was washed with water for several times in order to eliminate the unreacted glutaraldehyde.

In order to further confirm that functionalization modifies the polypyrrole thermal behaviour, the T_g values for pure polypyrrole and the three samples of functionalized polypyrrole were determined.

The influence of functionalization reaction on glass transition temperature (T_g) is revealed by DSC curves (Fig. 4).

The Tg for each sample represents the value which is assigned to the inflection point. The Tg values are given in Table 2. For the T_g values corresponding to the three samples of functionalized polypyrrole, one may notice a slight variation, the values varying between 66-72 ºC. Comparing the T_g values corresponding to the three samples of functionalized polypyrrole to the value corresponding to pure polypyrrole, it appears that functionalization does not lead to significant changes in the Tg value. The low differences between the Tg values assigned to the three samples of functionalized polypyrrole are probably due to the competition between intramolecular and intermolecular crosslinking with glutaraldehyde. Also, because of this competion the temperatures assigned to the amorphous ordering (Tmax, the temperature assigned to the peak from DSC for cooling processes) are different for the three functionalized polypyrrole samples. At the same time, these temperatures are different from the temperature corresponding to pure polypyrrole, confirming that functionalization reaction took place.

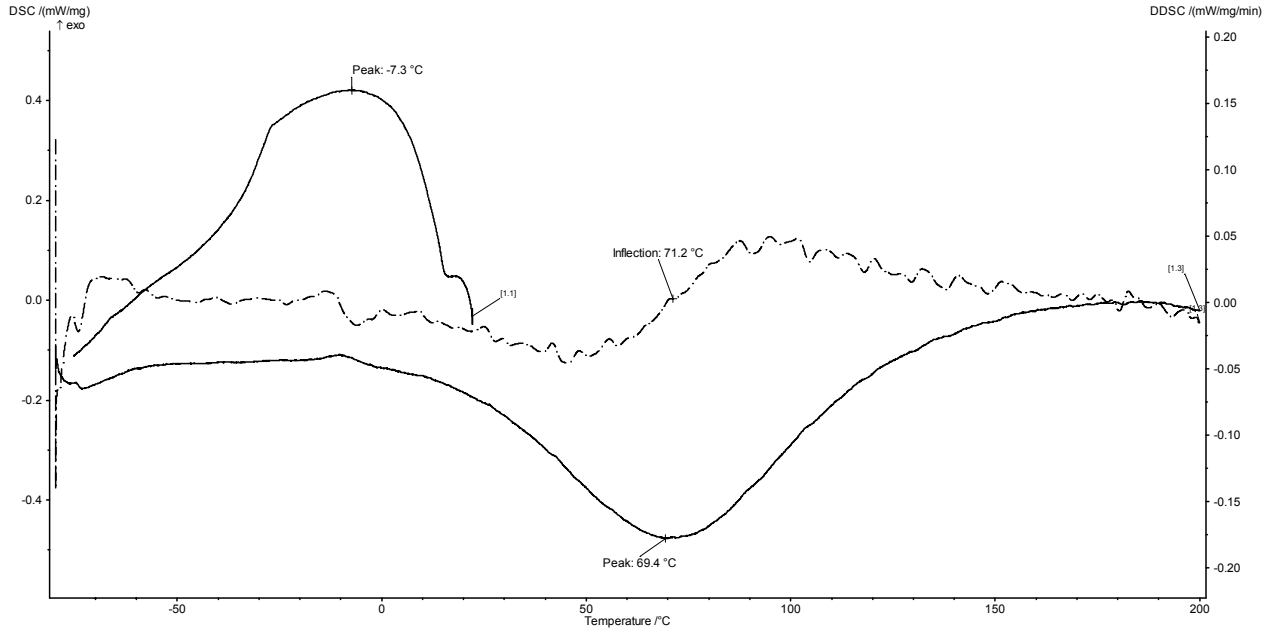

Fig. 4 – DSC curves of pure polypyrrole for heating (curve 1.3) and cooling (curve 1.1) processes and the corresponding first derivative (the curve with broken line) of this sample.

Table 2

Tg values and temperatures assigned to the amorphous ordering (T_{max}) for pure polypyrrole and three samples of functionalized polypyrrole revealed by DSC

Sample	T_g (ºC)	T_{max}(ºC)
PPY	71.2	-7.3
PPY-F1	66.3	4.9
PPY-F2	69.4	-14.7
PPY-F3	72.3	7.6

In order to further confirm PPy functionalization DMA tests were performed. From Fig. 5 one may observe that samples of functionalized polypyrrole obtained with different catalyst/PPY ratios exhibit different storage modulus compared to pure PPY. This is probably due to change of chemical composition by functionalization. From Fig. 6 it can be remarked that for functionalized polypyrrole the storage modulus decreases compared to pure polypyrrole. The decrease is more obvious for samples prepared with increased amounts of glutardialdehyde, fact which may be due to the increase of aliphatic groups which makes the structure more flexible. Fig. 7 shows that the storage modulus for the sample prepared at highest polypyrrole amount in the reaction mixture (solid/liquid ratio 1/112- curve 1) is much lower in comparison to that for pure PPY (curve 3) and for the samples obtained at lower solid/liquid ratio (curve 4 and 2). This fact shows that the samples prepared at solid/liquid ratio 1/137 and 1/150, because of the small content of polypyrrole, had not enough available –NH groups for bounding glutardialdehyde and that the solid /liquid ratio is a very important parameter for the functionalization reaction.

In order to emphasize that chemical composition was modified by functionalization, another sample of functionalized PPY was prepared. Before preparing this sample, PPY was heated with distilled water at 70 °C for 30 min., thus a reference with a similar thermal history as the functionalized samples being prepared which was then used for functionalization.

For reference functionalization a liquid phase (mixture of 9.98 mL water, 0.02 mL GLA, 0.136 mL concentrated sulphuric acid) was poured onto 0.1 g reference. Thus, functionalized polypyrrole (PPY-F) sample was obtained. Comparing the elemental compositions from XPS data (Table 3) the following features are observed: the reference exhibits less N, S, O than PPY dry powder and a higher amount of C, for PPY-F the carbon amount is higher than for the reference but it exhibits a less

amount of O, N, S, the reference and PPY-F samples also exhibit a small Si amount which perhaps is due to the dust (SiO_2) from air, absorbed onto the samples surface. The N, S and O content is lower for the reference compared to polypyrrole dry powder, which is due to the fact that after heating a mixture of polypyrrole and distilled water, the unreacted initiator (APS), is eliminated from polypyrrole. The carbon content increases because distilled water has absorbed CO_2 from atmosphere. These facts mean that before using PPY for functionalizing, it is necessary to purify it.

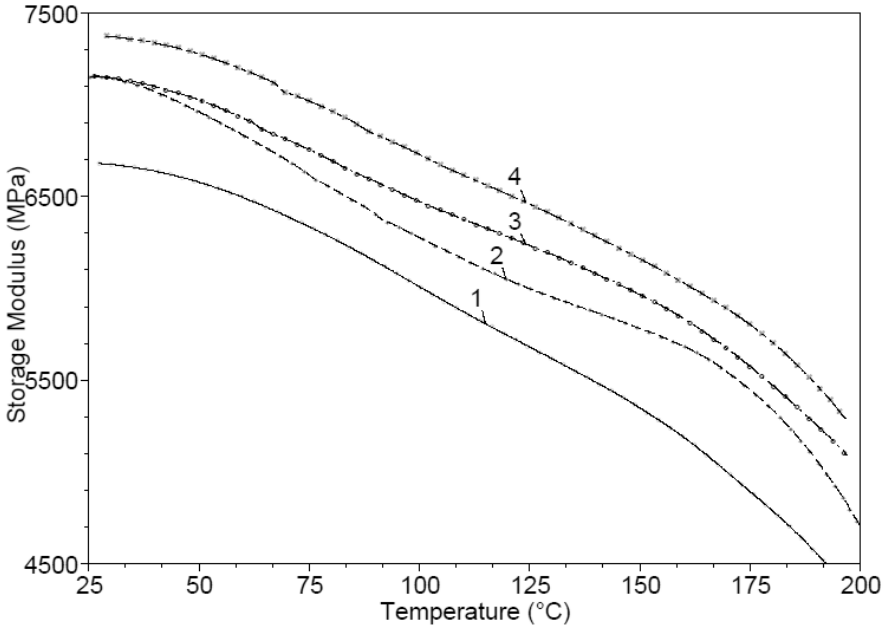

Fig. 5 – DMA curves for pure PPY(3) and for samples obtained with various catalyst /PPY ratios (mL H_2SO_4/g PPY): 0.163/0.100(1); 0.109/0.100 (2); 0.136/ 0.100(4).

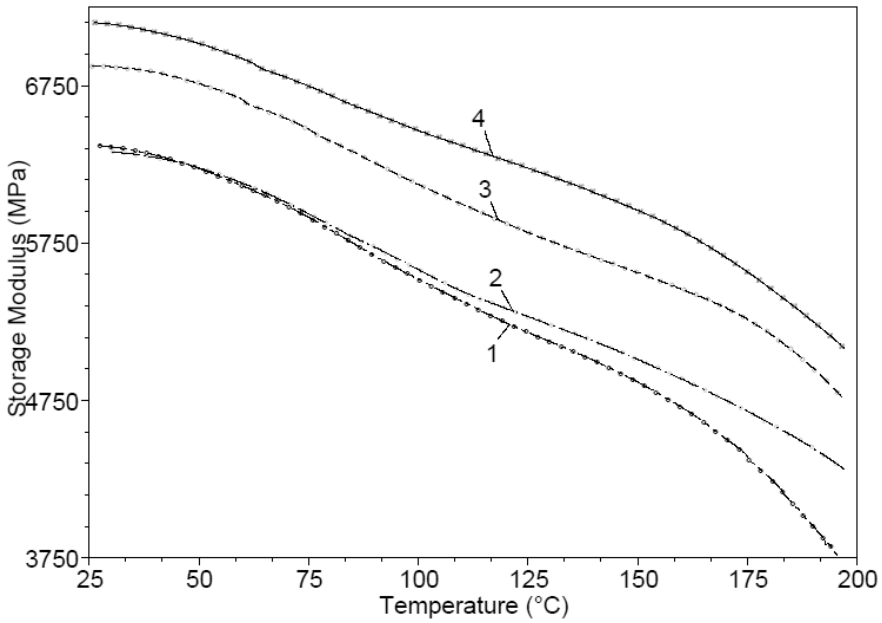

Fig. 6 – DMA curves for pure PPY (4) and samples obtained with various glutardialdehyde/water (GLA/W) ratios: GLA/W=1.50/8.50 (1); GLA/W=1/9 (2); GLA/W=0.25/9.75 (3).

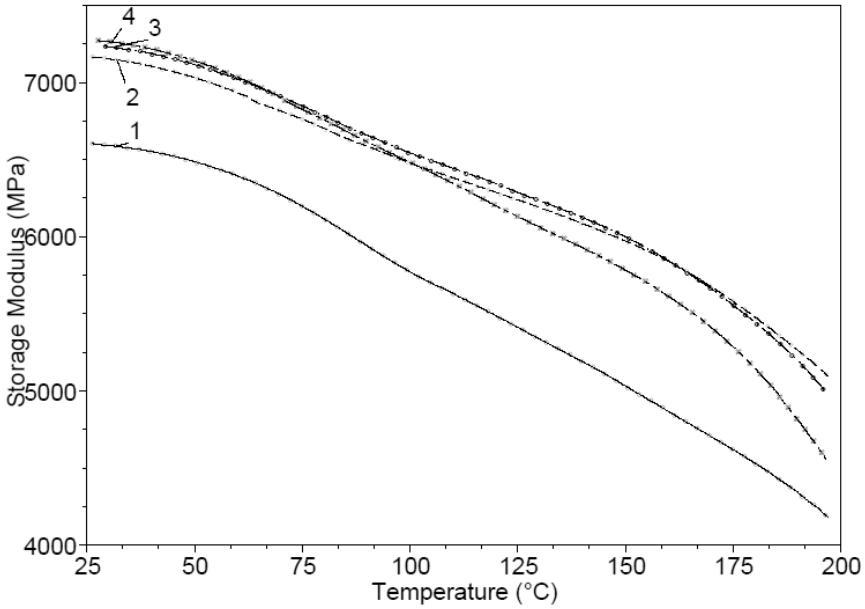

Fig. 7 – DMA curves for pure PPY (3) and samples obtained with various solid/liquid (S/L) ratio: S/L=1/112 (1); S/L=1/137 (4) S/L=1/150 (2).

The C content increase for PPY-F compared to reference is due to GLA bonding, because GLA exhibits a high C content. The N and S amount decreases after functionalization because GLA does not contain these atoms. All these features show that functionalization reaction took place.

Table 3

Elemental composition for PPY, REFERENCE, PPY-F (mass %)

Sample/Element	O	C	N	S	Si
PPY	25.9	56.8	13.9	3.4	
REFERENCE	19.5	64.7	13.6	1.6	0.6
PPY-F	19.2	65.6	13.6	1.0	0.6

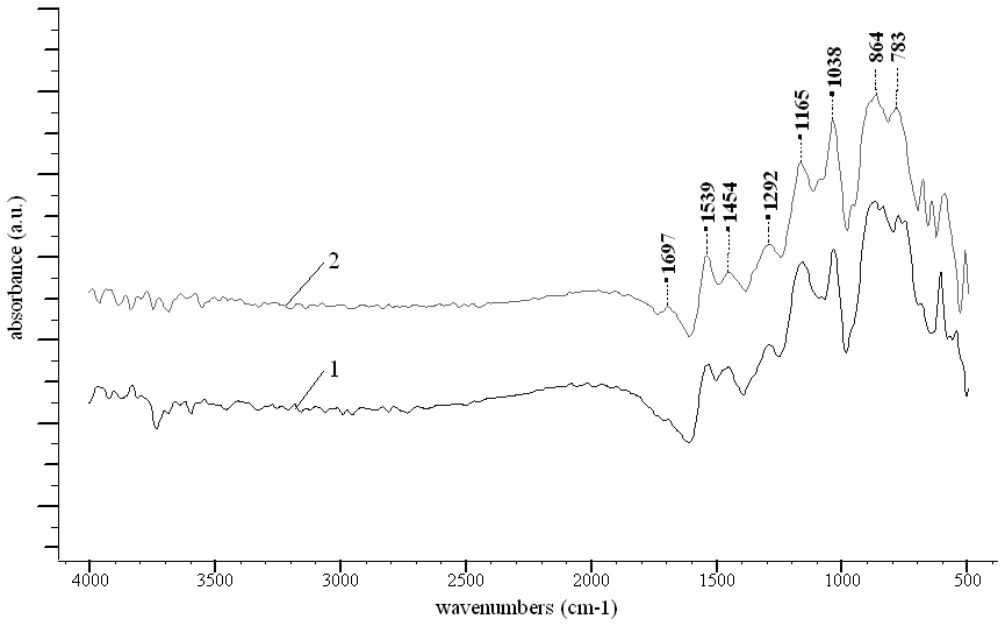

Fig. 8 – FTIR spectra for REFERENCE (1) and PPY-F (2).

In order to further confirm the differences between the pure PPY and PPY-F, FTIR spectra (Fig. 8) were recorded. The FTIR spectra exhibit the characteristic PPY absorptions. Characteristic PPY bands are given by: fundamental pyrrole rings vibrations (1539 cm^{-1} and 1454 cm^{-1}), in plane =C-H bond vibrations (1292 cm^{-1} and 1038 cm^{-1}), and the C-N bond stretching vibrations at 1165 cm^{-1}. The absorption bands from 870 and 780 cm^{-1} can be assigned to outside =C-H bond vibration. PPY functionalization is confirmed by amplitude increase and by the enlargement of the band from 1165 cm^{-1} assigned to C-N stretching vibration. In 600-1000 cm^{-1} frequency domain a slight change of the absorption bands can be noticed as a consequence of –CH (from PPY) and $–CH_2$ (from GLA) groups vibration superposition. The absorptions from 1697 cm^{-1} and 660 cm^{-1} can be assigned to unreacted compounds, which were eliminated by heating with distilled water, followed by drying.

EXPERIMENTAL

Materials

Pyrrole (PY) was supplied by Merck and distilled for further purification and then polymerized using ammonium persulphate as initiator in order to obtain polypyrrole (PPY). Ammonium persulphate was provided by Scharlau and used as received. Glutardialdehyde, aqueous solution 50% and sulphuric acid were received from Merck and used without further purification.

Sample synthesis

The PPY was synthesized by oxidative polymerization with ammonium persulphate, using a modification of a method reported in literature.[12] The modified procedure for PPY synthesis was described in our previous paper: [13] 5mL pyrrole were dissolved in 250mL water; then, 16.4g APS were added stepwise during two hours under continuous stirring, at 5°C. After that, the obtained slurry was filtered, washed and dried in oven at 50-60^{0}C for 6 h.

In order to synthesize functionalized PPY samples, firstly, the liquid phase was prepared by mixing the adequate amounts of water (8-9.75mL), glutardialdehyde (0.25-2mL) and sulphuric acid (0.109-0.163mL) in this order. Then, the liquid phase was poured onto polypyrrole (0.0667-0.1g) solid phase. The mixture thus obtained was heated at 70ºC for 30 min., then filtered and washed for five times with distilled water on the filter in order to eliminate the unreacted glutaraldehyde. Three samples of functionalized polypyrrole were synthesized in the same conditions (0.1 g PPY, 8 mL water, 2 mL glutardialdehyde, 0.136 mL sulphuric acid, 70 ºC, 30min.). The reference was obtained by heating PPY with distilled water at 70°C for 30 min. For synthesis of a reference functionalized PPY sample (PPY-F) a liquid phase (9.98mL water, 0.02mL GLA, 0.136mL concentrated sulphuric acid) was poured onto 0.1g reference and the mixture was maintained 30 min at 70 ^{o}C.

Sample characterization

Dynamic Light Scattering (DLS). The DLS analyses were registered on a Nano ZS MALVERN (Red Badge) equipment which determines sizes of particles in the range 0.6nm-6µm.

Thermogravimetric Analysis (TGA). The TGA curves were recorded on a Q 500 TA instrument. Each sample was heated from 20 to 400 °C at 10 °C/min heating rate under a constant nitrogen flow rate (100 mL/min).

Differential Scanning Calorimetry (DSC). The DSC curves were registered on a Netzsch 204 F1 Phoenix equipment using a heating rate of 5 °C/min. under a constant nitrogen flow rate (40 mL/min). Each sample was heated from -80 ºC to 200 ºC and then cooled at -80 ºC and reheated at 200 ºC.

Dynamic Mechanical Analysis (DMA). The DMA curves were recorded on a Q 800 TA Instrument, at 1 Hz frequency, from 25 °C to 200 °C using a heating rate of 3 ° C/min under air. The operating mode was temperature ramp, using powder clamp.

X-Ray Photoelectron Spectroscopy (XPS). The XPS spectra were recorded on a Thermo Scientific K-Alpha equipment, fully integrated, with an aluminium anode monochromatic source (1486.6 eV). The charging effects were compensated by an argon flood gun.

Fourier Transform Infrared Spectrometry (FTIR). The FTIR spectra were registered on a Able Jasco 4100 equipment using 32 scans and 4 cm^{-1} resolution in 500-4000 cm^{-1} region. The samples were analyzed using ATR unit.

CONCLUSIONS

At this stage of our research, the polymer functionalization degree is not still well controlled, but some general features appear. By the functionalization of polypyrrole, its stability is increased. The TGA and DTG curves confirm that functionalization reaction takes place and is reproducible. The functionalization is confirmed by the stability increase after functionalization (the maximum degradation temperature increases) as a consequence of methylene-ammonium (very stable compound) formation during functionalization. The functionalization reproducibility is proved by the low differences between the temperatures assigned to thermal decomposition of the three samples of functionalized polypyrrole. The DSC showed that functionalization does not lead to important Tg changes. Anyway, after functionalization the temperature assigned to the maximum at cooling processes changes, confirming that this reaction took place. After functionalization, important thermal stability changes are noticed, showing that functionalization takes place not only at polypyrrole particles surface, but also in the interior of these particles as

our previous paper,[14] by X-Ray Diffraction (XRD), proved. During polypyrrole functionalization the aliphatic groups content increases, leading to a more flexible structure. The higher flexibility causes the storage modulus decreasing, as DMA tests showed. FTIR spectra confirm pyrrole polymerization and polypyrrole functionalization. The XPS analyses prove that after functionalization, the surface elemental composition is modified. The XPS being a surface characterization technique, was used only to show the surface elemental composition changes due to PPY heating with distilled water and to PPY functionalization.

Acknowledgements: The work has been funded by the Sectoral Operational Programme Human Resources Development 2007-2013 of the Roumanian Ministry of Labour, Family and Social Protection through the Financial Agreement POSDRU/88/1.5/S/61178. This work was also supported by the BS Eranet project 7-045 IMAWATCO.

REFERENCES

1. D.H. Han, H. J. Lee and S. M. Park, *Electrochim. Acta*, **2005**, *50*, 3085-3092.
2. X. Yang, T. Day, Z. Zhu and Y. Lu, *Polymer*, **2007**, *48*, 4021-4027.
3. D. Mecerreyes, R. Stevens, C. Nguyen, J. A. Pomposo, M. Bengoetxea and H. Grande, *Synthetic Met.*, **2002**, *126*, 173-178.
4. B. Xi, "Novel conducting polymer structures for electrochemical actuators", Doctoral thesis, University of Wollongong, Australia, 2005.
5. L. Xu, W. Chen, A. Mulchandani and Y. Yan, *Angew Chem.*, **2005**, *44*, 6009-6012.
6. M. S. Ba-Shammakh, "Electropolymerization of pyrrole on mild steel for corrosion protection", Doctoral thesis, King Fahd University of Petroleum &Minerals, Dhahran, Saudi Arabia, 2002.
7. P. Saville, Polypyrrole Formation and Use, Defence R&D Canada Atlantic Technical Memorandum; DRDC Atlantic TM 2005-04, January 2005.
8. E. Georgescu, F. Dumitraşcu, F. Georgescu, C. Drăghici and M. M. Popa, *Rev. Roum. Chim.*, **2010**, *55*, 217-221.
9. F. Dumitraşcu, C. Drăghici, M. T. Căproiu, D. G. Dumitrescu, M. M. Popa, *Rev. Roum. Chim.*, **2009**, *54*, 923-926.
10. W. Prisanaroon-Ouajai, P. J. Pigram and A. Sirivat, *Jom-J. Min. Met. Mat. S.*, **2008**, *18*, 23-26.
11. K. Wanekaya, Y. Lei, E. Bekyarova, W. Chen, R. Haddon, A. Mulchandani and N. V. Myung, *Electroanal.*, **2006**, *18*, 1047-1054.
12. J. Honey, M. T. Rinku, J. Joe, J. Rani and K. T. Mathew, *Microw. Opt. Techn. Let.*, **2006**, *48*, 1324-1326.
13. T. Sandu, A. Sârbu, S. A. Gârea and H. Iovu, *UPB Sci Bull; Series B*, **2011**, *73*, 123-132.
14. T. Sandu, A. Sârbu, F. Constantin, E. Ocnaru, S. Vulpe, A. Dumitru and H. Iovu, *Revue Roum. Chim.*, **2011**, *56,* 875-882.

ACADEMIA ROMÂNĂ
Revue Roumaine de Chimie
http://web.icf.ro/rrch/

Rev. Roum. Chim.,
2012, *57*(3), 187-195

SCHIFF BASES OF 3-[(4-AMINO-5-THIOXO-1,2,4-TRIAZOLE-3-YL) METHYL]-2(3H)-BENZOXAZOLONE DERIVATIVES: SYNTHESIS AND BIOLOGICAL ACTIVITY

Solen URLU CICEKLI,[a] Tijen ONKOL,[a]* Selda OZGEN[b] and M. Fethi SAHIN[a]

[a] Gazi University, Faculty of Pharmacy, Department of Pharmaceutical Chemistry, 06330-Ankara, Turkey,
Fax: +90 312 223 5018; Tel: +90 312 202 3233
[b] Gazi University, Faculty of Pharmacy, Department of Microbiology, 06330-Ankara, Turkey,
Fax: +90 312 223 5018; Tel: +90 312 202 3262

Received June27, 2011

New Schiff base derivatives of 3-[(4-amino-5-thioxo-1,2,4-triazole-3-yl)methyl]-2(3*H*)-benzoxazolone with aromatic aldehydes have been synthesized under microwave irradiation. Structures of the synthesized compounds were confirmed by IR, ^{1}H-NMR and elemental analysis. Variable, but modest antimicrobial and antitubercular activity against the investigated strains of bacteria and fungi were observed. Among the derivatives obtained, 4-bromophenylmethylidene derivative **5j** revealed significant antibacterial activity against *P. aeruginosa*.

INTRODUCTION

1,2,4-Triazoles and their derivatives play important an role in medicinal, agricultural and industrial fields. In medicine, they can be used as antimicrobial,[1, 2] antitubercular,[3] anti-inflammatory[4] and analgesics.[5] There are numerous papers reporting the method of synthesizing 1,2,4-triazole Schiff bases and their diverse biological activities such as antioxidant,[6] antitumor,[7] antimicrobial[8-10] and antitubercular.[3,11]

The use of microwave irradiation (MWI) in organic synthesis has become increasingly popular within the pharmaceutical and academic areas due to its potential to accelerate the organic reactions and hence to improve the economic, environmental and operational aspects. Microwave irradiation in organic reactions offer several advantages over conventional homogeneous and heterogeneous reactions with respect to rate enhancement, higher yields, greater selectivity and ease of manipulation.[12, 13]

Starting from the known fact that 1*H*-1,2,4-triazole compounds have antimicrobial property, we synthesized new Shiff base derivatives of 3-[(4-amino-5-thioxo-1,2,4-triazole-3-yl)methyl]-2(3*H*)-benzoxazolone and tested them concerning the possible biological activity.

RESULTS AND DISCUSSION

A series of 3-[(4-substitutedphenyl-methylidene]amino-5-thioxo-1,2,4-triazol-3-yl) methyl]-2(3H)-benzoxazolone have been carried out by using microwave technique as shown in Scheme 1. Condensation of 2-aminophenol with urea resulted in rapid formation of 2(3H)-benzoxazolone **1** in high yield with enhanced reaction rate, when subjected to microwave irradiation under solvent-free condition.[14, 15]

* Corresponding author: tijen@gazi.edu.tr

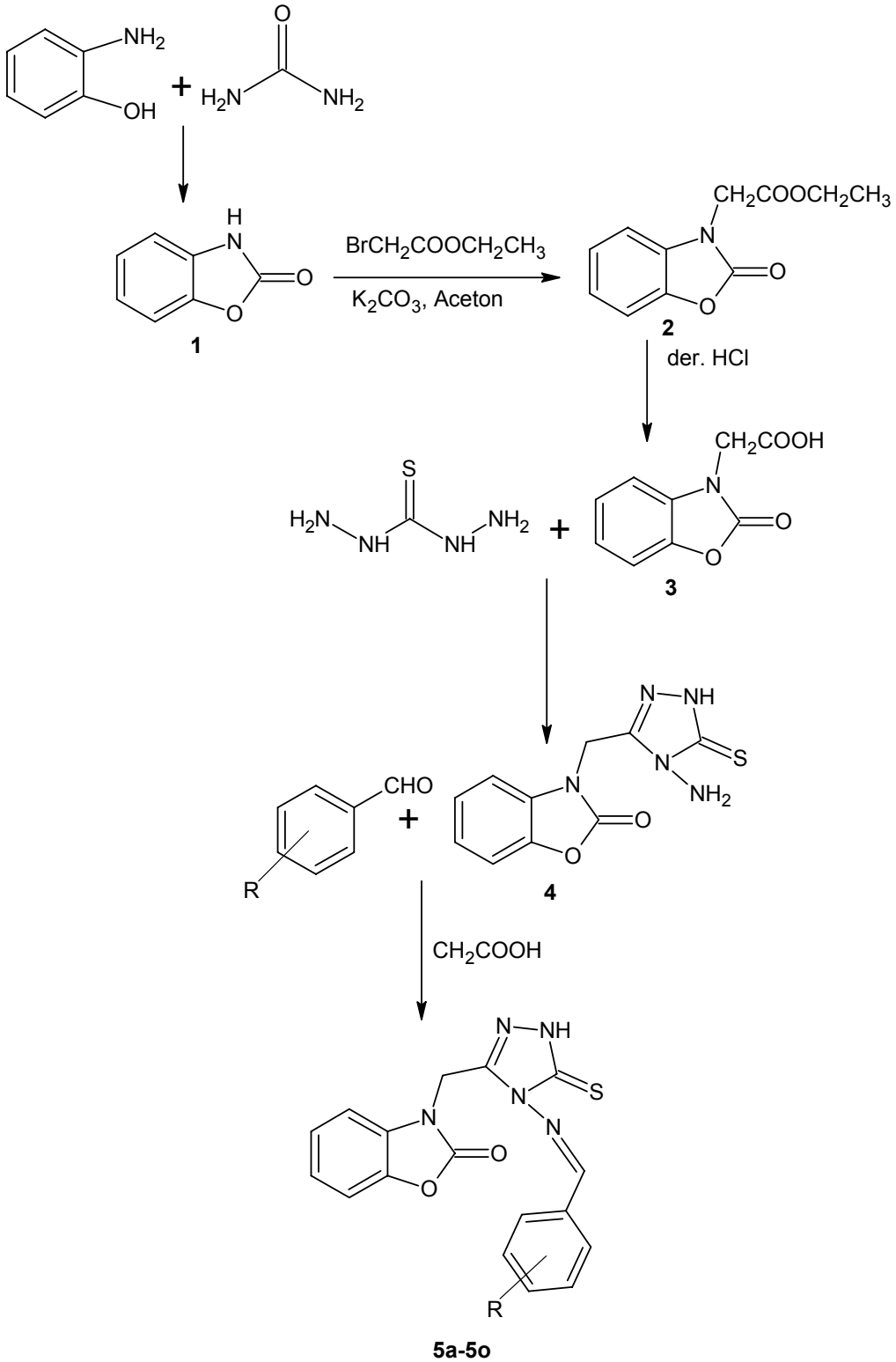

Scheme 1

2(3H)-benzoxazolone **1** was reacted with ethyl bromoacetate in the presence of potassium carbonate in microwave oven to obtain ethyl-(2(3H)-benzoxazolone-3-yl)acetate **2**. Synthesis of 2(3H)-benzoxazolone **1**, ethyl-(2(3H)-benzoxazolone-3-yl)acetate **2** and (2(3H)-benzoxazolone-3-yl)acetic acid **3** was accomplished according to the previously reported procedures.[16] 3-[(4-amino-5-thioxo-1,2,4-

triazol-3-yl)methyl]-2(3H)-benzoxazolone **4** was easily prepared from the reaction of (2(3H)-benzoxazolone-3-yl)acetic acid **3** and thiocarbohydrazide in oil-bath. 3-[(4-Amino-5-thioxo-1,2,4-triazol-3-yl)methyl]-2(3H)-benzoxazolone **4** was reacted with *o*/*p*-substituebenzaldehyde derivatives in acetic acid under microwave irradiation to give 3-[(*o*/*p*-substitutedphenylmethylidene]amino-5-thioxo-1,2,4-triazol-3-yl)methyl]-2(3H)-benzoxazolone **5a-5o** derivatives. Generally, Schiff bases are obtained in ethanol with an acid catalyst, but in our experiment 3-[(4-Amino-5-thioxo-1,2,4-triazol-3-yl)methyl]-2-benzoxazolone **4** was dissolved in acetic acid, that acted both as solvent and as catalyst.[17] Advantages of microwave irradiation such as high yield, short reaction time, pure product and easy work up prompted us to synthesize compounds under microwave irradiation.

The structures of the synthesized compounds were elucidated by IR, ^{1}H NMR spectra and elemental analysis.

In the IR spectra of all compounds, C=N and C=C bands were observed at about 1631-1462 cm^{-1} region and C=O stretching bands of 2(3H)-benzoxazolone were observed at 1782-1742 cm^{-1} region. IR spectroscopic data of the **5a-m** compounds, which have 3-[(4-substituephenyl-methylidene]amino-5-thioxo-1,2,4-triazol-3-yl) methyl]-2(3H)-benzoxazolone **4** structure, proved that these compounds were in the thionic form, as a result of the observation of C=S stretching bands at 1283-1233 cm^{-1} and the absence of an absorption at about 2600-2550 cm^{-1} region cited for SH group.

In the ^{1}H NMR spectra of compounds (**5a-m**) which were recorded in dimethylsulphoxide (DMSO)-d_6, NH proton of the Schiff base was seen as singlet at about 14.10-13.93 ppm. The signals due to 2(3H)-benzoxazolone methylene protons present in all compounds, appeared at 5.29-5.18 ppm, as singlet. The -N=CH proton of compounds **5a-m** appeared at 10.83-9.77 ppm as singlet. All other aromatic and aliphatic protons were observed at the expected regions.

The synthesized compounds were tested for their antibacterial activity against gram positive bacteria; *Staphylococcus aureus* ATCC 29213, methicillin-resistant *S. aureus* (MRSA, clinical isolate), *Enterococcus faecalis* ATCC 29212, *E. faecalis* (resistant to vancomycin, clinical isolate), gram negative bacteria; *Escherichia coli* ATCC 35218 producing extended spectrum β-lactamase and *E. coli* clinical isolate (ESBL), *Pseudomonas aeruginosa* ATCC 27853, *P. aeruginosa* (resistant to gentamicin, clinical isolate) and yeast-like fungi; *Candida albicans* ATCC 10231 and *Candida krusei* ATCC 6258 by using broth microdilution method. Ampicillin and gentamicin were used as standard antimicrobial agents and amphotericin B and fluconazole were used as standard antifungal agents (Table 2). The synthesized compounds were also tested *in vitro* for antimycobacterial activity against *Mycobacterium tuberculosis* H37RV ATCC 27294*, M. tuberculosis* (clinical isolate) by using MABA method. Ethambuthol was used as standard antimycobacterial agent. The results concerning the biological activity of the compounds are shown in Table 3. MICs were recorded as the minimum concentration of compounds which inhibit the growth of tested microorganisms.

Some synthesized compounds showed good to moderate activity with MIC value in the range of 32-128 μg/mL. Particularly, compounds **5e** and **5h** showed good activity (MIC value 128 μg/mL) against *E. coli* and compound **4** showed significant activity (MIC value 32 μg/mL) against *E. coli*. Moreover, **5e** and **5h** displayed comparable activity (MIC value 128 μg/mL) against *E. faecalis* and *E.coli* relative to the compound **4**.

For activity against *P. aeruginosa*, compounds **5j** yielded more promiosing activity, in comparison to other compounds synthesized, with MIC 64 μg/mL. All compounds showed weak or no activity against *S. aureus*. The results of antibacterial activity suggested that compounds with 2-hydroxy, 4-fluoro, and 4-bromo groups on the aromatic ring showed enhanced antibacterial activity among all the synthesized compounds.

Similar to antibacterial activity, the antifungal activity of the present compounds was not comparable to that of the standard drug Fluconazole due to the concentration variation. With respect to antifungal activity of the synthesized compounds, all compounds displayed antifungal activity against both *C. albicans* and *C. krusei* with MIC values of 128-512 μg/mL. Compounds **5e** and **5j** were as effective as compound **4** but were less active than the reference drug. Compounds **5c, 5g, 5n** and **5m** exhibited slightly inhibitory activity against *C. krusei* with MIC value of 128 μg/mL.

Table 1

Physico-chemical data of synthesis compounds (**5a-5o**)

Comp.	R	Crys. Sol.	Mp (^{o}C)	Yield (%)	Formula	Elemental Anal. Cal /Found.
4	-	EtOH-DMF	209	74	$C_{10}H_9N_5O_2S$	C:45.62 / 45.99 H: 3.45 / 3.76 N: 26.60 / 26.65
5a	**H**	Acetone-H_2O	225	27	$C_{17}H_{13}N_5O_2S$	C: 58.11 / 57.81 H: 3.73 / 4.15 N: 19.93 / 19.67
5b	**2-F**	EtOH-Acetone	232-34	59	$C_{17}H_{12}FN_5O_2S$	C: 55.28 / 55.09 H: 3.27 / 3.25 N:18.96 /19.05
5c	**2-Cl**	EtOH- DMF	231-33	36	$C_{17}H_{12}ClN_5O_2S$	C: 52.92 / 52.80 H: 3.13 / 3.16 N: 18.15 / 18.17
5d	**2-Br**	EtOH-Acetone	235	38	$C_{17}H_{12}BrN_5O_2S$	C: 47.45 / 47.13 H: 2.81 / 2.82 N:16.28 / 16.34
5e	**2-OH**	EtOH-Acetone	226	45	$C_{17}H_{13}N_5O_3S$	C: 55.58 / 55.32 H: 3.57 / 3.68 N: 19.06 / 19.01
5f	**2-CH_3**	EtOH-Acetone	221-22	58	$C_{18}H_{15}N_5O_2S$	C: 59.16 / 59.38 H: 4.14 / 3.95 N: 19.17 / 19.15
5g	**2-OCH_3**	EtOH-Acetone	237	55	$C_{18}H_{15}N_5O_3S$	C: 56.68 / 56.90 H: 3.96 / 3.99 N: 18.36 / 18.35
5h	**4-F**	2-Propanol	227-28	41	$C_{17}H_{12}FN_5O_2S$	C: 55.28 / 55.16 H: 3.27 / 3.50 N: 18.96 / 18.89
5i	**4-Cl**	EtOH	244-45	55	$C_{17}H_{12}ClN_5O_2S$	C: 52.92 / 52.73 H: 3.13/ 3.16 N: 18.15 / 18.22
5j	**4-Br**	EtOH- DMF	248-49	77	$C_{17}H_{12}BrN_5O_2S$	C: 47.45 /47.42 H: 2.81 / 2.89 N: 16.28 / 16.36
5k	**4-OH**	2-Propanol	247	45	$C_{17}H_{13}N_5O_3S$	C: 55.58 / 55.57 H: 3.57 /3.68 N: 19.06 / 19.03
5l	**4-CH_3**	EtOH-Acetone	231	62	$C_{18}H_{15}N_5O_2S$	C: 59.16 / 59.44 H: 4.14 / 4.10 N: 19.17 / 19.17
5m	**4-OCH_3**	EtOH- DMF	219-20	50	$C_{18}H_{15}N_5O_3S$	C : 56.68 / 56.58 H: 3.96 / 3.99 N: 18.36 / 18.42
5n	**4-CF_3**	EtOH-Acetone	243	39	$C_{18}H_{12}F_3N_5O_2S$	C : 51.55 / 51.55 H: 2.88 / 2.80 N: 16.70 / 16.67
5o	**4-$C(CH_3)_3$**	EtOH-Acetone	226-27	74	$C_{21}H_{21}N_5O_2S$	C: 61.90 / 61.99 H: 5.19 / 5.12 N: 17.19 / 17.16

Table 2

Antimicrobial activity results (MICs, µg/mL) of the synthesized compounds with the standard drugs

Comp.	A	B	C	D	E	F	G	H	I	J
4	256	256	128	256	32	128	256	128	128	256
5a	512	256	256	512	512	256	256	128	256	256
5b	512	256	512	512	512	512	256	256	256	256
5c	512	256	512	512	512	512	256	256	256	128

Table 2 (continued)

5d	512	256	256	512	512	512	256	256	256	256
5e	512	128	512	512	128	512	256	256	128	256
5f	512	256	512	512	256	512	256	256	256	256
5g	512	256	256	512	512	512	256	256	256	128
5h	512	256	128	512	128	512	256	256	256	256
5i	512	256	256	256	256	512	256	256	256	256
5j	512	128	512	256	512	512	64	256	128	256
5k	512	256	512	512	512	512	256	256	256	256
5l	512	256	256	512	512	512	256	256	256	256
5m	512	256	256	512	512	512	256	256	256	256
5n	512	256	256	512	256	512	256	256	256	128
5o	512	256	512	512	512	512	256	256	256	128
Ampicillin	0.5	-	0.5	0.5	-	>1024	-	-	-	-
Gentamicin	0.5	128	8	8	-	512	1	64	-	-
AmphotericinB	-	-	-	-	-	-	-	-	<0.03	0.5
Fluconazole	-	-	-	-	-	-	-	-	0.0625	32

A: *S. aureus* ATCC 29213, B: *S.aureus* isolated, C: *E. faecalis* ATCC 29212, D: *E.faecalis* isolated, E: *E.coli* ATCC 35218, F: *E.coli* isolated, G: *P. aeruginosa* ATCC 27853, H: *P.aeruginosa* isolated, I: *C. albicans* ATCC 10231, J: *C.krusei* ATCC 6258

Table 3

Antimycobacterial activity results (MICs, μg/mL)
of the synthesized compounds with the standard drugs

Comp.	*Mycobacterium tuberculosis* H37RV ATCC 27294	*Mycobacterium tuberculosis* isolated
4	128	512
5a	256	512
5b	256	512
5c	256	512
5d	128	512
5e	512	256
5f	512	256
5g	512	256
5h	256	512
5i	512	512
5j	512	512
5k	512	256
5l	512	512
5m	512	512
5n	512	256
5o	512	256
Etambuthole	4	1

The synthesized compounds showed moderate activity against mycobacteria with MIC values ranging from 128 to 512 μg/mL. Compounds **4** and **5d** showed better activity against *M. tuberculosis* H37Rv than the other compounds (MICs 128 μg/mL). The results of antimycobacterial activity showed that compounds with a halogen group on the aromatic ring showed good antimycobacterial activity among all the synthesized compounds.

MATERIALS AND METHODS

All chemicals and solvents, used in this study, were purchased from Aldrich, (Germany), Merck (Germany) and Acros (Germany) Chemical. Melting points of the compounds were recorded on an Electrothermal-9200 digital melting points apparatus and are uncorrected. Microwave reactions were carried out in MicroSYNTH Microwave Labstation at 1600 W (2 magnetrons 800Wx2). (Milestone S.r.l. Italy). ^{1}H-NMR spectra of compounds were recorded in DMSO-d_6 on Bruker 400 MHz NMR spectrometer. Chemical shifts were reported in parts per million relative to internal standard tetramethylsilane. FTIR spectra of the surface layer of grafted membranes were measured with a Perkin-Elmer 400 (USA) ATR attachment (32 scans, wavenumber 4000–650 cm^{-1}) and analyzed using the Spectrum v2.0 software.

2(3H)-Benzoxazolone **(1)**

2(3H)-benzoxazolone was prepared under microwave irradiation as previously reported. [14,15]

Ethyl (2(3H)-benzoxazolone-3-yl)acetate **(2)**

The mixture of 2(3H)-benzoxazolone (5 mmol), potassium carbonate (5.75 mmol) and ethyl bromoacetate (5.75 mmol) in 50 mL acetone was prepared in round bottom flasks, placed in a microwave oven and irradiated (350 W, 65°C) for 15 min. After completion of reaction (TLC), 100 mL iced water was added to the cooled (0-10°C) reaction mixture. After stirring for 1 h, the crude was filtered, washed with water, dried, and crystallized from ethanol. Structures of the products were confirmed by IR, ^{1}H-NMR spectra and the obtained result was compared with conventional sample's result prepared according to literature methods. [16]

(2(3H)-Benzoxazolone-3-yl)acetic acid **(3)**

Ethyl (2(3H)-benzoxazolone-3-yl)acetate (0.01mol) was refluxed in hydrochloric acid (50 mL) for 2 hours. The reaction mixture was cooled, and the precipitate was collected by filtration, washed with water, dried, and crystallized from water. [16]

3-[(4-amino-5-thioxo-1,2,4-triazol-3-yl)methyl]-2(3H)-benzoxazolone **(4)**

(2(3H)-benzoxazolone-3-yl)acetic acid (0.01 mol) and thiocarbohydrazide (0.01 mol) were fused at 160-170°C in an oil bath for 30 min. N,N-dimethylformamide (DMF) was added on the crude and crude was heated until it solves. Subsequently water was added to the reaction mixture and the precipate was filtered, dried and recrystallized from DMF-ethanol.

Yield, 74%, m.p 209°C. IR ν max/cm^{-1} 3278, 3179,1782, 1483, 1243. ^{1}H NMR (DMSO) δ13.63 (1H, s, NH), 7.36 (1H, d, H7), 7.22-7.13 (3H, m, H4, H5, H6), 5.62 (2H,s, CH_2), 5.11 (2H, s, NH_2).

General procedure for *3-[(4-{[phenylmethylidene] amino}-5-thioxo-1,2,4-triazol-3-yl)methyl]-2(3H)-benzoxazolone* **(5a-5m)**

To a suspension of *o*/*p*-substituted benzaldehyde (0.0022 mol) in glacial acetic acid (3 mL), 0.002 mol [(4-amino-5-thioxo-1,2,4-triazol-3-yl)methyl]-2(3H)-benzoxazolone was added. The reaction mixture was placed in microwave oven and irradiated for minutes changing between 15-30 min at 125 °C (300 W). After completion of the reaction by monitoring with TLC, the reaction mixture was kept overnight at room temperature. The precipitate was collected by filtration, washed with water, dried, and crystallized from appropriate solvent. (Table 1)

3-[(4-{[Phenylmethylidene]amino}-5-thioxo-1,2,4-triazol-3-yl)methyl]-2(3*H*)-benzoxazolone. (5a)

Yield, 27%, m.p 225°C. IR ν max/cm^{-1}, 3230, 1776, 1484, 1236. ^{1}H NMR (DMSO-d_6) δ 14.10 (1H, s, NH), 10.01 (1H, s, =CH), 7.85 (2H, d, Ar-H), 7.61 (1H, t, Ar-H), 7.54 (2H, t, Ar-H), 7.36 (1H, d, H7), 7.28 (1H, d, H4), 7.18 (1H, t, H6), 7.16 (1H, t, H5), 5.30 (2H, s, CH_2).

3-[(4-{[(2-Fluorophenyl)methylidene]amino}-5-thioxo-1,2,4-triazol-3-yl)methyl]-2(3*H*)-benzoxazolone. (5b)

Yield, 59 %, m.p 232-234°C. IR ν max/cm^{-1}, 3230, 1751, 1484, 1233. ^{1}H NMR (DMSO-d_6) δ 13.93 (1H, s, NH), 10.42 (1H,s, =CH), 7.94 (1H, T, Ar-H), 7.59-7.57 (1H, m, Ar-H), 7.33-7.25 (3H, m Ar-H, H7), 7.19 (1H, d, H4), 7.11 (1H, t, H6), 7.06 (1H, t, H5), 5.21 (2H, s, CH_2).

3-[(4-{[(2-Chlorophenyl)methylidene]amino}-5-thioxo-1,2,4-triazol-3-yl)methyl]-2(3*H*)-benzoxazolone. (5c)

Yield, 36 %, m.p 231-33°C. IR ν max/cm^{-1}, 3238, 1748, 1482, 1242. ^{1}H NMR (DMSO-d_6) δ 14.16

(1H, s, NH), 10.83 (1H, s, =CH), 8.13 (H, d, Ar-H), 7.64-7.43 (3H, m, Ar-H), 7.37 (1H, d, H7), 7.29 (1H, d, H4), 7.21-7.16 (2H, m, H6, H5), 5.33 (2H, s, CH_2).

3-[(4-{[(2-Bromophenyl)methylidene]amino}-5-thioxo-1,2,4-triazol-3-yl)methyl]-2(3*H*)-benzoxazolone. (5d)
Yield, 38 %, m.p 235 ^oC. IR ν max/cm^{-1}, 3248, 1744, 1480, 1269. ^1H NMR (DMSO-d_6) δ 13.93 (1H, s, NH), 10.72 (1H, s, =CH), 8.04-8.01 (1H, m, Ar-H), 7.71-7.69 (1H, m, Ar-H), 7.44-7.42 (2H, m, Ar-H), 7.28 (1H, d, H7), 7.20 (1H, d, H4), 7.11 (1H, t, H6), 7.06 (1H, t, H5), 5.24 (2H, s, CH_2).

3-[(4-{[(2-Hydroxyphenyl)methylidene]amino}-5-thioxo-1,2,4-triazol-3-yl)methyl]-2(3*H*)-benzoxazolone. (5e)
Yield, 45 %, m.p 226 ^oC. IR ν max/cm^{-1}, 3102, 1777, 1485, 1264. ^1H NMR (DMSO-d_6) δ 13.93 (1H, s, NH), 10.32 (1H, s, OH), 10.12 (1H, s, =CH), 7.72 (1H, d, Ar-H), 7.33 (1H, t, Ar-H), 7.26 (1H, d, H7), 7.19 (1H, d, H4), 7.12-7.03 (2H, m, H6, H5), 6.88 (1H, d, Ar-H), 6.81 (1H, t, Ar-H), 5.18 (2H, s, CH_2).

3-[(4-{[(2-Methylphenyl)methylidene]amino}-5-thioxo-1,2,4-triazol-3-yl)methyl]-2(3*H*)-benzoxazolone. (5f)
Yield, 58 %, m.p 221-222 ^oC. IR ν max/cm^{-1}, 3186, 1772, 1484, 1268. ^1H NMR (DMSO-d_6) δ 14.16 (1H, s, NH), 10.28 (1H, s, =CH), 7.84 (1H, d, Ar-H), 7.39 (1H, t, Ar-H), 7.29-7.18 (4H, m, Ar-H, H7, H4), 7.12(1H, t, H6), 7.06 (1H, t, H5), 5.21 (2H, s, CH_2), 2.40 (3H, s, CH_3).

3-[(4-{[(2-Methoxyphenyl)methylidene]amino}-5-thioxo-1,2,4-triazol-3-yl)methyl]-2(3*H*)-benzoxazolone. (5g)
Yield, 55 %, m.p 237 ^oC. IR ν max/cm^{-1}, 3233, 1750, 1485,1245. ^1H NMR (DMSO-d_6) δ 13.93 (1H, s, NH), 10.25 (1H,s, =CH), 7.82 (1H, d, Ar-H),7.50 (1H, t, Ar-H), 7.28 (1H, d,H7), 7.17 (1H, d, H4), 7.12-7.04 (3H, m, Ar-H, H5, H6), 6.96 (1H, t, Ar-H), 5.18 (2H, s, CH_2), 3.78 (3H, s, OCH_3)

3-[(4-{[(4-Fluorophenyl)methylidene]amino}-5-thioxo-1,2,4-triazol-3-yl)methyl]-2(3*H*)-benzoxazolone. (5h)
Yield, 41 %, m.p 227-228 ^oC. IR ν max/cm^{-1}, 3232, 1753, 1480, 1267. ^1H NMR (DMSO-d_6) δ 14.04 (1H, s, NH), 9.98 (1H, s, =CH), 7.95-7.91 (2H, m, Ar-H), 7.41-7.35 (3H, m, Ar-H, H7), 7.27 (1H, d, H4), 7.20 (1H, t, H6), 7.16 (1H, t, H5), 5.29 (2H, s, CH_2)

3-[(4-{[(4-Chlorophenyl)methylidene]amino}-5-thioxo-1,2,4-triazol-3-yl)methyl]-2(3*H*)-benzoxazolone. (5i)
Yield, 55 %, m.p 244-245 ^oC. IR ν max/cm^{-1}, 3298, 1744, 1484, 1241. ^1H NMR (DMSO-d_6) δ 14.06 (1H, s, NH), 10.06 (1H, s, =CH)), 7.88 (2H, d, Ar-H), 7.61 (2H, d, Ar-H), 7.36 (1H, d, H7), 7.27 (1H, d, H4), 7.20 (1H, t, H6), 7.17 (1H, t, H5), 5.30 (2H, s, CH_2)

3-[(4-{[(4-Bromophenyl)methylidene]amino}-5-thioxo-1,2,4-triazol-3-yl)methyl]-2(3*H*)-benzoxazolone. (5j)
Yield, 75 %, m.p 248-249 ^oC. IR ν max/cm^{-1}, 3258, 1759, 1462, 1265. ^1H NMR (DMSO-d_6) δ 14.06 (1H, s, NH), 10.06 (1H,s, =CH), 7.77 (4H, dd, Ar-H), 7.36 (1H, d, H7), 7.27 (1H, d, H4), 7.19 (1H, t, H6), 7.15 (1H, t, H5), 5.30 (2H, s, CH_2)

3-[(4-{[(4-Hydroxyphenyl)methylidene]amino}-5-thioxo-1,2,4-triazol-3-yl)methyl]-2(3*H*)-benzoxazolone. (5k)
Yield, 45 %, m.p 247 ^oC. IR ν max/cm^{-1}, 3236, 1747, 1484, 1283. ^1H NMR (DMSO-d_6) δ 14.07 (1H, s, NH), 10.41 (1H, s, OH), 9.64 (1H, s, =CH), 7.66 (2H, d, Ar-H), 7.35 (1H, d, H7), 7.26 (1H, d, H4), 7.19 (1H, t, H6), 7.14 (1H, t, H5), 6.89 (2H, d, Ar-H), 5.25 (2H, s, CH_2)

3-[(4-{[(4-Methylphenyl)methylidene]amino}-5-thioxo-1,2,4-triazol-3-yl)methyl]-2(3*H*)-benzoxazolone. (5l)
Yield, 62 %, m.p 231 ^oC. IR ν max/cm^{-1}, 3265, 1754, 1462, 1238. ^1H NMR (DMSO-d_6) δ 14.07 (1H,s, N), 9.92 (1H,s, =CH), 7.74 (2H, d, Ar-H), 7.37-7.33(3H, m, Ar-H, H7), 7.26 (1H, d, H4), 7.19 (1H, t, H6), 7.17 (1H, t, H5), 5.28 (2H,s, CH_2), 2.39 (3H,s, CH_3)

3-[(4-{[(4-Methoxyphenyl)methylidene]amino}-5-thioxo-1,2,4-triazol-3-yl)methyl]-2(3*H*)-benzoxazolone. (5m)
Yield, 50 %, m.p 219-220 ^oC. IR ν max/cm^{-1}, 3189, 1756, 1482, 1253. ^1H NMR (DMSO-d_6) δ 14.07 (1H,s, NH), 9.77 (1H, s, =CH), 7.79 (2H, d, Ar-H), 7.36 (1H, d, H7), 7.26 (1H, d, H4), 7.19 (1H, t, H6), 7.15 (1H, t, H5), 7.08 (2H, d, Ar-H), 5.27 (2H,s, CH_2), 3.86 (3H,s, OCH_3)

3-[(4-{[(4-Trifluoromethylphenyl)methylidene]amino}-5-thioxo-1,2,4-triazol-3-yl)methyl]-2(3*H*)-benzoxazolone. (5n)
Yield, 39 %, m.p 243 ^oC. IR ν max/cm^{-1}, 3276, 1742, 1462, 1239. ^1H NMR (DMSO-d_6) δ 14.07 (1H, s, NH), 10.19 (1H,s, =CH), 7.99 (2H, d, Ar-H), 7.81 (2H, d, Ar-H), 7.27 (1H, d, H7), 7.20 (1H,

d, H4), 7.11 (1H, t, H6), 7.07 (1H, t, H5), 5.23 (2H, s, CH_2)

3-[(4-{[(4-Trifluoromethylphenyl)methylidene] amino}-5-thioxo-1,2,4-triazol-3-yl)methyl]-2(3*H*)-benzoxazolone. (5o)

Yield, 74 %, m.p 226-227 ^oC. IR ν max/cm^{-1}, 3289, 1751, 1484, 1239. ^1H NMR (DMSO-d_6) δ 14.07 (1H, s, NH), 9.91 (1H, s, =CH), 7.78 (2H, d, Ar-H), 7.56 (2H, d, Ar-H), 7.36 (1H, d, H7), 7.26 (1H, d, H4), 7.20 (1H, t, H6), 7.17 (1H, t, H5), 5.27 (2H, s, CH_2), 1.32 (9H,s, CH_3)

Microbiological studies

Microdilution method: Standard strains of *P. aeruginosa* ATCC 27853, *E. coli* ATCC 25922, *E.coli* ATCC 35218, *S. aureus* ATCC 29213, *E. faecalis* ATCC 29212, clinical isolates of these microorganisms and *C. albicans* ATCC 10231, *C.krusei* ATCC 6258 were included in the study. Resistance in clinical isolates was determined by disc diffusion method according to the guidelines of clinical and laboratory standards institute (CLSI).[18] Standard powders of ampicillin trihydrate, gentamicin sulfate, amphotericin B and fluconazole were obtained from the manufacturers. Stock solutions were dissolved in pH 8 phosphate buffered saline (PBS) (ampicillin trihydrate) and distilled water (gentamicin sulfate and amphotericin B). All bacterial isolates were subcultured in Mueller Hinton Agar (MHA; Merck) plates and incubated overnight at 37°C. The solutions of the newly synthesized compounds and standard drugs were prepared and diluted at 2048, 1024, 512,… 0.0625 μg/mL concentrations in the wells of microplates within the liquid media. Bacterial susceptibility testing was performed according to the guidelines of CLSI M100-S18.[19] The bacterial suspensions used for inoculation were prepared at 10^5 CFU/mL by diluting fresh cultures at MacFarland 0.5 density (10^7 CFU/mL). Suspensions of the bacteria at 10^5 CFU/mL concentrations were inoculated to the two-fold diluted solution of the compounds. There were 10^4 CFU/mL bacteria in the wells after inoculations. Mueller Hinton Broth (MHB; Merck) was used for diluting the bacterial suspension and for two-fold dilution of the compound. Dimethylsulphoxide (DMSO), phosphate buffer saline (PBS), pure microorganisms and pure media were used as control wells. A 10 μL bacteria inoculum was added to each well of the microdilution trays. The trays were incubated at 37°C and minimum inhibitory concentration (MIC) endpoints were read after 24 h of incubation. All organisms were tested in triplicate in each run of the experiments. The lowest concentration of the compound that completely inhibits macroscopic growth was determined and MICs were reported. *Candida* were subcultured in sabouraud dextrose agar (SDA; Merck) plates and incubated at 35°C for 24-48 h. Susceptibility testing was performed in RPMI-1640 medium with L-glutamine (Sigma) buffered with 3-morpholinopropane-1-sulfonic acid (MOPS) (pH 7) (Sigma) and culture suspensions were prepared through the guideline of CLSI M27-A3.[20] Yeast suspensions were prepared according to McFarland 0.5 density and a working suspension was made by a 1:100 dilution followed by a 1:20 dilution of the stock suspension ($2.5x10^3$ CFU/ml). A 10 μL yeast inoculum was added to each well of the microdilution trays. The trays were incubated at 35°C and MIC endpoints were read after 48 h of incubation. All organisms were tested in triplicate in each run of the experiments. The lowest concentration of the compound that completely inhibits macroscopic growth was determined and MICs were reported.

Microplate alamar blue assay (MABA): *Mycobacterium tuberculosis* H37RV ATCC 27294 were subcultured on Middlebrook 7H11 agar (Becton Dickinson). Culture suspensions were prepared in 0.04 % (v/v) between 80-0.2 % bovine serum albumin (Sigma) at MacFarland 1 density. Suspensions were then diluted 1:25 in 7H9GC broth 4.7 g of Middlebrook 7H9 broth base (Difco), 20 mL of 10 % (vol/vol) glycerol, 1 g of Bacto Casitone (Difco), 880 mL of distilled water, 100 mL of oleic acid, albumin, dextrose and catalase (Sigma). Compounds were dissolved in dimethylsulphoxide (DMSO; Merck) at a final concentration of 4096 μg/mL and sterilized by filtration using 0.22 μm syringe filters (millipore) and used as the stock solutions. The stock solutions of the agents were diluted within liquid media. Stock solutions of EMB (Sigma) were prepared in deionized water. The solution of the newly synthesized compounds and standard drugs were prepared and diluted at 4096, 2048, 1024, 512,… 0.0625 μg/mL concentrations in the wells of microplates within the liquid media.

The plates were sealed with parafilm and were incubated at 37 °C for 5 days. Fifty microliters of a freshly prepared 1:1 mixture of 10X alamar blue (AbD Serotec) reagent and 10 % between 80 was added to the control well. The plates were incubated at 37°C for 24 h. Control well turned

pink and the reagent mixture was added to all wells in the microplate. The microplates were resealed with parafilm and were incubated for 24 h at 37°C and the colours of all wells were recorded. A blue colour in the well was recorded as no growth and a pink colour was scored as growth. The MIC was defined as the lowest drug concentration which prevented a colour change from blue to pink.[21]

Acknowledgements: This study was supported by Gazi University BAP. Project Number 02/2009-03.

REFERENCES

1. Z.A. Kaplancıklı, G. Turan-Zitouni, A.Ozdemir and G. Revial, *Eur. J. Med. Chem.*, **2008**, *43*, 155-159.
2. H. Bayrak, A. Demirbas, N. Demirbas and S.A. Karaoglu, *Eur. J. Med. Chem*., **2009**, *44*, 4362-4366.
3. G.V.S. Kumar, Y. Rajendraprasad, B.P. Mallikarjuna, S. M. Chandrashekar and C. Kistayya, *Eur. J. Med. Chem*., **2010**, *45*, 2063-2074.
4. M.F.E. Shehry, A.A. Abu-Hashem and E.M.E Telbani, *Eur. J. Med. Chem*., **2010**, *45*, 1906-1911.
5. S. P. Aytaç, B.Tozkoparan, F. B.Kaynak, G. Aktay, O. Goktas and S. Unuvar, *Eur. J. Med. Chem*., **2009**, *44*, 4528-4538.
6. P.Valentina, K. Ilango, M.Deepthi, P. Harusha, G. Pavani, K. L. Sindhura and C.H.G. Keerthanan, *J. Pharm. Sci. Res*., **2009**, *1*, 74-77.
7. G.Q. Hu, L.L.Hou, S.Q. Xie and W. L. Huang, *Chinese J. Chem*., **2008**, *26*, 1145-1149.
8. B. R. Abdel-Wahab, H. A. Abdel-Aziz and E. M. Ahmed, *Monatsh Chem*., **2009**, *140*, 601-605.
9. B. P. Mallikarjuna, B.S. Sastry, G.V.S.Kumar, Y. Rajendraprasad, S.M. Chandrashekar and K. Sathisha, *Eur. J. Med. Chem*., **2009**, *44*, 4739-4746.
10. S. Balram, M. S. Ranawat, R. Sharma, A. Bhandari and S. Sharma, *Eur. J. Med. Chem*., **2010**, *45*, 2938-2942.
11. M. Shiradkar, G.V. S.Kumar, V. Dasari, S. Tatikonda, K. C. Akula and R. Shah, *Eur. J. Med. Chem*., **2007**, *42*, 807-816.
12. A. K. Man and R. Shahidan, *J. Macromolecular Sci., Part A: Pure and Applied Chemistry*, **2007**, *44*, 651-657.
13. C. O. Kappe, *Angew. Chem. Int. Ed*., **2004**, *43*, 6250-6284.
14. S. Cankara, "Studies on the synthesis and cox inhibitory activities of some 6-(thiazole-4-yl)-2-oxo-3*H*-benzoxazole derivatives", MsD Thesis, Department of Pharmaceutical Chemistry, Faculty of Pharmacy, Gazi University, Ankara, Turkey, 2007.
15. G. Eren, S. Ünlü, M.T. Nuñez, L. Labeaga, F. Ledo, A. Entrena, E. Banoğlu, G. Costantino and M. F. Şahin, *Bioorg. Med. Chem*., **2010**, *18*, 6367-6376.
16. T. Onkol, Y. Dundar, B.Sırmagul, K. Erol and M.F. Sahin, *J. Fac. Pharm. Gazi*, **2002**, *19*, 15-24.
17. X. H. Sun, Y. Tao, Y. F. Lıu and B.Chen, *Chinese J. Chem*., **2007**, *25*, 1573-1576.
18. Clinical and Laboratory Standards Institute (CLSI) (formerly NCCLS), "Performance Standards for Antimicrobial Disk Susceptibility Tests Approved Standard, M2-A9", Clinical and Laboratory Standards Institute, 940 West Valley Road, Wayne, Pennsylvania, USA, 2006.
19. Clinical and Laboratory Standards Institute (CLSI) (formerly NCCLS), "Performance Standards for Antimicrobial Susceptibility Testing 18th Informational Supplement. CLSI M100-S18", Clinical and Laboratory Standards Institute, 940 West Valley Road, Wayne, Pennsylvania, USA, 2008.
20. Clinical and Laboratory Standards Institute (CLSI) (formerly NCCLS): "Reference method for broth dilution antifungal susceptibility testing yeast; approved standard, M27-A3", Clinical and Laboratory Standarts Institute, 940 West Valley Road, Wayne, Pennsylvania, USA, 2008.
21. S.G.F. Franzblau, R.S. Witzig, J.C. Mclaughlin, P. Torres P., G.Madico, A. Hernandez, M.T. Degnan, M. B. Cook, V.K. Quenzer, R. M. Ferguson and R. H. Gilman, *J. Clin. Microbiol*., **1998**, 362-366.

ACADEMIA ROMÂNĂ
Revue Roumaine de Chimie
http://web.icf.ro/rrch/

Rev. Roum. Chim.,
2012, *57*(3), 197-202

DESIGNING OF DRILLING FLUIDS USING NANO SCALE POLYMER ADDITIVES

Mihaela MANEA*

Petroleum – Gas University of Ploieşti, Wells Drilling, Extraction and Transport of Hydrocarbons Department, Petroleum and Gas Engineering Faculty, 39 Bucureşti Bdv., 1000519, Ploieşti, Roumania

Received July 15, 2011

Drilling fluids, dispersed systems that have to meet specific technological requirements in order to be used in the process of oil wells drilling have been recently intensly studied. The major aim of the research is to increase the technological efficiency of these systems, to make them environmentally friendly and economical. The paper presents the designing of novel drilling fluids together by applying nanotechnology to wells drilling technology. The author focused on low solid content water-based drilling fluids prepared with polymers. Two polymers were tested to adjust specific properties and their performance was studied comparatively for particles sizes in micro and nano scale. Treatments of alkalisation and density increase were performed on an initial system, evaluating the response to them by measurements on the entire set of standard properties.

INTRODUCTION

Wells drilling is a major part of petroleum industry worldwide and it requires a high level of knowledge and technology.[1] An extremely important role is given to the technology of drilling fluids, which are dispersed systems that must fulfill various functions with direct influence on the drilling operation performance.[2]

Therefore, in the past decades there has been an increased interest for new products in the area of drilling fluids and extensive researches and developments have been carried out to improve those systems. The main motivation is represented by the technological factor, for instance when drilling at high depths and/or horizontally; another one comes from the strict environmental regulations imposed on toxic and non biodegradable materials, especially in offshore drilling. [3]

This paper refers to water-based drilling fluids prepared with certain additives that help to adjust one or more properties; these additives are mainly polymers. This wide class of materials is well-known for its industrial applications in different fields.[4,5] They are mostly used because of their specific properties such as rheological behaviour,[6,7] ability to form hydrogels, capacity of interaction with other solid particles by bridging and encapsulation etc. [8]

The use of natural hydrophilic colloids[9] to the preparation of drilling fluids was introduced first by Chillingarian in 1950.[9] Among those there was a number of natural gums like: Shiraz, Ghatti and Tragacanth. Since then, polymer additives were introduced and studied to a great extend in oil industry; not only in the drilling technlogy, but also in reservoir engineering. [10,11]

The technological advantages of using water based polymer containing drilling fluids are good slurry suspension and transport properties, as the gel process occurs rapidly and the shear stress at low shear rates are high. These qualities also prevent slurry layer formation in the horizontal sections of the slanting hole. In addition, the hydration and dispersion inhibition of the clay that comes from the productive strata, is the result of encapsulating action of the macromolecular chains towards the clay colloids. It can also be mentioned

* Corresponding author: mihaela_manea2002@yahoo.com

the reduction of the friction at the drill pipe because of the slurry encapsulation mechanism and the deposition of a polymeric film on the well walls as well as on the metallic elements of the drill tool. The use of water based polymer containing drilling fluids help to diminish the charge on the solids control equipment at the surface as there is a low solid content.

In the most recent years, nanotechnology has taken a remarkable advance in many scientific fields;[12,13] the drilling fluids technology, a big profitable domain with a great potential, could not fall apart. Therefore, a particular effort is dedicated to the application of nano technology to the design of drilling fluids, considering the increased flexibility of those systems. Solid nano particles dispersed may offer unique properties to a drilling fluid or can simply influence its properties in certain ways. From a practical point of view, the presence of nano sized solid particles in a drilling fluid is worth to be studied, evaluated and, eventually, controlled. Introducing nano-sized additives in the drilling fluids technology is extremely new and therefore, promising.

EXPERIMENTAL

The preparation of water based drilling fluids involved gradual addition of materials under continuous stirring at 3000 rpm and letting them mix and interact with the system for minimum 30 minutes.

The materials used were: Xanthan gum, a polysaccharide acting as rheology controller, provided by C.P. Kelco; calcium carbonate, weighting agent of fine granulation (d_{10}<4 μm; d_{50}<25 μm; d_{90}<80 μm), commercially named Avacarb, from Ava Drilling Fluids & Services S.p.A.; sodium hydroxide, in aqueous solution 50%, added to adjust the pH, a product of Chimopar S.A. Roumania; a polymer synthesized used as a filtrate reducer additive.[14]

The set of standard properties measured for the prepared drilling fluids included: density, determined with the mud balance; the conventional viscosity using the Marsh funnel; the rheological parameters and gel resistance, calculated with data obtained from measurements at FANN 35A viscosimeter.[15] The rheology study was completed with measurements performed with a Brookfield PVS rheometer. In addition, the filtrate volume was measured with the Baroid filter press; for the filtrate pH the data was acquired using a Techne pHmeter, model 3505; finally, the filter cake thickness was determined with a penetrometer Dreamscience.

The nano particles were obtained by grinding with a Fritsch Pulverisette planetary mill having an agate bowl and 20 agate ball of 20 mm diameter; their particle size distribution was measured by the dynamic light scattering method (DLS) with a Red Badge Nano Sizer Coulter.

RESULTS AND DISCUSSION

The designing of a new water based drilling fluid started taking as a model the Flo-Pro system. [16] The initial mixture was composed by water, Xanthan gum and the fluid loss reducer synthesized by the authors. The additive properties of this polymer are due to its capacity of forming hydrogels by absorption of free water from the system. The material is also pH sensitive, its swelling capacity increases in alkali medium. [17]

The optimization of the initial system consisted, first, in a treatment with sodium hydroxide. It resulted in creating an alkali medium of dispersion which increased the efficiency of the viscosifier, the Xanthan gum. Next, a weighting operation with calcium carbonate was done, considering the relative low density that the initial system has.

Table 1 presents the properties of the initial system and of the systems obtained after performing treatments. These properties are density, ρ_n, Marsh funnel viscosity, $\mathbf{V_M}$, apparent viscosity, $\eta_{ap,}$ behavior index, *n,* consistency index, *k*, gel strength at 1 and 10 minutes, $\theta_{1'}$, $\theta_{10'}$, cummulative filtrate volume, Vf, the filtrate pH, and the cake thickness, *t*.

Table 1

Properties of the initial system and of the systems obtained after treatments

System	ρ_n, kg/m^3	V_M, s	η_{ap}, Ns/m^2	*n*	*k*	$\theta_{1'}$, N/m^2	$\theta_{10'}$, N/m^2	Vf, cm^3	pH filtrate	t, mm
A	1000	46	18	0.525	0.48	4.3	5.3	9.0	7.0	0.5
B	1000	49	20,5	0.451	0.92	5.7	6.7	7.3	11.0	0.5
C	1170	48	24	0.494	0.82	5.7	6.7	7.6	9.0	2.3
D	1370	51	33.5	0.483	1.23	5.7	6.7	7.8	8.5	2.8

A – water, Xanthan gum 2.5%wt, fluid loss reducer 3%wt

B – water, Xanthan gum 2.5%wt, fluid loss reducer 3%wt, NaOH

C – water, Xanthan gum 2.5%wt, fluid loss reducer 3%wt, NaOH, calcium carbonate 2.5%wt

D – water, Xanthan gum 2.5%wt, fluid loss reducer 3%wt, NaOH, calcium carbonate 4.5%wt

It can be observed that the pH is 11 after adding sodium hydroxide and has a continuous decrease when adding calcium carbonate. This fact is explained by formation of calcium hydroxide, consuming the OH^- ions existing in the medium after sodium hydroxide dissociation. This treatment has a major impact on the cumulative volume of filtrate by decreasing it, an important improvement to the drilling fluid. Even at lower values of pH, the fluid loss reducer polymer maintains good performances by retaining free water from the system.

When adding the weightning agent, together with adjusting the density, the flow parameters are slightly increased due to the contribution of extra solid particles to viscosity. This effect is explained by the interactions between these chemicaly inert particles through static forces, as well as by their interaction with the continuous medium through friction forces. In addition, the presence of calcium carbonate particles may induce a screening effect for the long macromolecular chains and it causes a slight decrease of the behaviour index, *k*, at the first addition.

As far as the caking phenomena is concerned, the solids laden fluid deposits a thicker filter cake once the calcium carbonate is added. Still, the cake is an elastic and impermeable polymeric film upon which the solid particles settle.

The same set of measurements was performed on a drilling fluid prepared in the same manner, only the polymers were ground to a nano metric scale. After grinding, their particle size was determined, as shown in Fig. 1.

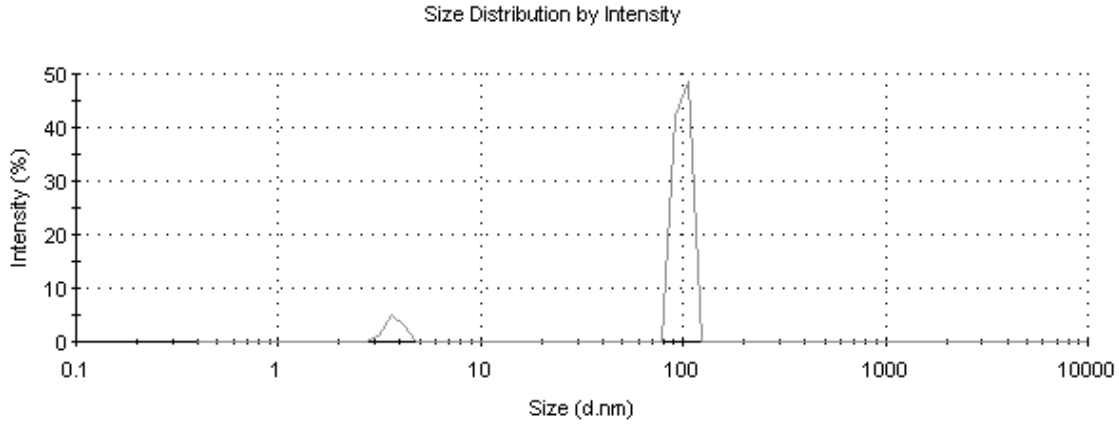

a. Xanthan gum

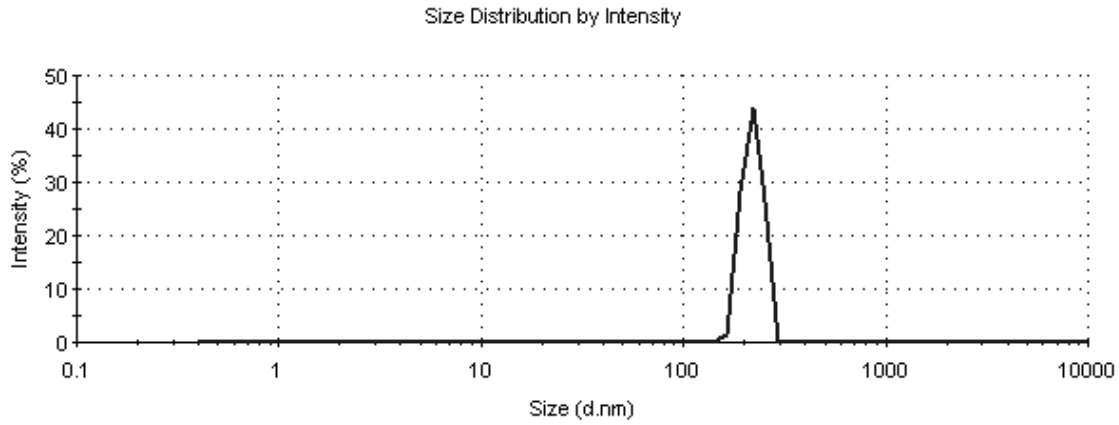

b. Filtrate loss reducer

Fig. 1 – The particle size distribution at nanometric scale.

It can be seen that the Xanthan gum has an average size diameter of around 100nm, while the fluid loss reducer was brought to about 200nm. Both particle size curves show an unimodal distribution. Furthermore, when referring to the nano scale additive, it means these particle size additives.

The values of the measured properties, the same as presented in Table 1, are given in Table 2.

Table 2

Properties of the drilling fluids prepared with nano scale sized additives

System	ρ_n, kg/m^3	V_M, s	η_{ap}, Ns/m^2	*n*	*k*	$\theta_{1'}$, N/m^2	$\theta_{10'}$, N/m^2	Vf, cm^3	pH filtrate	t, mm
E	1000	38	14	0.479	0.32	3.2	4.1	6.4	7.0	0.5
F	1000	41	18.5	0.389	0.75	4.3	5.0	3.8	11.5	0.5

E – water, nano Xanthan gum 2.5%wt, nano fluid loss reducer 3%wt
F – water, nano Xanthan gum 2.5%wt, nano fluid loss reducer 3%wt, NaOH

Comparing to the data in Table 1, it is noticeable that the flow parameters are slightly lower for the case of drilling fluids with nano additives, including the gel strength at one and ten minutes rest. Considering that these systems are to be further weightened by adding solid particles, the previous set of measurements showed that the flow characteristics are to be increased. Nevertheless, the influence of pH is obvious in the sense of enhancing the efficiency of the Xanthan gum, the viscosity controling agent. This aspect is revealed both through the rheological parameters, as well as through the gel resistance.

As far as the fluid loss reducer agent is concerned, it gains better properties of keeping the cumulative volume of filtrate at low values. It is due to the fact that when the polymer is brought to smaller particle sizes, namely to nano metric scale, the total specific area is considerably increased; thus, the interaction area with the continuous medium is a lot bigger and, so, the swelling capacity of this polymer is more significant. At basic pH, it can be seen that the performance of the fluid loss reducer is clearly intensified, in a synergetic effort with the viscosity controling agent.

The rheological behaviors of the drilling fluids prepared in this study are presented in Fig. 1. The rheological model considered for the aqueous, free clay and polymer containing systems is the Ostwald de Waele one.[18]

A first glance observation of the profiles in Figs. 2 and 3 confirms the choosing of the Ostwald de Waele model. Looking at the graphs in Fig. 2, it is obvious the synergic effect of pH and of $CaCO_3$ presence to increase the flow resistance of the system. Meanwhile, as seen from Fig. 3, the flow curves for nanometric scale additives show a similar profile, but at lower absolute values.

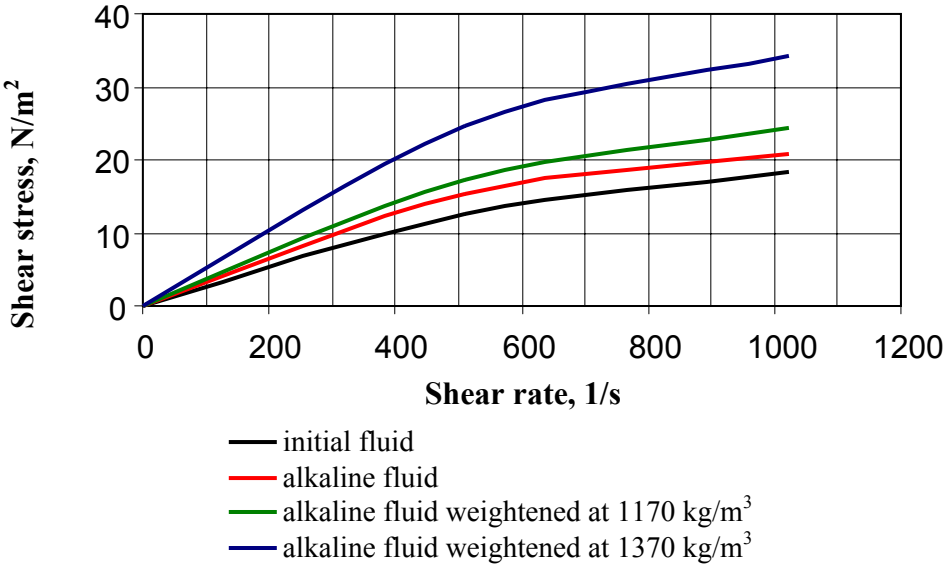

Fig. 2 – Flow curves of the drilling fluids designed with standard sized additives.

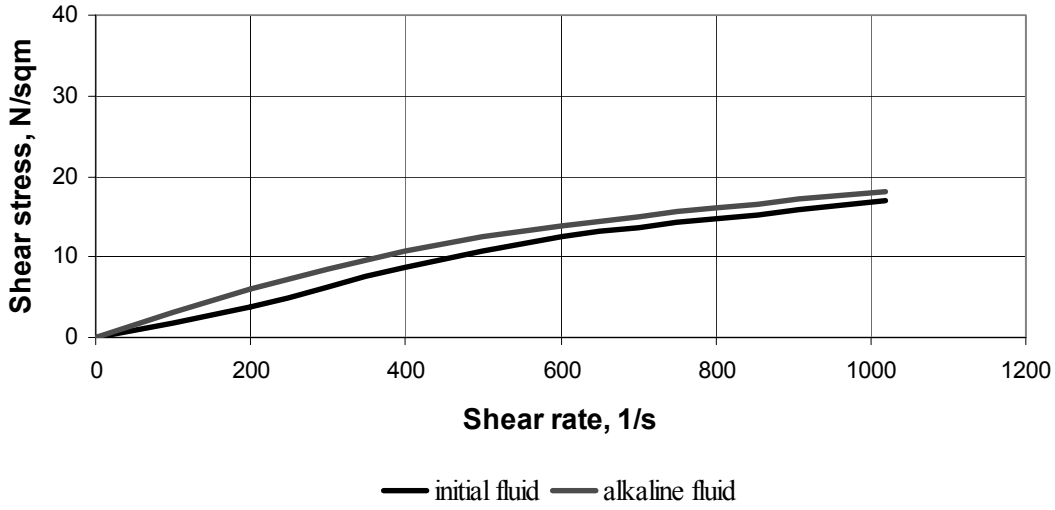

Fig. 3 – Flow curves of the drilling fluids designed with nano metric scale additives.

CONCLUSIONS

This paper is presenting a new approach to the study of drilling fluids by analyzing the influence of additives granulometry to all standard properties. Furthermore, the comparison of drilling fluid performances depending on the particle sizes of the additives used goes to the level of nano scale. It is a breaking through subject in the field of drilling technology.

In addition, the study refers to a new polymer material that is meant to be introduced as fluid loss reducer. Its efficiency and response to different treatments is tested here at laboratory stage.

The experimental results lead to several conclusions. First, the polymer synthesized by the authors provides good fluid loss reduction, both in neutral medium and, especially, in alkali medium. In addition, the fluid loss reducer is more efficient if ground to nanometric sizes.

In an alkali medium, after adding sodium hydroxide, the efficiency of the Xanthan gum, as a viscosifier, is better; the weighing treatment with calcium carbonate has a flocculating effect, seen by the increase of the filtrate volume and higher rheological parameters.

The materials used to formulate the drilling fluids in this study act in synergy to create dispersion with good structure properties, though at nano metric scale, the additives are not more efficient; the gel strength increases when adding a small amount of calcium carbonate, then remains constant when increasing the amount of it.

The drilling fluids designed in this study are viable and robust systems, compatible to other systems, already existing on the market.

Acknowledgments: Authors recognize financial support from the European Social Fund through POSDRU/89/1.5/S/54785 project: "Postdoctoral Program for Advanced Research in the field of nanomaterials".

REFERENCES

1. J. Bergenholtz, J. F. Brady and M. Vicic*, J. Fluid Mech.,* **2002**, *456*, 239.
2. R.P. Chhabra and J.F. Richardson, "Non-Newtonian Flow and Applied Rheology", Second Edition: Engineering Applications, Butterworth-Heinemann/IChemE, 2008.
3. ASME Shale Shaker Committee, "Drilling Fluids Processing Handbook", Elsevier, 2005.
4. K.W. Lem, J.R. Haw, D.S. Lee, C. Brumlik, S. Sund, S. Curran, P. Smith, S. Brauer and D. Schmidt, *Nanotech.*, **2010**, *1*, 889.
5. M. Manea, *Rev. Chim. (Bucharest)*, **2009**, *60,* 1231.
6. G.V. Chilingarian and P. Vorabutr, *Dev. Petr. Sci.,* **1981**, *11*, 17.
7. A. Y. Dandekar, "Petroleum Reservoir Rock and Fluid Properties", CRC Press, 2006.
8. W.B. Russel, D.A Saville and W.R. Schowalter, "Colloidal Dispersions", Cambridge University Press, 1999.
9. Y. J. Azar and G. R Samuel., "Drilling Engineering", PennWell Co., SUA, 2007.
10. C.J. Tucker, *Nanotech*, **2010**, *1*, 846.
11. M.G. Popescu and M. Manea, "Fluide de foraj şi cimenturi de sondă. Îndrumar de laborator", UPG Ploieşti, 2008.
12. M.G. Popescu, "Fluide de foraj şi cimenturi de sondă", UPG Ploieşti, 2002.
13. C.S. Satish, K.P. Satish and H.G. Shivakumar, *Indian J. of Pharm. Sci.*, **2006**, *68*, 133.

14. M. Manea, C.G. Dussap, J. Troquet and L. Avram, *Le 4ème Coll. Fr.-Rou. de Chim. Appl. (Clermont-Ferrand)*, **2006**, 171.
15. D. Urban and K. Takamura, "Polymer Dispersions and Their Industrial Applications", Wiley-VCH, 2002.
16. P.A. Williams, "Handbook of Industrial Water Soluble Polymers", Wiley-Blackwell, 2007.
17. R.K. Gupta, "Polymer and Composite Rheology", Marcel Dekker, 2000.
18. G. Allan Stahl, D.N. Schulz, "Water-soluble Polymers for Petroleum Recovery", Springer, 1988.

ACADEMIA ROMÂNĂ
Revue Roumaine de Chimie
http://web.icf.ro/rrch/

Rev. Roum. Chim.,
2012, *57*(3), 203-208

MONITORIZING METHYLENE BLUE INCLUSION IN REVERSE MICELLAR NANOSTRUCTURES

Monica Elisabeta MAXIM, Gabriela STÎNGĂ,* Alina IOVESCU, Adriana BĂRAN, Cornelia ILIE and Dan F. ANGHEL

Department of Colloids, Institute of Physical Chemistry "Ilie Murgulescu", Roumanian Academy, 202 Spl. Independentei, 060021 Bucharest, Roumania, Tel/Fax: ++40213121147

Received October 12, 2011

Methylene blue (MB) inclusion in nanostructured systems formed by sodium bis(2-ethylhexyl) sulfosuccinate (AOT) reverse micelles, water and organic solvents (*i.e.*, *iso*-octane, *n*-hexane) is investigated by UV-Vis, static fluorescence and dynamic light scattering. The spectroscopic signals of methylene blue are blue shifted in reverse micelles compared to those in water. The probe senses a more nonpolar microenvironment in reverse micelles formed in *n*-hexane compared to that in *iso*-octane. The results are discussed in terms of optimization the methylene blue solubilization in nanoconfined media.

INTRODUCTION

Reverse micelles are aggregates formed by surfactants in nonpolar solvents in presence of very small amounts of water. In such structures, the hydrophilic head groups of the surfactants are oriented towards water, the hydrocarbon tails are embedded into the nonpolar solvent, and the systems are isotropic and thermodynamically stable.[1,2] The micellar core is characterized by the hydration degree, w_0, which is the water to surfactant molar ratio. The nanoscopic water drops are a model of those in the live systems and this explains the popularity of reverse micelles as model of biomembrane/water interface. The inner core of reverse micelles, the "water pool", is able to solubilize hydrophilic biomolecules and reverse micelles are unique medium for enzymatic catalysis,[3-6] protein extraction,[7-9] and protein refolding.[10-12]

Dye molecules are often employed to probe the structure of live systems. MB is exploited to sentinel lymph node mapping,[13] to treat oncological, cardiovascular and ophthalmic diseases,[14] or to delay the onset of Parkinson's and Alzheimer's syndromes.[15-17] Inspired by the medical applications of methylene blue, our attention was directed towards the use of MB in the spectroscopic investigation of confined water in reverse micelles. The spectroscopic data were correlated with those obtained from dynamic light scattering measurements. This work aims to shed more light on the oil/water interface following the location of MB in the reverse micelles obtained with sodium bis(2-ethylhexyl) sulfosuccinate (AOT) in different solvents, and at various hydration degrees.

EXPERIMENTAL

Reagent grade *iso*-octane, *n*-hexane, AOT from Aldrich, and methylene blue from Fluka were used as received. The molecular structures of the MB and AOT are shown in Fig. 1.

The water was Milli-Q, and the reverse micellar solutions are prepared by the injection method.[18] The concentrations of surfactant and dye in reverse micelles are of 0.1 M and 1.3 x 10^{-5} M, respectively.

Optical absorption spectra are recorded on a Varian Cary 100 Bio spectrophotometer. Fluorescence measurements are

* Corresponding author: gstinga@gmail.com

carried out on an Edinburgh Instruments FLS 900 spectrofluorimeter with excitation set at 514 nm. Dynamic light scattering data are collected on a ZetaSizer, Nano ZS, Malvern Instruments. The analysis was performed at a laser wavelength of 633 nm and an angle of 173°.

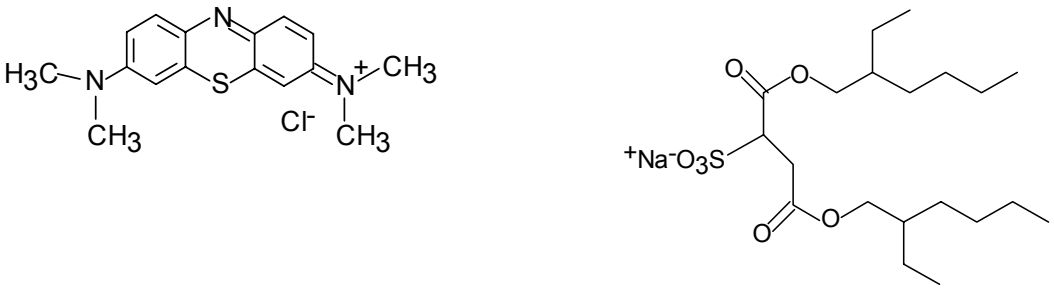

Fig. 1 – The molecular structures of methylene blue and sodium bis(2-ethylhexyl) sulfosuccinate.

RESULTS AND DISCUSSION

Fig. 2 presents our dynamic light scattering data in terms of the hydrodynamic diameter of reverse AOT micelles in *iso*-octane and *n*-hexane. They show a linear dependence of the hydrodynamic diameter on w_0. The results are in agreement with the data obtained by Sechler *et al.*[19] who state for AOT reverse micelle in *iso*-octane a linear increase in water droplet size with the hydration degree. In the present study we use an organic solvent with a linear alkyl chain, *n*-hexane, that shows a similar size/hydration degree linear behavior and a marked decrease of nanodroplet size as compared to that in micellar systems formed with branched alkyl chain hydrocarbons like *iso*-octane. The progressive raising of water concentration in the AOT/organic solvent system allows the formation of reverse micelles whose dimensions depend on the water to surfactant molar ratio.

Fig. 3A shows the absorption behavior of MB in bulk water and AOT/water/*iso*-octane reverse micelle at different hydration degrees. The spectra reveal the presence of two species of MB (monomer and dimer) that have been previously identified in water.[20] In aqueous solution, the MB monomer has the absorption peak at 664 nm and the MB dimer appears as a shoulder around 600 nm. The absorption spectra in reverse micelles resemble those in water. Moreover, our results show the increase of absorbance of the MB monomer with the hydration degree and the blue-shift of the absorption peak by 6 nm as compared to water.

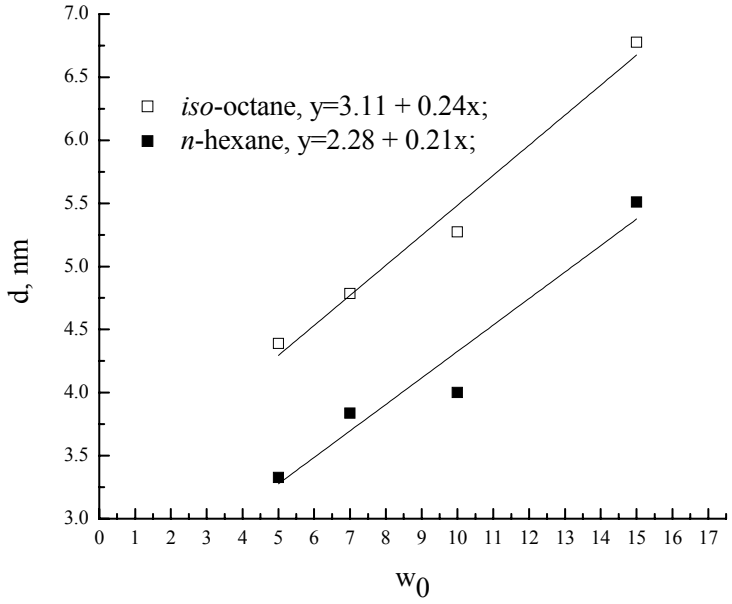

Fig. 2 – The hydrodynamic diameters of AOT reverse micelles *vs*. the hydration degree. The solid lines are the least-squares fits, and the squared correlation coefficients from bottom to top are r^2=0.9173 and r^2=0.9708.

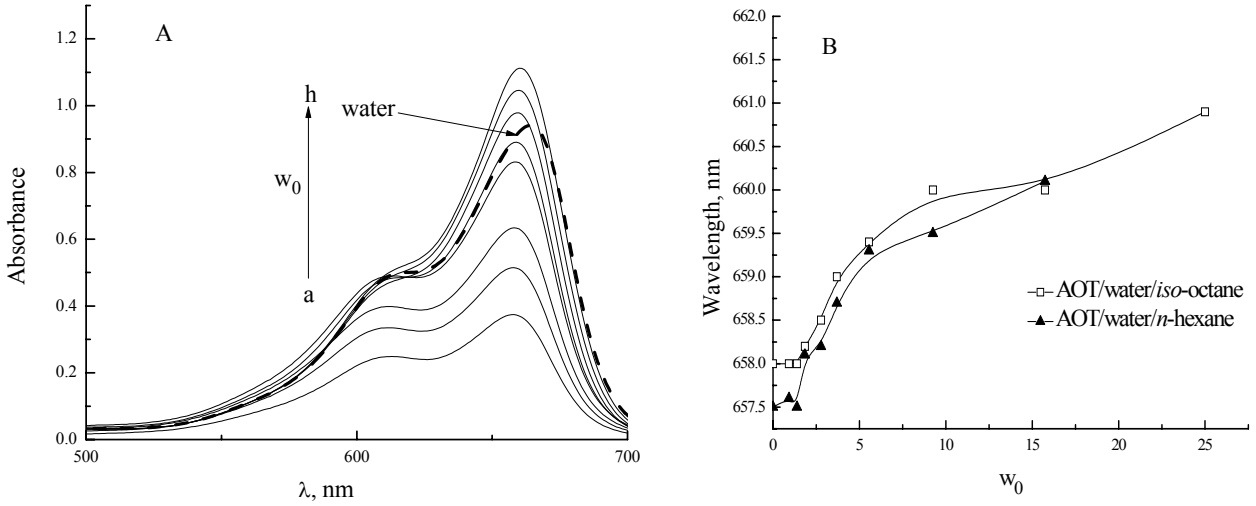

Fig. 3 – Absorption spectra of 1.3 x 10^{-5} M methylene blue in bulk water (dashed line) and at different hydration degrees (w_0) of reverse micelles (solid line; From a→h, w_0=0; 0.93; 1.4; 1.85; 3.7; 5.56; 9.3; 15.74) (A). The variation of MB absorption maximum wavelength in different AOT/water/organic solvent systems, *vs*. hydration degrees (B).

The variation of MB monomer absorption maximum in the AOT reverse micelles obtained with two solvents, *iso*-octane and *n*-hexane, at different hydration degrees appears in Fig. 3B. The shape of curves is similar in both solvents. At low hydration degrees up to w_0 = 1.4, the absorption maximum doesn't change. By raising the hydration degree a steep red shifting is recorded, followed by a slight increase of the absorption maximum wavelength. The results are along with those previously reported in the reverse micellar system of Triton X-100, *n*-hexanol and cyclohexane investigated using methyl orange.[21] Other results pointing out a blue shift of the maximum absorption of MB as compared to water were interpreted by a smaller polarity sensed by the probe.[5,22] Our data show that the micelles prepared in *n*-hexane have the smallest polarity. This organic solvent has a short linear alkyl chain able to accommodate easier into the surfactant hydrophobic tail than the more bulky *iso*-octane diminishing the water amount from the micellar host. Yuan *et al*., studied the structure of water in AOT/water/*iso*-octane system by dissipative particle dynamics simulation method and the data reveal the presence of several types of water.[23] There is water located in the hydrophobic palisade of the micelle (captured water), at the periphery of micelles around the polar beads of surfactant molecules (bound water) and in the micellar core (free water). For low hydration degrees, one may consider that, in the interfacial region of our systems, there are those water molecules captured and not bonded to the surfactant polar groups. This assumption relies on the disordered structure of the micelles at molecular level that allows to some water molecules to stay around the hydrocarbon tails of AOT in micelles producing water of very low density. These water molecules behave like monomers or dimers and are capable to penetrate the interfacial layer.[24] In such regions, even if the density of water is very low and compactness of micelle is high, the probe is captured and solubilized. For w_0 in between 1.4 and 9.3, the ionic layer of AOT/water/*iso*-octane reverse micelle contains water molecules bound to the sodium ions of the sulfonate groups. Due to its cationic character, MB tends to be linked to negatively charged groups of the surfactant. By increasing the hydration degree, the interactions between the water and counterions enhance to the detriment of those between the cationic MB and negatively charged polar groups, leading to a further weakening of the electrostatic interaction between SO_3^- and Na^+. The plateau begining at w_0=9.3 can be safely ascribed to the free water from the micellar core by analogy with previous data by Hou *et al.*[25] In the Triton X-100/1-butanol/*n*-octane/water systems they observed bulklike water at w_0=5.3 a much lower value than in our systems.

In the next approach we did aging test of the reverse micelles. Fig. 4 shows the change of absorbance maximum of the dye monomer *vs*. the

hydration degree at a time span from two hours to three weeks. The recorded absorbancies did not change denoting stable systems in time. The results show a good relationship between the MB inclusion in reverse micelles and the stability in time of micellar matrix structure. At the same time, the obtained data reveal that at $w_0<3.7$ there is a hyperchromic shift of the absorption peak of MB with increasing of w_0 denoting a further inclusion of dye in the micellar host. For $w_0>3.7$, the absorption remain constant suggesting the saturation of micellar host with dye. At this hydration degree, the absorbance peak of MB monomer is a maximum (Fig. 3A), being higher than the dye's signal in *n*-hexane and bulk water. This demonstrates that in the water-pool of micelles the methylene blue reaches a higher local concentration than in bulk water. Such a phenomenon is similar to that observed in micellar catalysis, when the rate constant increases because the reactants are concentrated inside the micelles.[26,27]

The effect of water content of the reverse micelles upon the MB solubilization was investigated by static fluorescence. Fig. 5 shows the variation of emission maxima of the MB monomer solubilized in reverse micelles formed in *iso*-octane and *n*-hexane as a function of w_0. The curves have an ascending part, eventually followed by a plateau and a descending zone. The fluorescence data have a similar trend to those of UV-VIS, and show a raise of emission to $w_0=3.7$ (in the system with *iso*-octane). This means that the probe is gradually solubilized within the water pool of micelles. Above a hydration degree of 3.7, the emission is constant but gradually decreases when $w_0=9.3$. Fig. 5 also shows that MB is less concentrated into the micellar nanocage, since its emission signal diminishes ($w_0>9.3$). Comparing the shift in the MB emission in AOT/water/*n*-hexane with that in AOT/water/*iso*-octane it is observed that the probe presents a weaker fluorescence signal for the same value of w_0. This indicates that the probe senses the difference in size of the water droplet in the systems prepared with *n*-hexane and *iso*-octane.

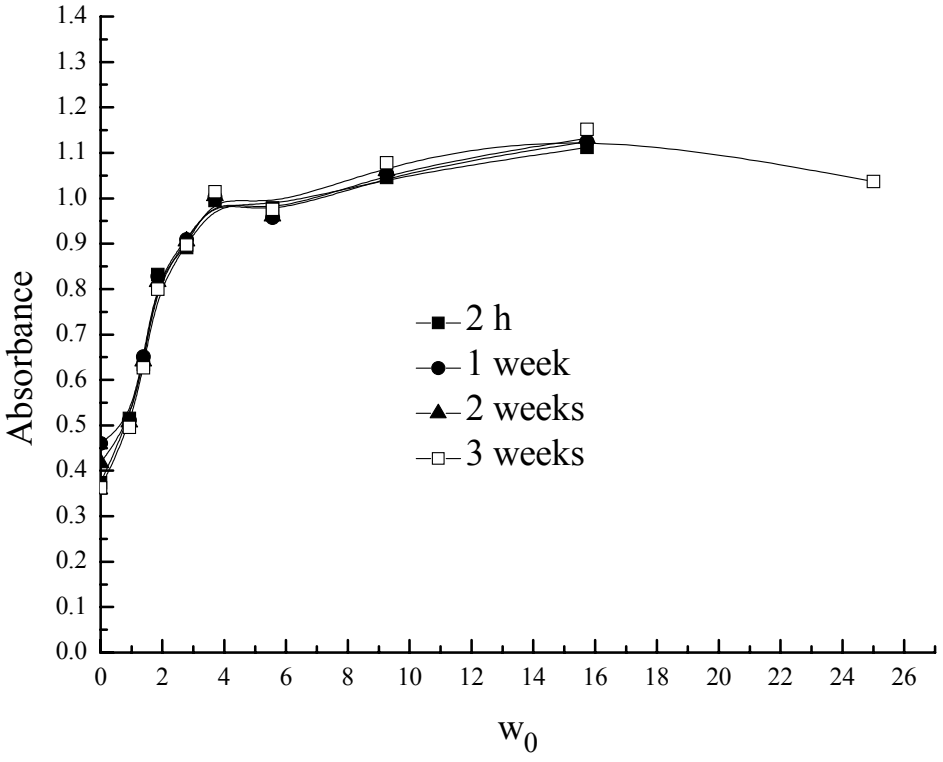

Fig. 4 – Maximum of absorbance values
at different times *vs*. hydration degrees of AOT/water/*iso*-octane micelles.

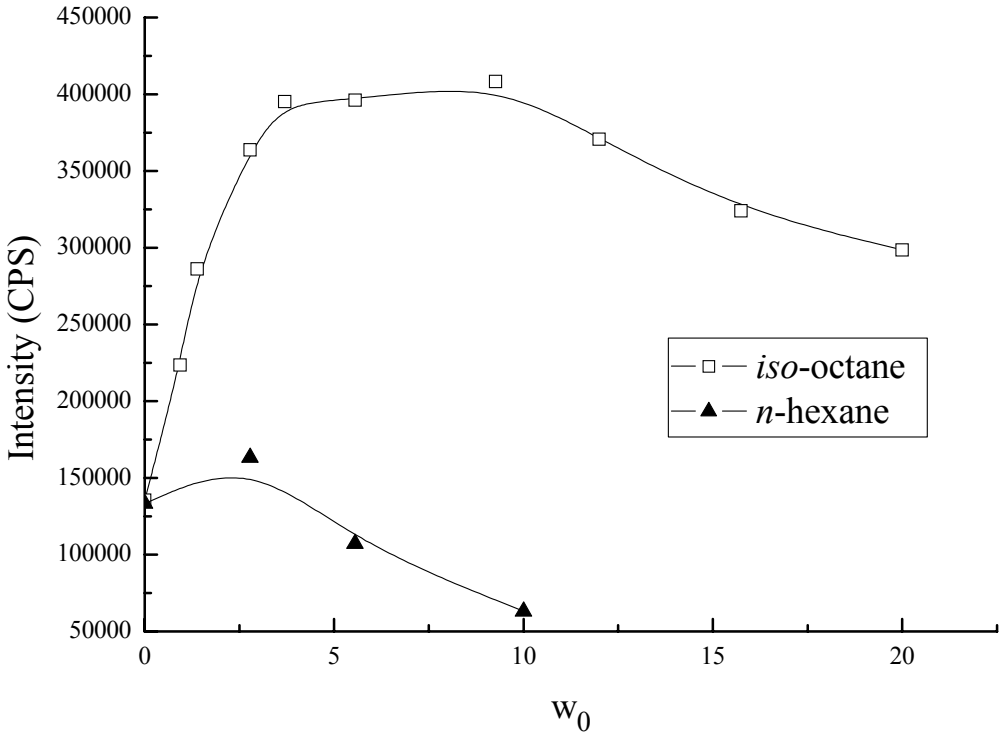

Fig. 5 – The variation of MB emission maxima in AOT reverse micelles at different w_0.

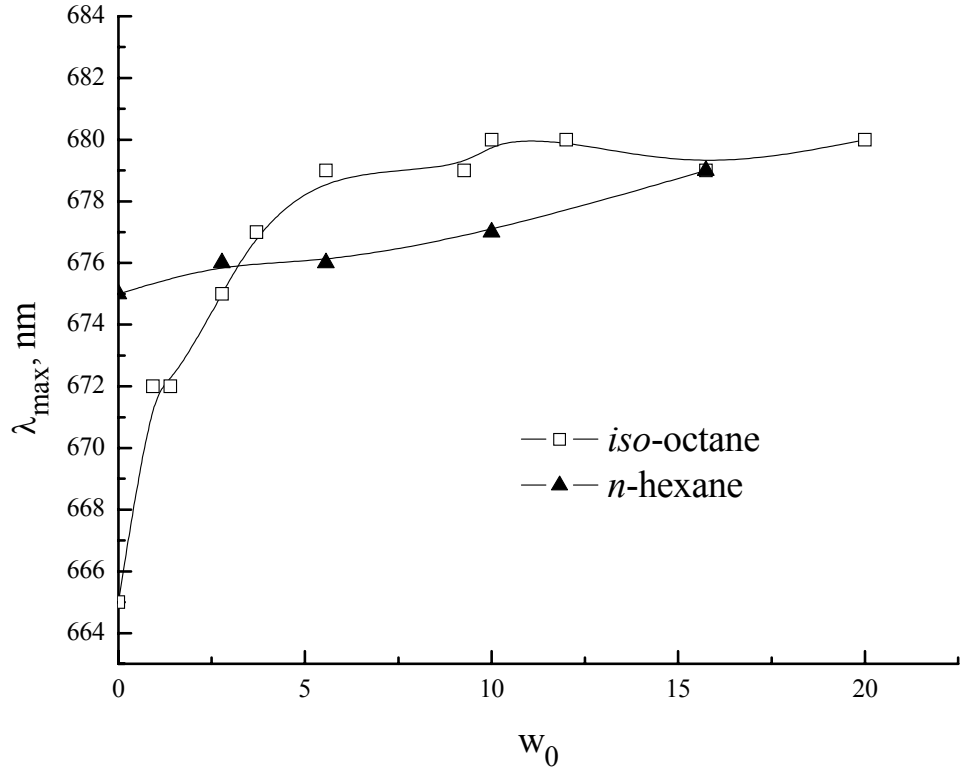

Fig. 6 – The variation of MB emission maximum wavelength (λ_{max}) as a function of hydration degree in reverse micellar systems.

Fig. 6 illustrates the change of the maximum wavelength (λ_{max}) of emission in reverse micelles prepared with *iso*-octane or *n*-hexane. A blue shift of the fluorescence maximum compared to that in water ($\lambda_{max,water}$=686 nm) was observed. By analogy with the electronic spectra discussed above, a blue shift denotes that the microenvironment is less polar than bulk water.

The shift induced by the organic solvent is of 21 nm for *iso*-octane and of 11 nm for *n*-hexane. At the same time, one may observe that λ_{max} of MB in *iso*-octane displays a progressive red shift of 12 nm (from 665 to 677 nm) with the increase of w_0. This change became smaller and reaches a plateau when the hydration degree is higher than 3.7, meaning that MB is completely dissolved into the water pool of reverse micelles. The phenomenon can be explained admitting that MB senses, at low w_0, the interfacial region of reverse micelle. As w_0 increases, the probe moves towards the bulk water. A different situation appeared in case of AOT/water/*n*-hexane when a small increase of λ_{max} with w_0 is recorded. A weak dependence of λ_{max} on w_0 for this system indicates that the probe is located in a region of the reverse micelles that is hardly penetrated by water.

The fluorescence measurements confirm that linear hydrocarbons penetrate better the surfactant layer, raising the spontaneous curvature of the reverse micelle and decreasing the amount of incorporated water. As a consequence, in the reverse micelles formed in *n*-hexane, the quantity of solubilized MB decreases as proved by our absorbance and fluorescence data.

CONCLUSIONS

Spectroscopic absorption and fluorescence properties of methylene blue are different in the water pool of the AOT reverse micelles as compared to those in bulk water. MB experiences a less polar microenvironment in the reverse micelles formed in *n*-hexane than in *iso*-octane and the bulk water. The dye has a higher local concentration in the micellar host than in bulk water. This depends on the hydration degree and the organic solvent.

Acknowledgements: This paper is a part of the research program "Colloids and dispersed systems" of the "Ilie Murgulescu" Institute of Physical Chemistry, financed by the Roumanian Academy. The authors gratefully acknowledge the support of the EU (ERDF) and Roumanian Government allowing for acquisition of research infrastructure under POSCCE O 2.2.1 project INFRANANOCHEM – Nr. 19/01.03.2009.

REFERENCES

1. M. J. Rosen, "Surfactants and Interfacial Phenomen", 3rd edition, John Wiley & Sons, New York, 2004, p. 157.
2. D. B. Dadyburjor, T. E. Fout and J. W. Zondlo, *Cat. Today*, **2000**, *63*, 33-41.
3. M. Goto, C. J. Medeiros and T. A. Hatton, *Biotech. Bioeng.*, **1997**, *11*, 141-143.
4. R. D. Falcone, M. A. Biasutti, N. M. Correa, J. J. Silber, E. Lissi and E. Abuin, *Langmuir*, **2004**, *20*, 5732-5737.
5. R. O. Anarbaev, A. L. Rogozina and O. I. Lavrik, *Biophys. Chem.*, **2009**, *141*, 11-20.
6. E. V. Kudryashova, V. L. Bronza, A. A. Vinogradov, A. Kamyshny, S. Magdassi and A. V. Levashov, *J. Colloid Interface Sci.*, **2011**, *353*, 490-497.
7. S. S. Lee, B. K. Lee, J. S. Choi and J. P. Lee, *Bull. Corean Chem. Soc,* **2001**, *22*, 897-902.
8. A. Sivasamy, P. I. Rasoanto, B. V. Ramabrahmam and G. Swaminathan, *J. Sol. Chem.*, **2005**, *34*, 33-42.
9. S. H. Mohad-Setapar, R. J. Wakeman and E. S. Tarleton, *Chem. Eng. Res. Design*, **2009**, *87*, 833-842.
10. V. N Dorovska-Taran, C. Veeger and A. J. W. G. Visser, *Eur. J. Biochem.,* **1993**, *218*, 1013-1019.
11. E. Abuin, E. Lissi, M. A. Biasutti and R. Duarte, *Protein J.*, **2007**, *26*, 475-479.
12. F. Farivar, A. A. Moosavi-Movahedi, Y. Sefidbakht, K. Nazari, J. Hong and N. Sheibani, *Biochem. Eng. J.*, **2010**, *49*, 89-94.
13. M. Chu, Y. Wan, *J. Biosci. Bioeng.*, **2009**, *107*, 455-459.
14. H. J. Hah, G. Kim, Y. E. Koo Lee, D. A. Orringer, O. Sagher, M. A. Philbert and R. Kopelman, *Macromol. Biosci.*, **2011**, *11*, 90-99.
15. G. Anderson, A. R. Noorian, G. Taylor, M. Anitha, D. Bernhard, S. Srinivasan and J. G. Greene, *Exp. Neurol.,* **2007**, *207*, 4-12.
16. M. Oz, D. A. Lorke and G. A. Petroianu, *Biochem. Pharmacol.*, **2009**, *78*, 927-932.
17. R. H. Schirmer, H. Adler, M. Pickhardt and E. Mandelkow, *Neurobiol. Aging*, **2011**, doi:10.1016/j.neurobiolaging.2010.12.012.
18. P. L. Luisi, M. Giomini, M. P. Pileni and B. H. Robinson, *Biochim. Biophys. Acta*, **1988**, *947*, 209-246.
19. T. D. Sechler, E. M. DelSole and J. C. Deak, *J. Colloid Interface Sci.*, **2010**, *346*, 391-397.
20. P. Mukerjee and A. K. Gosh, *J. Am. Chem. Soc.*, **1970**, *92*, 6419-6424.
21. L. Qi and J. Ma, *J. Colloid Interface Sci.*, **1998**, *197*, 36-42.
22. S. K. Mehta, K. Kaur, K. K. Bhawna and K. K. Bhasin, *Colloid Surf. A*, **2009**, *339*, 217-223.
23. S. L. Yuan, G. W. Zhou, G. Y. Xu and G. Z. Li, *J. Dispers. Sci. Tech.*, **2004**, *25*, 733-739.
24. P. Calandra, G. Di Marco, A. Ruggirelo and V. T. Liveri, *J. Colloid Interface Sci.*, **2009**, *336*, 176-182.
25. Z. Hou, Z. Li and H. Wang, *Colloid. Polym. Sci.*, **2001**, *279*, 8-13.
26. J. H. Fendler, E. J. Fendler "Catalysis in Micellar and Macromolecular Systems", Academic Press, New York, 1975, p. 98-100.
27. G. Stîngă, D. M. Mihai, A. Iovescu, A. Băran and D. F. Anghel, *Rev. Roum. Chim.*, **2005**, *50*, 767-775.

ACADEMIA ROMÂNĂ
Revue Roumaine de Chimie
http://web.icf.ro/rrch/

Rev. Roum. Chim.,
2012, *57*(3), 209-213

MICROWAVE-ASSISTED α-PINENE ACIDIC CATALYTIC ISOMERISATION

József Zsolt SZÜCS-BALÁZS,[a] Maria COROŞ,[a] Diana MOLNAR[a] and Mircea VLASSA[b*]

[a] "Raluca-Ripan" Institute of Chemistry Research, Babeş-Bolyai University, 30 Fântânele, 400294, Cluj-Napoca, Roumania
[b] Faculty of Chemistry and Chemical Engineering, Babeş-Bolyai University, 11 Arany János, 400028, Cluj-Napoca, Roumania

Received October 14, 2011

A comparative study of microwave assisted α-pinene acidic catalytic isomerisation reactions with near-critical water procedure under microwave irradiation is presented. This study can be performed because in both cases the mechanism is similar, namely an acidic-catalyzed rearrangement. The non-critical method technique is milder using a lower temperature and pressure and a shorter reaction time than near-critical water conditions. The general aspect of the selectivity of the reaction products is changed, being higher for α-terpinolene and γ-terpinolene and lower for limonene and camphene compared to the non-critical conditions.

INTRODUCTION

Because of its use as a fragrance intermediate and for technical applications, α-pinene **(1)** is a key compound among industrially used terpenes.[1] From the reaction of α-pinene with acetic acid two series of products can be obtained (see Scheme 1): esters - bornyl- **(16)**, fenchyl- **(12)** and α-terpinyl-acetate **(9)** and compounds with the p-menthadiene structure, resulted by isomerisation reactions such as camphene **(11)**, limonene **(7)**, terpinolene **(8)**, α-terpinene, γ-terpinene, *p*-cymene and α-phellandrene.

The esters usually are prepared in two steps (first step, the treatment of α-pinene with liquid mineral acid and second step, the esterification with acetic anhydride in the presence of liquid mineral acids),[2,3] but this method shows the disadvantage of too large amount of catalysts, corrosion of equipments, complicated technique and serious environmental pollution. From these reasons, many researches[2-8] have been done to develop a clean process with a high selectivity towards the esterification products starting directly from α-pinene. Compared with the current two-step process, this direct process is more convenient for the preparation of esters. A lot of studies are dedicated to enhance the selectivity of products and the conversion of the reagents.[4-8]

In the case of isomerisation reactions the yields of the products strongly depend on the acidity and on the pore structure of catalyst, the nature of the acidic sites (Brønsted or Lewis) and the operating conditions.[9,10]

During the last two decades there has been a great interest in the application of microwave energy as a means of rate enhancement in synthesis,[11] due to the fact that the chemical reactions are affected by overheating, polarization, dielectric properties, solvent sensitivity, spin alignment and (partially) nuclear spin rotation produced by microwave irradiation. This framework represents the major effects of microwaves, which are not always equally important. In this field many reviews[12-17] or books[18-21] have been published. In the terpene chemistry microwaves were applied for solvent free microwave distillation[22] and very seldom in the synthesis of these compounds.[23]

* Corresponding author: mvlasa@chem.ubbcluj.ro

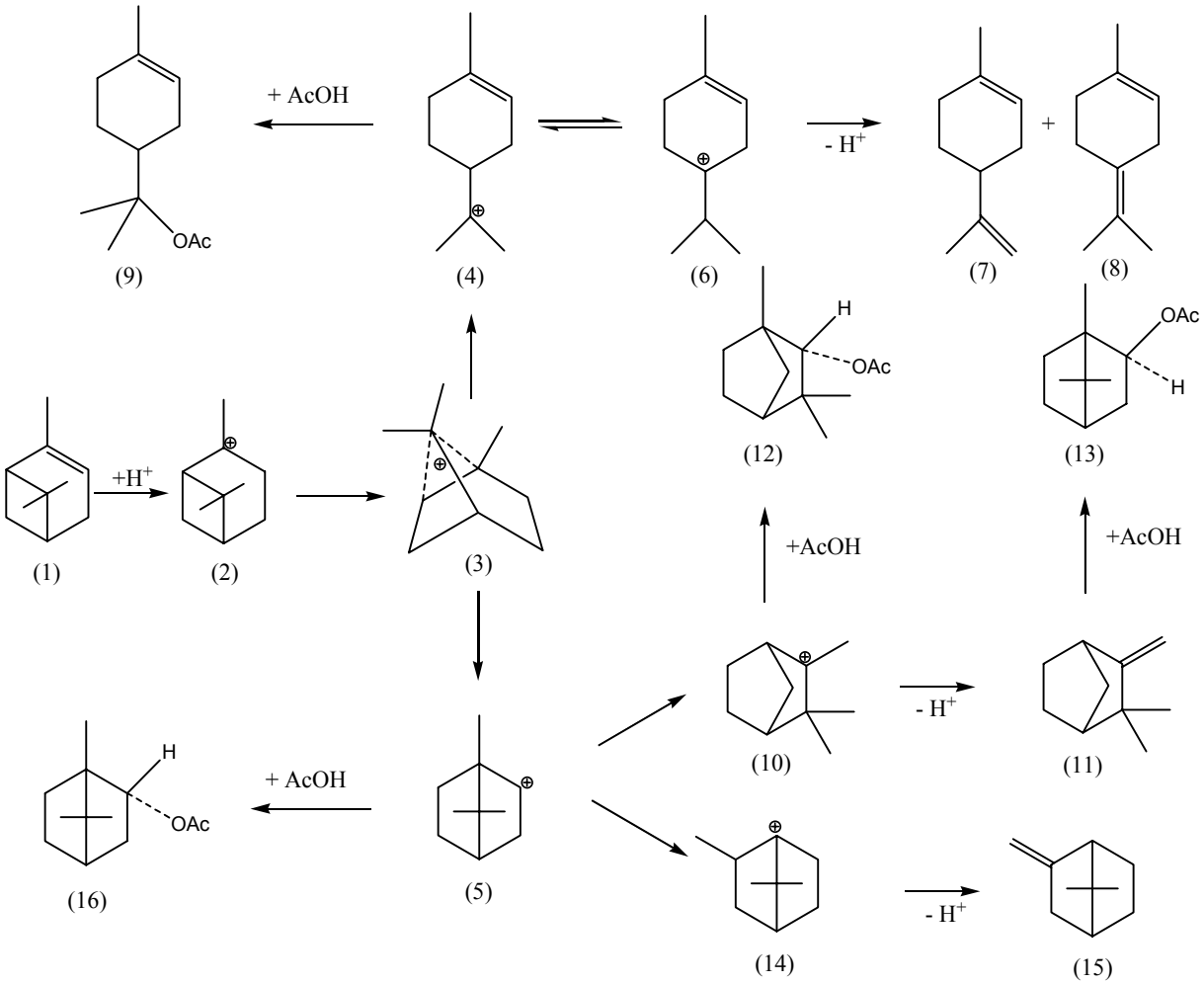

Scheme 1

Stolle[23] achieved the isomerisation of α- and β-pinene in near-critical water and supercritical lower aliphatic alcohols. Generally, two pathways occur – pyrolysis, when supercritical alcohols were used, or acidolysis, when supercritical water was employed. The different behavior in function of the solvent used can be explained by increased availability of the protons in near-critical water (heated at 270°C and at 80 bar) when the autoprotolysis of the water is enhanced. In this case, the main products of the reaction were from the p-menthadiene series. When supercritical alcohols were used thermal pyrolysis took place, due to the formation of radical reaction intermediates.

We achieved a comparative study of the acidic catalytic reactions of α-pinene with microwave activation with the reaction in near-critical water conditions assisted by microwave irradiation, in order to examine, working in milder conditions, the differences that appear in the reaction yields and the selectivity of the products.

RESULTS AND DISCUSSIONS

Experiments were conducted in order to study the behavior of α-pinene in acetic acid with or without different acidic catalysts. After cooling the mixture to ambient temperature the conversion of α-pinene was found to be almost quantitative in all reactions.

Taking into consideration the fact that we used acetic acid as solvent and as catalyst, both acidolysis and esters products were obtained (see Table 1).

Examining the results (Table 1) we can see that for the preparation of bornyl and fenchyl acetate the best method is to work only in the presence of acetic acid, for iso-bornyl acetate is recommended to use acetic acid in the presence of *para*-toluenesulfonic acid and for terpenyl acetate boric acid is the best choice.

The results obtained under microwave irradiation in the presence of the acidic catalyst were compared with those obtained in near-critical water method by Stolle (see Table 2).[23] This fact is

possible because these authors sustain that by using near-critical water the availability of protons is enhanced, the main products of the reaction being from the p-menthane series. This behavior can be attributed to proton-catalyzed rearrangement mechanism, and the addition of other acids-catalyzing reactants like mineral acids, zeolites or heteropolyacids is not necessary.

In the case of rearrangement of **(1)** in near-critical water under microwave irradiation the majority of products originated from the acidolysis reaction pathway, as in case of our experiments. This can be explained by the fact that from the two competitive reactions, namely the pyrolitic ring cleavage and reaction via carbocations (produced by addition of a proton to the double bond) the first one has a higher activation energy. Stolle[23] worked at 270°C and this temperature was not high enough to pyrolyze great amounts of **(1)**, and, as a result, only small quantities of pyrolytic products were formed (see Table 2).

Table 1

Conversion and selectivity of the products formed by isomerisation of α-pinene using acetic acid and other acidic catalysts under microwave irradiation

No	Catalyst	C (%)	Selectivity (%)										
			Isomerisation products						Ester products				Unknown
			Bicyclic terpenes		Monocyclic terpenes								
			Fen	Cf	α-T	Lim	γ-T	T	Fac	Bac	iso-Bac	Tac	
1	A.A.	99	4.2	11	1.6	39.7	1.4	11.4	9.3	15.4	1	2	3
2	A.A.+$B(OAc)_3$	98	4.3	14.7	1.9	32.9	1.9	12.8	6.6	12	1.2	7.4	4.3
3	A.A.+H_3BO_3	98	4.1	13.5	09	32.4	1.6	11.6	6.6	11.6	0.7	9.1	8.6
4	A.A.+B_2O_3	97	4.3	14.5	4.4	32.5	3.3	17.7	4.8	10.1	2.2	2	4.6
5	A.A.+APTS	100	1.1	10.2	0.1	17.9	5.3	9.9	3.2	4.6	14.3	2.1	31.3

A.A. = Acetic acid, Fen = Fenchene; Cf = Camphene; T = Terpinolene; α-, γ-T = α-, γ-Terpinene; Lim = Limonene; Fac = Fenchyl acetate; Bac = Bornyl acetate; iso- Bac = iso-Bornyl acetate; Tac = Terpenyl acetate; C = Conversion, APTS = *para*-Toluenesulfonic acid.

Table 2

Results of rearrangement of α-pinene in near-critical water, with 100% conversion, according to Stolle and coworkers [23*]

Compound	Yield (%)	Reaction type
Limonene	14	P,A
Alloocimene	9	P
Pyronene	4	P
Terpinolene	20	A
γ-Terpinene	24	A
α-Terpinene	12	A
α-Phellandrene	2	A
p-Cymene	5	A
Camphene	3	A
Unknown	7	?

*Reaction conditions: 250 µl α-pinene, 15 ml 0.03 M NaCl solution, 80 ml quartz vessel, heating 10 min, reaction time 60 min, cooling 20 min, P_{max}: 1.2 kW, microwave Synton 3000. A = Acidolysis, P = Pyrolysis.

Working in milder conditions than Stolle,[23] in our case the pyrolitic reactions did not occur, and as a result alloocimene and pyronene were not formed (Tables 1 and 2). Also the general aspect of the product yields is dramatically changed. Thus, in the case of our reaction conditions the higher yields were obtained in the case of limonene (39.7% in presence of acetic acid compared to 14% in near-critical water method) and of camphene (14.7% in boric acetate in acetic acid compared to 3% in near-critical water procedure). For terpinolene the yields are approximately the same (17.7% in presence of boric oxide compared to 20% in near-critical water). For α-terpinene and γ-terpinene the yields are better in near-critical water method (12% and 24%, respectively, compared to only 4.4% in the presence of boric oxide in acetic acid and 5.3% in the presence of *para*-toluenesulfonic acid in acetic acid, respectively, in our method). We cannot identify α-phellandrene and

p-cymene, products that appear in traces in near-critical water method (2% and 5%, respectively). *p*-Cymene can be formed as a side reaction of the endocyclic α-terpinene and γ-terpinene isomers due to their tendency to form the thermodynamic stable aromatic compounds. The reason that we could not observe the formation of p-cymene consisted in a very low yield of α-terpinene and γ-terpinene isomers obtained in our case.

The isomerisation products/ester products ratio is in favor of the isomerisation one (see Table 3). Both products of the reactions have the same starting mechanism, namely addition of the proton to a double bond. By the addition of acetic acid to the resulted carbocations the esters are formed; the isomerisation products appear by a rearrangement of the carbocations. According to these observations, to name the formation of bornyl-, isobornyl-, terpenyl-, and fenchyl-acetate an esterification reaction, as sometimes appear in literature,[8] is incorrect.

Table 3

Isomerisation products/esterification products ratio

No	Catalyst	Selectivity (%)		Isomerisation products/ esterification products
		Isomerisation products	Esterification products	
1	A.A.	69.4	27.7	2.5
2	A.A.+$B(OAc)_3$	68.4	27.1	2.5
3	A.A.+H_3BO_3	64.1	28.1	2.3
4	A.A.+B_2O_3	77.0	19.2	4.0
5	A.A.+APTS	44.6	24.2	1.8

A.A= Acetic acid

EXPERIMENTAL

The microwave reactions were carried out in a CEM Discovery Labmate microwave oven with irradiation powder of 300 W; with continuous irradiation on all power range in 1W steps. The power of the microwave irradiation could be controlled via a pressure-, temperature-, or power-regulated program. The temperature of all vessels was controlled by IR-sensor. The feedback control of the pressure was made by pressure sensor Discovery IntrelliVent and pressure attenuator Discover IntrelliVent. In this case, the power input was limited by temperature T_{lim}= 150°C, pressure p_{lim}= 17 bar and power = 0.1 kW. For heating up to T_{lim} 6 min and for cooling down 20 min were used. The 10 ml glass vessels were used and were filled with maxim 5 ml of solution.

The GC analysis was carried out using a Hewlett Packard 5890 series II instrument. SPB^{TM} capillary column (60m x 0.32mmx0.25μm film thickness) and SUPELCOWAX^{TM} 10 capillary column (60 m x 0.32 mm x 0.5μm film thickness) were used with H_2 as carrier gas (0.2 ml/min). The second capillary column is more polar than the first one and both were used for analysis of all reaction products. Both capillaries were used for analysis of each compound. FID detector temperature was 270°C. GC oven temperature was kept at 60°C for 3 min and programmed to 210°C at a rate of 4°C/min, and kept constant at 210°C for 20 min; split ratio was adjusted to 80:1. The injector temperature was set to 260°C. The qualitative and quantitative analysis of the mixtures of reactions was made using internal standards.

Reaction of α-pinene with acetic acid, solid acidic catalysts under microwave conditions

The mixture of α-pinene (6 g, 0.043 mmol), acetic acid (7.92 g, 0.132 mmol) and catalyst (0.06 g) was heated into microwave oven at 150°C. Microwave power was 100 W and pressure was 6 bars. The reaction mixtures were analyzed in all methods by GC.

CONCLUSIONS

In conclusion, compared to near-critical water method, the procedure that uses microwave assisted of α-pinene acidic catalysis isomerisation reactions in non-critical conditions is milder, using a lower temperature (150°C compared to 270°C), a lower pressure (6 bar compared to 80 bar) and a shorter reaction time (45 min compared to 90 min). The general aspect of the reaction selectivity is changed, being higher for limonene and camphene and lower for α-terpinene and γ-terpinene than in near-critical water procedure.

REFERENCES

1. "Ulmanns Encyclopedia of Industrial Chemistry", 5th edition on CD-Rom, VCH, Veinheim, 1996.
2. J. G. Graeme, F. H. Camila and J. WE. Roderick, *Appl. Catal. A. Gen*., **2001**, *209*, 269-277.
3. Z. Cheng, "Process Technology of Natural Resin", China Forestry Publishing House, 1996.
4. O. Zeitschel, *US Patent*, 907941, 1906.
5. S. Winstein, E. Grundwald and H.W. Jones, *J. Am. Chem. Soc*., **1951**, *73*, 2700-2707.
6. G. Valkanas, *J. Org. Chem*., **1976**, *41*, 1179-1183.

7. C. M. Williams and D. Whittaker, *J. Chem. Soc. (B),* **1971**, 668-672.
8. S. Liu, C. Xie, S. Yu, F. Liu and K. Ji, *Catal. Commun*., **2008**, *9*, 1634-1638.
9. N. Besun, F. Ozkan and G. Gunduz, *Appl. Catal. A. Gen*., **2002**, *224*, 285-297.
10. D. M. Roberge, D. Buhl, J. P. Niederer and W. Holderich, *Appl. Catal. A. Gen*., **2001**, *215*, 111-124.
11. (a) R. Butnariu and I.I. Mangalagiu, *Bioorg. Med. Chem*., **2009,** *17*, 2823-2829; (b) Gh. Zbancioc and I. I. Mangalagiu, *Synlett*, **2006**, *5*, 804-806; (c) C. Afloroaei, M.Vlassa, A. Becze, P. Brouant and J. Barbe, *Heterocyclic Commun*., **1999**, *5*, 249-252; (d) S. V. Filip, I. A. Silberg, E. Surducan, M. Vlassa and V. Surducan, *Synthetic Commun*., **1998**, *28*, 337-345; (e) A. Burczyk, A. Loupy, D. Bogdal and A. Petit, *Tetrahedron*, **2005**, *61*, 179-188; (f) W. P. Fang, Y. T. Cheng, Y. R. Cheng and Y. J. Cherng, *Tetrahedron*, **2005**, *61*, 3107-3113; (g) C. Kuang, Q. Yang, H. Senboku and M. Tokuda*, Tetrahedron,* **2005**, *61*, 4043-4052; (h) M. Iannelli, V. Alupei and H. Ritter*, Tetrahedron*, **2005**, *61*, 1509-1515; (i) B. Desai, T. N. Danks and G. Wagner*, J. Chem. Soc., Dalton Trans*. **2004**, 166-171.
12. B. A. Roberts and C. A. Strauss, *Acc. Chem. Res*., **2005**, *38*, 653-661.
13. B. L. Kappe, *Angew. Chem. Int. Ed*., **2004**, *43*, 6250-6284.
14. B. L. Hayes, *Aldrichim. Acta*, **2004**, *37*, 66-76.
15. A. De la Hoz, A. Diaz-Ortiz and A. Moreno, *Chem. Soc. Rev*., **2005**, *34*, 164-178.
16. C. R. Strauss, *Aust. J. Chem*., **1999**, *52*, 83-96.
17. I.I. Mangalagiu, *Curr. Org. Chem*. **2011**, *15*, 730-752.
18. A. Loupy (Ed), "Microwaves in Organic Synthesis", Wiley-VCH, Weinheim, 2002.
19. A. Loupy (Ed), "Microwaves in Organic Synthesis", vol 1, 2nd edition, Wiley-VCH Verlag GmbH and Co.KgA, Weinheim, 2006.
20. J. P. Tierney and P. Lidstrom, Assisted Organic Synthesis, Blackwell, Publ.Ltd, Oxford (UK), 2005.
21. C. O. Kappe and A. Stadler, Microwaves in Organic Syntyhesis, Wiley-VCH, Weinheim, 2005.
22. (a) M. E. Lucchesi, F. Chemat and J. Smadja, *J. Chromatogr. A*. **2004**, 1043, 323-327; (b) Idem, *Flavour Frag. J.,* **2004**, *19*, 134-138.
23. T. Szuppa, A. Stolle and B. Ondruschka, *Org. Biomol. Chem*., **2010**, *8*, 1560-1567.

ACADEMIA ROMÂNĂ
Revue Roumaine de Chimie
http://web.icf.ro/rrch/

Rev. Roum. Chim.,
2012, *57*(3), 215-222

NUMERICAL STUDY OF DILUENT INFLUENCE ON BURNING VELOCITY OF ACETYLENE-AIR MIXTURES

Codina MOVILEANU,[a] Maria MITU,[a] Venera GIURCAN,[a] Adina MUSUC,[a]
Domnina RAZUS[a*] and Dumitru OANCEA[b]

[a] Roumanian Academy, "Ilie Murgulescu" Institute of Physical Chemistry, 202 Spl.Independentei, 060021Bucharest, Roumania
[b] Department of Physical Chemistry, University of Bucharest, 4-12 Regina Elisabeta Blvd., 030018 Bucharest, Roumania

Received November 1, 2011

In the present paper, the numerical study of 1-D adiabatic laminar premixed flames of acetylene-air and acetylene-air-diluent (stoichiometric acetylene-air mixtures containing various amounts of Ar, N_2 or CO_2) was carried out at room temperature and atmospheric pressure, using two software packages (INSFLA, based on Warnatz mechanism and COSILAB, based on GRI mechanism). The kinetic modelling provides the normal burning velocities and the profiles of temperature and heat release rate across the flame front. For the stoichiometric acetylene-air mixture, the burning velocities computed with GRI mechanism agree well with experimental values from literature while the burning velocities computed with the Warnatz mechanism are underestimated. Dilution by increasing amounts of diluents determines the decrease of burning velocity, of maximum flame temperature and of heat release rate, determined by decrease of overall reaction rate between fuel and oxidant in the reaction zone and of heat and mass transfer rates between the burnt and unburnt gases.

INTRODUCTION

The acetylene combustion with air or oxygen has a considerable chemical and industrial interest and importance. The high enthalpy of formation of acetylene determined by the presence of the triple C≡C bond results in flame temperatures higher than those normally obtained from other hydrocarbon fuels; therefore acetylene is widely used in industrial welding and cutting and also in other applications where high temperature flames are required, such as photometry and atomic absorption.[1] The combustion reactions of acetylene are of wider significance, since acetylene is formed as an intermediate in the combustion of fuel-rich mixtures of other hydrocarbons and plays an important role in soot formation.[2] Knowledge of acetylene combustion is important also with respect to industrial hazards presented during acetylene manufacture and its wide using for chemical synthesis. This is particularly so since acetylene is capable of sustaining a self-decomposition flame, while in mixture with oxygen it readily detonates.[3] The laminar burning velocities for acetylene-air mixtures are also substantially higher than those of any other hydrocarbon mixture for the same equivalence ratio.[4, 5]

Among characteristic propagation parameters, the normal burning velocities are key properties for modelling the turbulent combustion, optimization of internal combustion engines and the design and construction of venting devices. Reliable values of burning velocities for gaseous acetylene-air mixtures are found in literature, from various measurements on premixed flames, under stationary or non-stationary conditions.[6-12] The burning velocities of acetylene with air over lean to rich fuel concentrations, at various initial pressures between 0.5 and 20 atm were measured by means of the spherical bomb technique.[6-8] For the stoichiometric mixture at ambient initial pressure and temperature, burning velocities ranging within 125 cm/s [6] and 135 cm/s [8] were reported. Other

* Corresponding author: drazus@icf.ro; drazus@yahoo.com

measurements on outwardly propagating spherical flames in a constant-pressure chamber [9] for various equivalence ratios and pressures up to 5 atm, confirmed the previously found burning velocity (125 cm/s) for the stoichiometric mixture at 1 bar. Slightly higher burning velocities of acetylene-air, for mixtures with an equivalence ratio between 1.1 and 1.3 were found by measurements with the burner technique, using moist acetylene-air mixtures (0.3 vol.% H_2O (vap)) at 1 bar:[10] the authors found S_u =144 cm/s for the stoichiometric mixture and S_u =154 cm/s for the most reactive mixture (equivalence ratio φ = 1.2). In this case, the burning velocity was determined by direct photographic records; improved measurements based on Schlieren records of flames stabilized over a Bunsen burner delivered S_u =155 cm/s for the stoichiometric mixture and S_u =168 cm/s for the most reactive mixture (equivalence ratio φ = 1.25) at ambient initial conditions.[11] Recent measurements on acetylene-air mixtures at ambient initial conditions were made with the counter-flow twin flames technique;[12] the burning velocity of the unstretched flame in the stoichiometric mixture was found to be S_u=135 cm/s.

The fuel/air ratio, as well as the addition of inert diluents, strongly affects both the kinetics and thermodynamics of the combustion process and consequently the observable properties like the burning velocity, thus being used in many practical applications. The dilution effects on the burning velocity of fuel/air mixtures are frequently studied using Ar, N_2 and CO_2 gases having quite different physical and chemical properties.

Several comprehensive kinetic models for the combustion of unsaturated hydrocarbons were reported in literature.[13-17] Their validation was made by comparison between the computed and measured values of a few global parameters, such as the normal burning velocity and/or the ignition delay and ignition temperature, for the examined fuels under extensive variations of their state parameters. Among them, the models developed by Warnatz *et al.*[13, 18-20] for flames of C1-C4 hydrocarbons and by the Gas Research Institute[17] for natural gas-air flames were considered adequate and were tested for acetylene-air and acetylene-air-inert flames. The computed burning velocities of the stoichiometric acetylene-air and acetylene-air-inert mixtures with various dilution degrees will be discussed in comparison with available literature data. The results will be compared with those computed for other fuel-air-diluent systems, in order to correlate the observed burning velocity variation with physical and/or chemical factors.

COMPUTER PROGRAMS AND DATA EVALUATION

The kinetic modelling of acetylene-air and acetylene-air-diluent flames was made with packages INSFLA, developed by Warnatz and coworkers[20] and COSILAB version 3.0.3, developed by Rogg and Peters.[21] One-dimensional, premixed laminar free flames were considered, assuming the mechanism CH_4-C_4 (53 chemical species and 592 elementary reactions) with updated values of rate coefficients for the rate-limiting reactions in acetylene-air oxidation as reported by Heghes.[22] Another mechanism taken into account was the GRI mechanism – version 3.0 (53 chemical species and 325 elementary reactions).

The input data were taken from thermodynamic and molecular databases of Sandia National Laboratories, USA, according to the international standard (format for CHEMKIN).

RESULTS AND DISCUSSION

The kinetic modelling of flame propagating in gaseous acetylene-air and acetylene-air-diluent mixtures of given initial composition, pressure and temperature provides the laminar burning velocity S_u and the profiles of the volumetric rate of heat release, dQ/dt, of temperature and of concentration for all chemical species taken into account, describing the flame structure. The modelling refers to stable one-dimensional (1-D) laminar, premixed free flames.

A set of results obtained for the stoichiometric acetylene-air flame ([C_2H_2] = 4.02 vol. %) diluted with various amounts of CO_2 at ambient initial conditions are given in Fig. 1, where normal burning velocities computed by the two mechanisms (Warnatz and GRI, respectively) are plotted against diluent concentration. A good agreement between literature data referring to the stoichiometric acetylene-air mixture [6, 8-10] is found for the burning velocities computed by means of the GRI mechanism; comparatively, the burning velocities computed with the Warnatz mechanism are lower at any diluent concentration.

The normal burning velocities of the stoichiometric acetylene-air mixture in the presence of various diluents, at ambient initial conditions, are drawn in Fig. 2. As expected, CO_2 dilution has the highest influence on burning velocities, since CO_2

has a larger influence on mixture heat capacity and on heat dissipation rate in comparison with nitrogen and argon.

This effect was already observed for stoichiometric ethylene-air and propylene-air mixtures, for computed and measured burning velocities, as well.[23, 24] Similar dependencies were obtained for both mechanisms used in the present computations, at various initial pressures between 1 and 5 bar.

A set of representative data obtained in the present computations for stoichiometric acetylene-air mixture diluted with 10% diluent, is given in Table 1, together with data characteristic of the stoichiometric acetylene-air mixture at ambient initial conditions: the maximum flame-front temperature (T_{max}), the flame front width (d_{fl}) and the normal burning velocity (S_u). Both data sets confirm the decrease of the maximum flame temperatures and burning velocities and the increase of flame front width of acetylene-air flames in the presence of diluents.

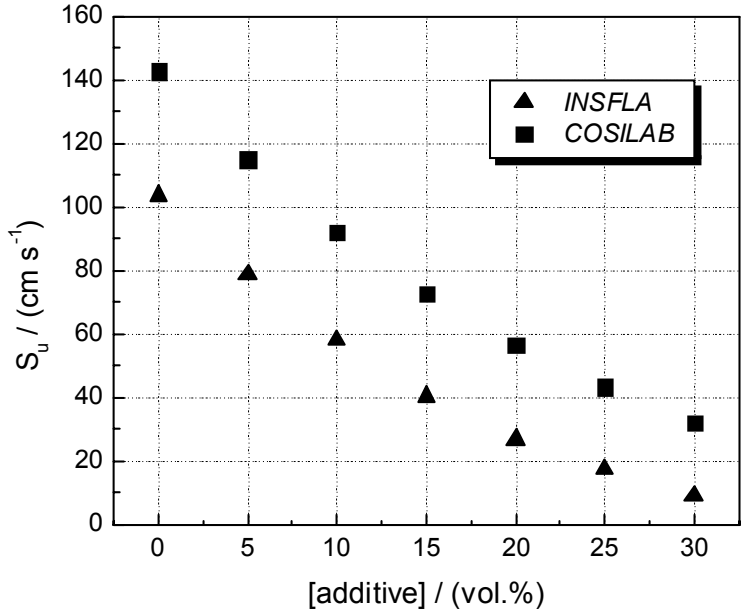

Fig. 1 – Computed normal burning velocities
for stoichiometric C_2H_2-air-CO_2 mixtures at p_0 = 1 bar and T_0 = 298 K.

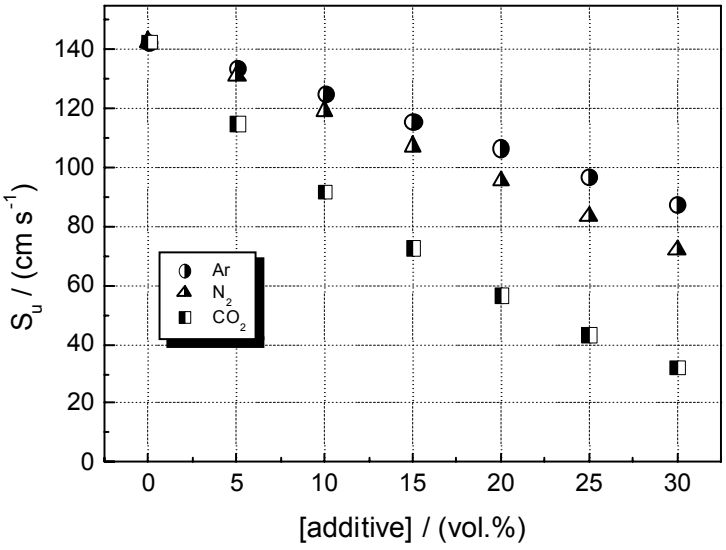

Fig. 2 – Computed burning velocities using GRI mechanism
for stoichiometric acetylene-air mixtures diluted with various diluents.

Table 1

Characteristic parameters of the stoichiometric acetylene-air and acetylene-air-10% diluent flames at ambient pressure and temperature

	INSFLA				COSILAB			
	no diluent	argon	nitrogen	carbon dioxide	no diluent	argon	nitrogen	carbon dioxide
T_{max} / K	2569.6	2507.1	2472.9	2371.5	2125.0	2053.3	2020.9	1935.0
d_{fl} / mm	0.449	0.512	0.542	0.654	-	-	-	-
S_u / (cm s^{-1})	103.7	87.10	80.79	57.99	142.76	125.13	119.23	92.10

Significant differences are revealed between data obtained with the two mechanisms, determined by adopting different reaction routes; they are maintained even for the relative (normalized) flame front temperatures, defined as $T_{\max,rel} = T_{\max} / T_{\max}^0$ (where $T_{\max}$ is the temperature of fuel-air-diluent flame and $T_{\max}^0$ is the temperature of fuel-air flame without diluent) and for the relative burning velocities, defined as $S_{u,rel} = S_u / S_u^0$ (S_u is the burning velocity of fuel-air-diluent mixture and S_u^0 is the burning velocity of fuel-air mixture without diluent). Taking into account the better agreement between burning velocities of acetylene-air computed with GRI mechanism and the reference data from literature, we will discuss only results computed by means of this mechanism.

Comparison of relative burning velocities computed for stoichiometric C_2H_2-air and stoichiometric C_3H_8-air mixtures in the presence of various diluents reveals systematic differences between the two fuels. For each examined diluent, the relative burning velocities of C_3H_8-air-diluent are lower in comparison with burning velocities of C_2H_2-air-diluent, as seen in Fig. 3. Identical dependencies were obtained for the relative flame front temperatures, proving that dilution effect is influenced not only by diluent nature and concentration but also by the combustion heat of examined fuels.

Additional information on diluent influence on C_2H_2-air flames is obtained from heat release rates, computed for atmospheric flames, plotted in Fig. 4. The decrease of heat release rates by dilution is determined mostly by the diminution of acetylene and oxygen concentrations and of the amount of evolved heat, able to sustain the flame propagation. The typical examples are acetylene-air-N_2 and the acetylene-air-Ar mixtures (the upper plots in Fig. 4). In addition, dilution by CO_2 maintains the diminution of fuel content, adding the specific influence of this diluent: its ability to dissociate and to dissipate heat by radiation. However, the effect of carbon dioxide dissociation is less important when diluent amount is increased because the flame temperature is lower and does not support an extensive dissociation.[25]

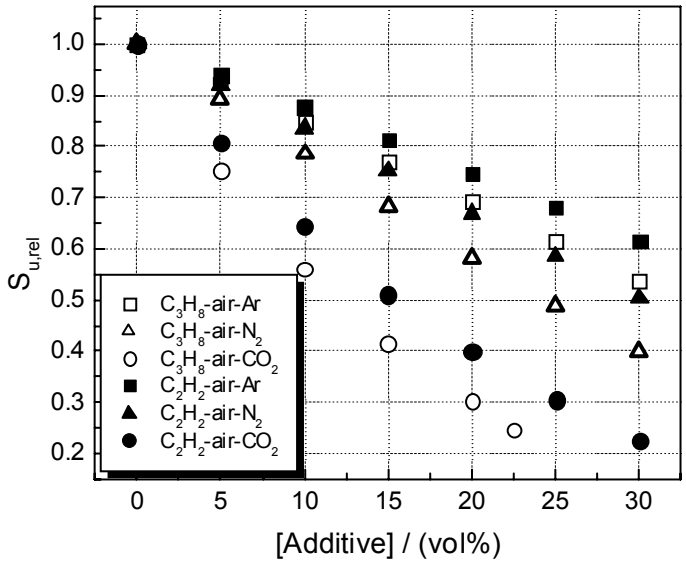

Fig. 3 – Relative burning velocities of C_2H_2-air-diluent and C_3H_8-air-diluent mixtures at p_0 = 1 bar and T_0 = 293K, computed with GRI mechanism.

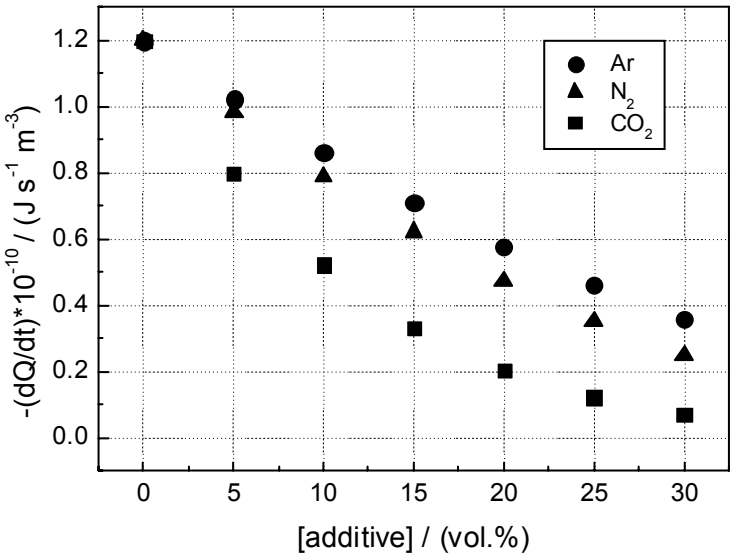

Fig. 4 – Heat release rate from acetylene-air-diluent flames, at p_0 = 1 bar and T_0 = 298 K.

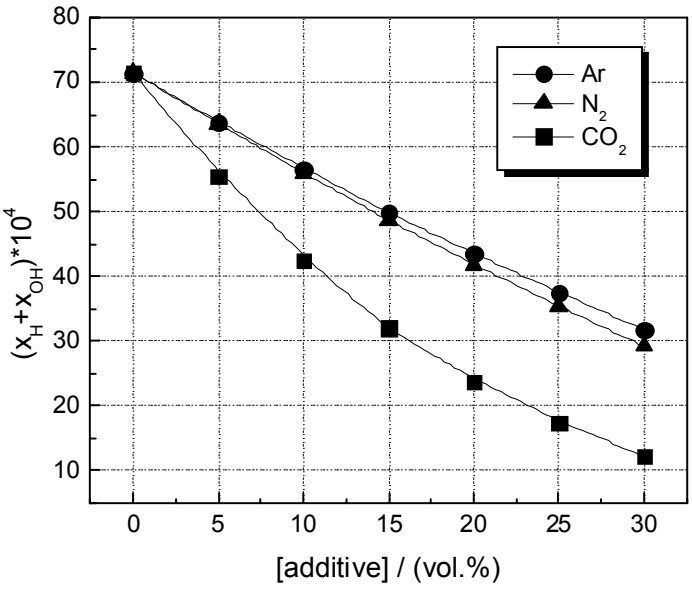

Fig. 5 – Total mass fractions of H and OH in the flame front of the stoichiometric acetylene-air mixtures diluted with various amounts of Ar, N_2 and CO_2 at p_0 = 1 bar and T_0 = 298 K.

The diluent influence upon flame propagation is observed also by examination of the total mass fraction of H and OH radicals, the chain carriers that influence most significantly the fuel consumption reaction.[20] In Fig. 5, a plot of the total mass fractions of H and OH against diluent concentration is given. The decrease of the mass fractions of examined radicals with dilution is larger in flames diluted with carbon dioxide, as compared to flames diluted by nitrogen or argon.

Good correlations were found between the normal burning velocities and the maximum flame temperatures for all examined diluents, as seen from Fig. 6. In the range of high flame temperatures, data laye practically on the same plot; they differentiate in the low temperatures range. Similar dependencies were found for many other systems: C_2H_4-O_2-N_2 [24] and CH_4-O_2-N_2-CO_2 or H_2-O_2-N_2-CO_2 where oxygen-enriched air was used, with different enrichment factors.[26]

The correlation of normal burning velocities with flame temperatures, illustrated by data in Fig. 6, can be used to evaluate the overall activation energy of the combustion process.

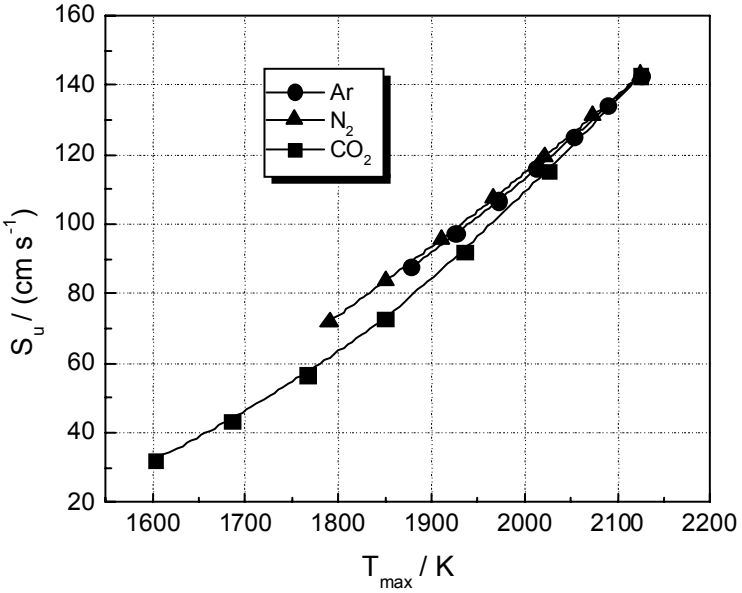

Fig. 6 – Correlation between the normal burning velocities and maximum flame temperatures for acetylene-air-diluent mixtures, obtained by GRI mechanism.

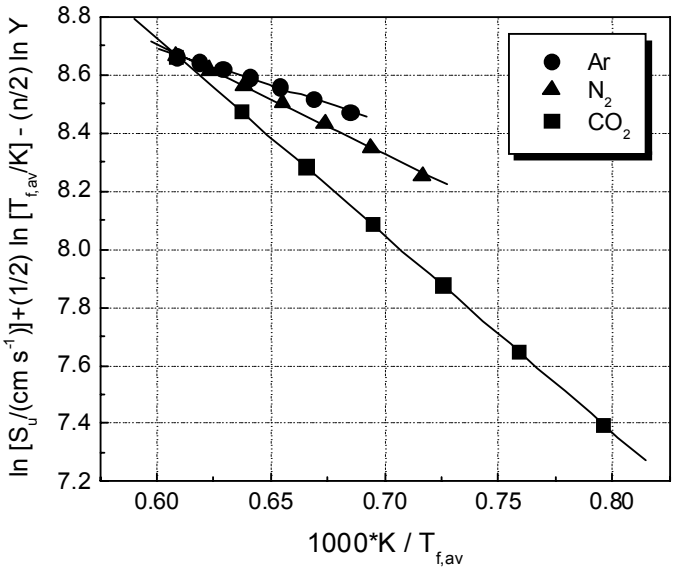

Fig. 7 –Variation of normal burning velocities and average flame temperatures, for acetylene-air-diluent mixtures.

The overall activation energy of acetylene-oxygen reaction within the flame front, in the presence of different diluents, was calculated from equation:

$$\ln S_u + \frac{1}{2}\ln T_{fl,av} - \frac{n}{2}\ln Y = const - \frac{E_a}{2R \cdot T_{fl}} \quad (1)$$

derived by Burke *et al.*[27] for any fuel-oxygen-inert mixture where the flame temperature is varied by dilution. In eq. (1), $T_{fl,av}$ is the average temperature within the flame front, Y is the mole fraction of reactive components (fuel + oxidant) in the examined mixture and n is the overall reaction order for the reaction between fuel and oxidant. The average flame temperature was calculated with the relationship:[27]

$$T_{fl,av} = T_0 + 0.74 \cdot \left(T_{fl} - T_0\right) \quad (2)$$

where T_0 is the initial temperature of flammable mixture and T_{fl} is the maximum flame temperature in the flame front. The overall reaction order, n, was considered 2.0, according to data referring to propane-air mixtures.[28] An additional evaluation of the same data used $n = 1.8$, as found for ethylene-air and propylene-air.[23, 24]

Table 2

Activation energies of acetylene oxidation in the presence of various diluents

	Ar	**N_2**	**CO_2**
E_a, kJ/mol (based on n = 2.0)	41.5 ± 1.1	63.2 ± 1.5	112.7 ± 0.30
E_a, kJ/mol (based on n = 1.8)	49.3 ± 1.0	68.3 ± 0.80	115.9 ± 0.30

The plots of the left member of equation (1) (with n = 2) against the reciprocal value of average flame temperature, for the stoichiometric acetylene-air mixture diluted with Ar, N_2 and CO_2 are given in Fig. 7. The slopes of the linear correlations gave the overall activation energies.

A typical set of data is given in Table 2. Quite small differences were obtained, for each examined diluent, when the overall reaction order varied from 1.8 to 2.0.

The overall activation energies of acetylene oxidation in flames with O_2, in the presence of diluents, are much lower in comparison with the activation energies of other fuels with oxygen, *e.g.* E_a = 146 kJ/mol for stoichiometric C_3H_6-air-Ar mixtures and 207 kJ/mol for stoichiometric C_3H_6-air-CO_2 mixtures;[29] E_a = 97.2 kJ/mol for C_2H_4-air-N_2, 134.4 kJ/mol for C_2H_4-air-Ar and 158.6 kJ/mol for C_2H_4-air-CO_2.[24] For all fuels, the largest activation energies are calculated for mixtures diluted with CO_2 ; they account for the steeper decrease of burning velocities of fuel-air-CO_2 (in comparison with other fuel-air-diluent mixtures) when CO_2 concentration increases.

CONCLUSIONS

A computational study of flame propagation in stoichiometric acetylene-air-diluent mixtures (diluents: argon, nitrogen, and carbon dioxide, with concentrations between 5-30 vol.%) was performed by using the Warnatz mechanism developed for combustion of C1 - C4 hydrocarbons with air and the GRI mechanism, developed for combustion of natural gas with air. The study provides the burning velocities of examined mixtures at p_0 = 1 bar and T_0 = 298 K, together with temperature, flame front width, species concentrations and profiles of heat release rate across the flame front. A better agreement between computed and experimental burning velocities was obtained by using GRI mechanism.

A strong influence of the inert diluents on the normal burning velocity, maximum flame temperature, concentration of active radical species and heat release rate in the flame front was observed. Dilution by increasing amounts of diluents determines the decrease of the burning velocity, maximum flame temperature and heat release rate, for all investigated diluents. Among them, CO_2 was found the most efficient, followed by N_2 and Ar. The explanation relies on the larger influence of carbon dioxide on the total heat capacity and heat dissipation rate in comparison to nitrogen and argon. The differentiation of the dilution effect is clearly reflected in the overall activation energies: 41.5 kJ/mol (C_2H_2-air-Ar), 63.2 kJ/mol (C_2H_2-air-N_2) and 112.7 kJ/mol (C_2H_2-air-CO_2), indicating the maximum dilution efficiency of CO_2.

Acknowledgements: This work was supported by CNCSIS–UEFISCSU, project number PNII – IDEI code 458/2008. The authors gratefully thank Prof. U. Maas (Institut fűr Technische Verbrennung, Karlsruhe, Germany) and Dr. D. Markus (PTB, Braunschweig, Germany) for the permission to run the program INSFLA and for the provided assistance.

REFERENCES

1. A. Williams and D. B. Smith, *Chem. Rev.*, **1970**, *70*, 267-293.
2. I. Glassman, *22nd Symposium (International) on Combustion*, **1988**, 295-311.
3. M. G. Zabetakis, "Flammability characteristics of combustible gases and vapors", U.S. Departament of Interior, 1965, Bureau of Mines Bulletin 627.
4. C.K. Law, "A compilation of experimental data on laminar burning velocities" in "Reduced Kinetic Mechanisms for Applications in Combustion Systems", N. Peters and B. Rogg, Eds., Springer Verlag, New York, 1993, p. 15-26.
5. B. Lewis and G.von Elbe, "Combustion, Flames and Explosion of Gases", Academic Press, New York and London, 3-rd Edition, Chapter 3, 1987.
6. J. T. Agnew and L. B. Graiff, *Combust. Flame,* **1961**, *5*, 209-219.
7. C.J. Rallis, A. M. Garforth and J. A. Steinz, *Combust. Flame*, **1965**, *9*, 345-356.
8. B. E. Milton and J. C. Keck, *Combust. Flame*, **1984**, *58,* 13-22.
9. G. Jomaas, X. L. Zheng, D. L. Zhu and C. K. Law, *30th Symposium (International) on Combustion*, **2005**, 193-200.
10. G. J. Gibbs and H.F. Calcote, *J. Chem.Eng. Data*, **1959**, *4*, 226-237.
11. R. Gunther and G. Janisch, *Chem.-Ing. Tech.*, **1971**, *43, 1*, 975- 978.
12. F. N. Egolfopoulos and C.K. Law, *23nd Symposium (International) on Combustion*, **1990**, 471-478.

13. J. Warnatz, *18th Symposium (International) on Combustion*, **1981**, 369-384.
14. J. A. Miller, R. E. Mitchell, M. D. Smooke and R. J. Kee, *19th Symposium (International) on Combustion*, **1982**, 181-196.
15. C. K. Westbrook and F. L. Dryer, *Progr. Energy Combust. Sci.* **1984**, *10,* 1-57.
16. P. Dagaut, J.C. Boettner and M. Cathonnet, *Intern. J. Chem. Kinet.,* **1990**, *22*, 641-664.
17. GRI Mech 3.0, Gas Research Institute USA, under http://www.me.berkeley.edu.
18. J. Warnatz, *Ber. Bunsenges. Phys. Chem.*, **1978**, *82*, 643-649.
19. U. Maas and J. Warnatz, *Combust. Flame,* **1978**, *74*, 53-69.
20. J. Warnatz, U. Maas and R. Dibble, "Combustion", 3rd Edition, Springer Verlag Berlin, Heidelberg and New York, 2001.
21. Cosilab, version 3.0.3., Rotexo-Softpredict-Cosilab GmbH & Co KG, Bad Zwischenhahn, **2011**.
22. C. Heghes, "C1-C4 Hydrocarbon Oxidation Mechanism", Ph.D. Thesis, 2006, Heidelberg University**.**
23. D. Razus, C. Movileanu and D. Oancea, *19th International Symposium on Combustion Processes*, **2005**, p.221-229.
24. C. Movileanu, D. Razus and D. Oancea, *Energy & Fuels*, **2011**, *25*, 2444-2451.
25. F. Halter, F. Foucher, L. Landry and C. Mounaim-Rousselle, *Combust. Sci. Technol.,* **2009**, *181*, 813-827.
26. A. Di Benedetto, V. Di Sarli, E. Salzano, F. Cammarota and G. Russo, *Int. J. Hydrogen Energy,* **2009**, *34*, 6970-6978.
27. R. Burke, F. Dewael and A. van Tiggelen, *Combust. Flame*, **1963**, *7*, 83-87.
28. V. Brinzea, M. Mitu, D. Razus and D.Oancea, *Rev. Roum. Chim*, **2010**, *55*, 55-61.
29. D. Razus, C. Movileanu, V. Branzea and D. Oancea, *Analele Univ.Bucureşti-Chimie*, **2005**, *14* (I-II), 209-214.

ACADEMIA ROMÂNĂ
Revue Roumaine de Chimie
http://web.icf.ro/rrch/

Rev. Roum. Chim.,
2012, *57*(3), 223-227

HYALURONIC ACID DETECTION FROM NATURAL EXTRACT BY DIODE ARRAY-CAPILLARY ELECTROPHORESIS METHODS

Eugenia Dumitra TEODOR,[a*] Georgiana TRUICĂ[a,b] and Gabriel Lucian RADU[a,b]

[a] National Institute for Biological Sciences, Centre of Bioanalysis, 296 Spl. Independentei, Bucharest 060031, Roumania, tel/fax: +4021.2200900
[b] University Politehnica Bucharest, Faculty of Applied Chemistry and Materials Science, 1-7 Polizu Str., Bucharest 011061, Roumania

Received November 28, 2011

Hyaluronic acid (HA) was separated by capillary electrophoresis (CE) under normal polarity in phosphate buffer pH 7.4. HA-derived monosaccharide obtained after hydrolysis with trifluoroacetic acid and derivatization with 4-aminobenzoic acid ethyl ester were separated by capillary electrophoresis under normal polarity in borate buffer pH 11. Both CE methods are simple and reliable for quantifying of HA in several natural extracts. The sensitivity of the methods (18.6±0.36 μg/mL detection limit for intact HA and 1.09 ±0.07 μg/mL for derivatized monosaccharide) is acceptable for an UV detection and to evaluate the content of HA in connective tissues extracts and, eventually, in cosmetic and pharmaceutical formulations.

INTRODUCTION

Hyaluronic acid (hyaluronan, HA) is an acidic linear non-sulfated glycosaminoglycan (GAG) formed from disaccharide units containing *N*-acetylglcosamine and glucuronic acid, generally found in animal tissues. Hyaluronan has molecular weight usually in the order of 10^5–10^7 Da[1] and has many biological roles, some requiring its presence in small quantities (*e.g.,* as a proteoglycan organizer in cartilage) whereas in others, it is the most important structural/functional entity (*e.g.,* its presence in vitreous, synovial fluid, ovarian follicles or skin)[2-5]. It is used as a diagnostic factor for many diseases such as tumours, rheumatoid arthritis and liver diseases, in ophthalmology and in skin care.[6-10] HA is highly hygroscopic, biocompatible and biodegradable biopolymer, very attractive for biomaterials fabrication. It is intensively used in cosmetics, surgery and drug delivery.[11-13]

Because it is expensive, it was replaced by chitosan or associated with chitosan and collagen. Recently, the interest for HA rose again being used intensively, especially in cosmetic formulation for its anti-aging properties (hydrating and radical scavenger properties).

The aim of this work is to evaluate the content of HA in some extracts from bovine or swine vitreous using capillary electrophoresis (CE) methods. Other analytical methods were former used, such carbazole/orcinol reaction for quantitative assay of glucuronic acid and high performance liquid chromatography (HPLC) with UV detection for quantification of derivatized N-acetylglucosamine.[14]

CE is an attractive separating technique for HA, or other GAGs because their negative charge assures the resolving power even in the presence of other contaminants and HA could be detected intact or hydrolyzed. CE also offers a high separation efficiency, short analysis time, low consumption of materials and automated and reproducibility of analysis.[15]

An attempt was made to find a cheaper and simple method regarding the equipment and experimental protocol, but, in the same time, with a

* Corresponding author: eu_teodor@yahoo.com

good sensitivity and reproducibility for determination of HA from natural extracts or cosmetic formulations. Two methods were tested, one for intact HA which allows us to evaluate molecular mass, and other for hydrolyzed GAGs (or other polysaccharides). These methods are useful for a suitable chemical evaluation of some extracts and to utilize them in biomaterials fabrication (wound dressing, drug delivery etc). In addition, the second method could be used for monosaccharide content evaluation in other extracts (plants, yeasts etc).

RESULTS

Detection of intact HA

Using standard HA solution (conc. 20-800 μg/mL) the following calibration curve was obtained by CE separation of standard HA (rooster comb, Fig. 1):

$$A = 0.4459c - 8.2951;\ R^2 = 0.9975;$$
$$\text{LoD} = 18.6 \pm 0.36\ \mu g/mL$$

where A = peak area, c = concentration of HA, and LoD = detection limit; the limit of detection was defined as the concentration resulting from a signal to noise ratio of 3.

1. Detection of hydrolyzed HA

Table 1 summarises the main characteristics of the CE separation of ABEE derivatized carbohydrates and Fig. 2 contains the electropherogram illustrating the separation of five derivatized monosaccharide in 15 minutes. The derivatization reagent, ABEE is neutral at BGE pH and the excess of reagent is well separated from the derivatized monosaccharide peaks, which are very well differentiated (Fig. 2).

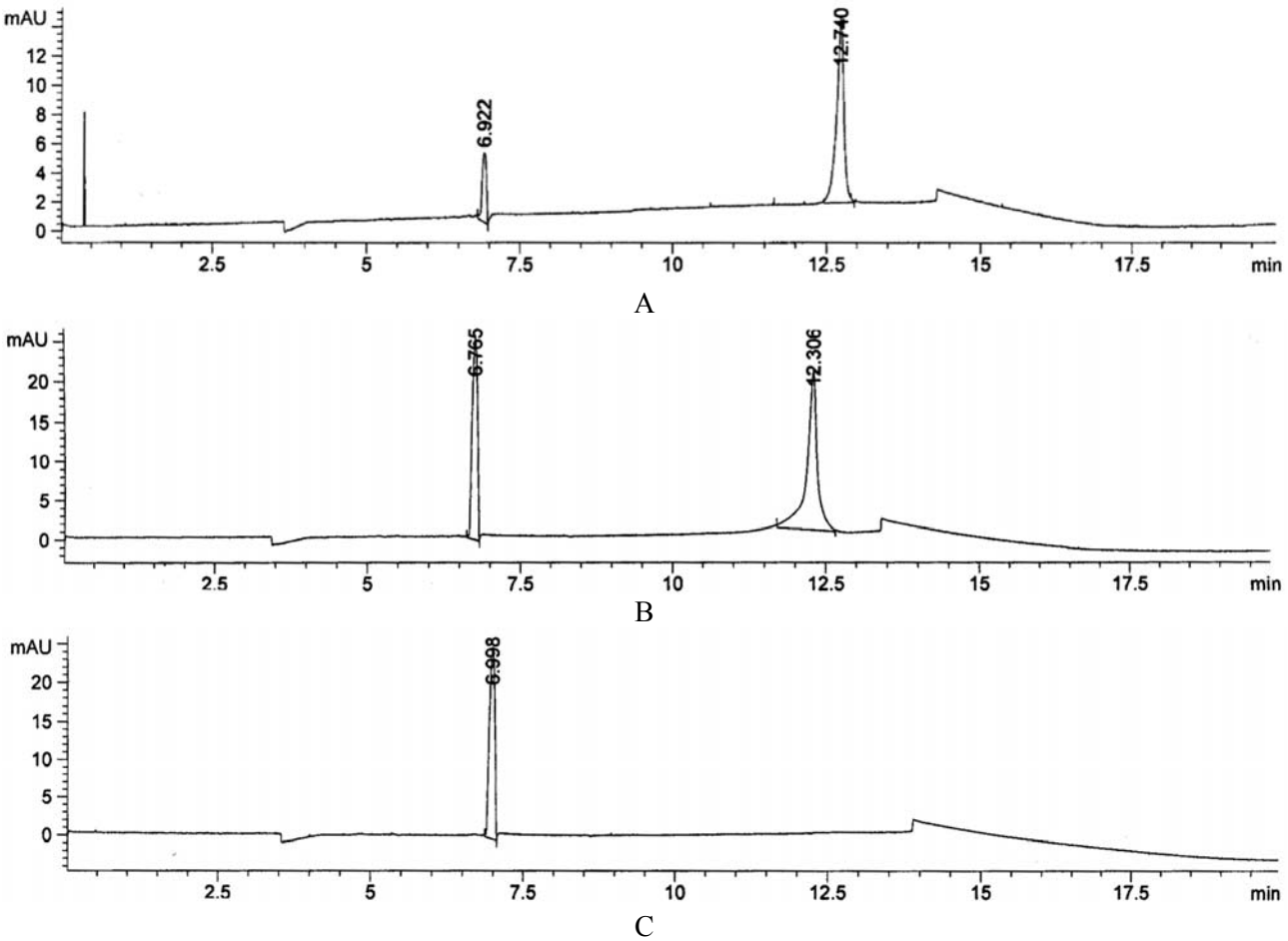

Fig. 1 – Electropherogram for standard HA, 300 μg/mL (A) and 800 μg/mL (B) and for HA sample (our extract from bovine vitreous) (C).

The separation of derivatized glucuronic acid and N-acetyl glucosamine from hydrolyzed HA, standard (Sigma) and from our extracts, are given in figures 3 and 4. Several artefact peaks appeared in the vicinity of N-acetyl glucosamine, probably due to degradation products. The recovery rates of standard HA are between 89 and 92%, and the quantification of HA in our extracts based on calibration curves of glucuronic acid and N-acetyl glucosamine show HA content between 72 and 75%.

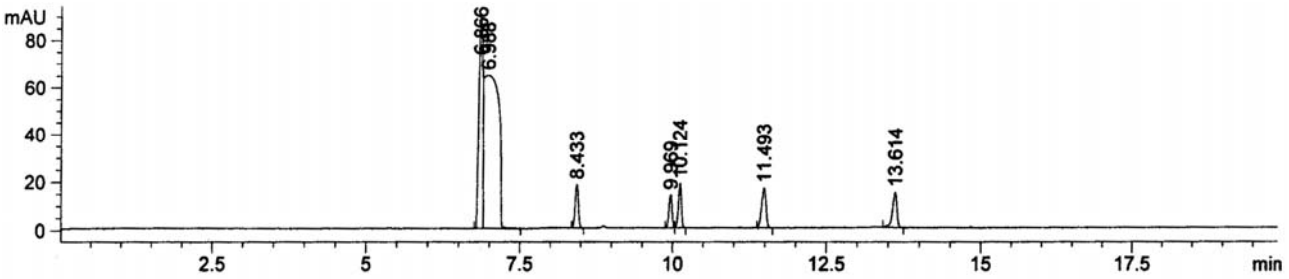

Fig. 2 – Electropherogram of mixed derivatized standard monosaccharides; 6.966 – derivatization reagent excces; 8.433-2-deoxy D-ribose; 9.969-N-acetyl D-glucosamine; 10.124-D-glucose; 11.493-D-galactose; 13.614-D-glucuronic acid.

Table 1

The main characteristics of the ABEE derivatization method

Compound	**Calibration curve equation**	**R^2**	**LoD (μg/mL)**	**LoQ (μg/mL)**
N-acetyl D-glucosamine	*A = 2.1371c – 1.7583*	0.9959	0.82 ±0.11	2.74 ±0.21
D-glucose	*A = 3.1372c – 2.7872*	0.9953	0.89 ±0.12	2.96 ±0.17
D-galactose	*A = 3.8645c – 3.2642*	0.9954	0.84 ±0.05	2.81 ±0.09
D-glucuronic acid	*A = 3.6804c – 4.0266*	0.9976	1.09 ±0.07	3.64 ±0.12
2-deoxy D-ribose (IS)	*A = 2.8494c – 2.3391*	0.9959	0.82 ±0.02	2.73 ±0.23

LoD=detection limit; LoQ= quantification limit (signal/noise ratio of 3)

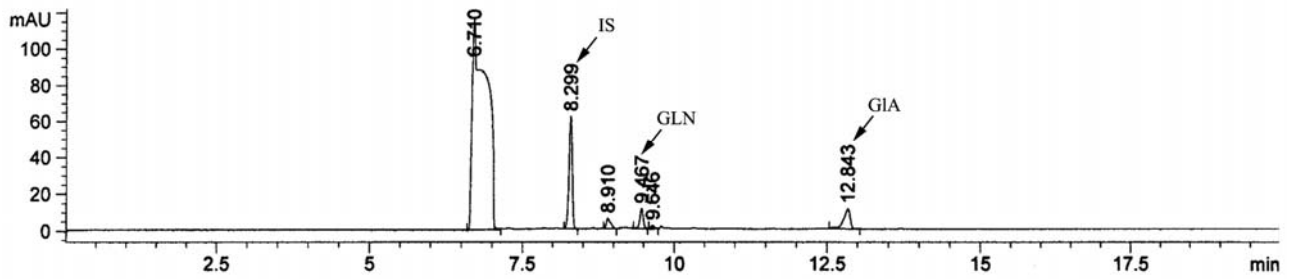

Fig. 3 – Electropherogram of standard hydrolyzed HA (rooster comb); 6.710 –derivatization reagent excces; 8.299-2-deoxy D-ribose; 9.467-N-acetyl D-glucosamine (NAc-GLN); 12.843-D-glucuronic acid (GlA).

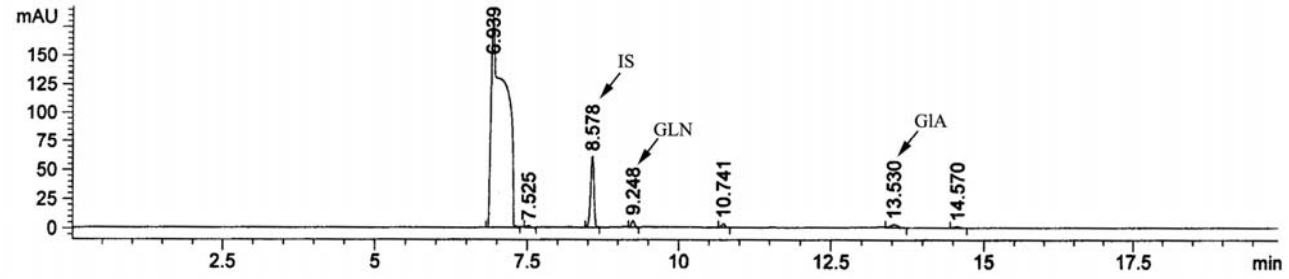

Fig. 4 – Electropherogram of hydrolyzed HA sample (our extract from bovine vitreous).

DISCUSSION

The electropherograms for intact standard HA (rooster comb, Figs. 1A and 1B) are very interesting because two peaks were obtained, the first at 6.7-6.9 minutes and the second at 12.3-12.7 minutes. Other research works in similar conditions[16-17] obtained a single peak for HA. In our case, the first peak appears only at concentrations higher than 100μg/mL HA, and the second is representative and appear for the beginning (from 20 μg/mL). The similar results were obtained with HA from umbilical cords.

Our samples present a single peak, at any solution concentration, at 6.8-6.9 minutes (Fig. 1C). These results confirm our previous studies[14] regarding the molecular mass of HA extracted by us from bovine or swine vitreous. Comercial hyaluronic acid (Sigma) has a major fraction with high molecular mass (not mentioned, but probably around of 10^6 Da) and a smaller fraction with medium molecular mass (probably around $2x10^5$ Da). Our extracted HA has only the fraction with medium molecular mass. The quantification of HA in our extracts based on calibration curve show a content between 75 and 78 % in all the samples.

The results are appropriate because they reveal a high content of HA in our extracts, and the medium molecular mass is suitable for its use in biomaterials fabrication (wound dressing hydrogels or other cosmetic formulations). [18-19]

The second method is more complicated because implies derivatization procedure but has the advantage to be suitable for other glycosaminoglycans or polysaccharides. Capillary electrophoresis with DAD detection is not a very sensitive procedure, but for our purposes is very suitable, rapid (~ 15 minutes for a run), very low consumption of reagents (order of mL) and reliable. For this stage of our needs, the methods did not need validation.

EXPERIMENTAL

HA (from rooster comb and from human umbilical cords), benzocaine (ABEE/4-aminobenzoic acid ethyl ester), D-glucuronic acid and N-acetyl D-glucosamine were purchased from Sigma, reagent grade di-potassium hydrogen phosphate and potassium di-hydrogen phosphate were supplied from Riedel-de Haën, sodium cyanoborohydride (CBH) from Aldrich and D-glucose, D-galactose and 2-deoxy D-ribose were supplied from Merck.

Our extraction method of partially purified-HA, essentially that of Danishefsky, 1966[20] consists in extraction of HA from bovine or swine vitreous with sodium chloride solution, and precipitation with cetylpiridinium chloride and ethanol.[14]

CE detection of intact HA

An Agilent CE system with diode array detector (190-600 nm) was used. Fused-silica capillaries HPCE standard, 50 μm id, 72 cm length were obtained from Agilent Technologies. The capillaries were preconditioned for 15 min with 1M sodium hydroxide before first run. The separations conditions were: +20 kV voltages, 30°C capillary temperature, 15 min migration time and the detection set to 193 and 195 nm. The preconditioning conditions were: before each run, flush the capillary for 7 minutes with 0.1 N sodium hydroxide, water for 3 minutes, and background electrolyte (BGE for 7 minutes. After each run the capillary was flushed for 7 minutes with background electrolyte (BGE).

The background electrolytes used were: 40 mM di-sodium hydrogen phosphate, 40 mM sodium dodecyl sulphate and 10 mM sodium tetraborate, pH 9[16] and 20 mM reagent grade di-potassium hydrogen phosphate and potassium di-hydrogen phosphate, pH 7.4.[17]

The second procedure, with 20 mM phosphate buffer pH 7.4 turned out to be most suitable with regard to peak shape and analysis time and was used in further experiments. All buffer solutions were filtered through membrane filters of 0.45 μm.

HA extracts from bovine vitreous humour[14] and standard HA solutions were prepared by dissolving 1 mg/mL HA in sodium chloride 0.4 M. All the experiments were made in triplicates.

CE detection of hydrolyzed HA

The same Agilent CE system and fused-silica capillaries were used. Carbohydrates derivatized with 4-aminobenzoic acid ethyl ester were separated by CE with an alkaline borate BGE.[21] Briefly, the derivatization procedure is as folows: just before use, dissolve 1 mg CBH in 100 μL of 10% (w/v) ABEE disolved in 10% acetic acid in methanol; 49 μL of this solution is mixed with 1 μL sugar standard (100 mg/mL in water) and heat for 15-20 min at 80°C. After completion of the reaction methanol is added to the total volume of 2 mL.

Background electrolyte used (after many trials) was 200 mM borate buffer, pH 11. The separations conditions were: +25 kV voltages, 30°C capillary temperature, 20 min migration time and the detection set to 306 nm. The preconditioning conditions were: before each run, flush the capillary for 7 minutes with 0.1 N sodium hydroxide, water for 3 minutes, and BGE for 7 minutes. After each run the capillary was flushed for 7 minutes with BGE. The resulting peak areas are average values from three consecutive electropherograms.

Commercials HA and our HA extracts were hydrolyzed with 3M trifluoroacetic acid (TFA) (20 mg HA in 2 mL 3 M TFA) for 6 hours at 100°C and derivatized as above. An internal standard (IS, 2-deoxy-D-ribose) was added in each sample.

CONCLUSIONS

Two simple and reliable CE methods to determine of HA from extracts were applied and

optimized according to our experimental conditions. The sensitivity of the methods (18.6±0.36 μg/mL detection limit for intact HA and 1.09±0.07 μg/mL for derivatized monosaccharide) is in the range for an UV detection and appropriate for actual and further purposes, to evaluate the content of HA in other connective tissues extracts and, eventually in cosmetic and pharmaceutical formulations. In our opinion, the method for determination of intact HA is more convenient than HPLC or CE methods which involve derivatization procedures, because is very simple, rapid and economical. In addition, some information about the hydrodynamic volume of the molecule is obtaining, this fact being important for further utilization of the extracted HA. Recently, an elaborated agarose-gel electrophoresis method was reported for molecular mass calculation of HA.[22, 23]

The second CE method is appropriate in the case that other glycosaminoglycans are present beside HA in the extracts (e.g. chondroitin sulphate, data not shown) and could be applied to a large range of polysaccharides extracted from natural sources. Both methods proved a HA content in our natural extracts between 72 and 78%.

Acknoledgements: The research was supported by Nucleu-Biodiv grant no. PN 09-360106/2009.

REFERENCES

1. T.C Laurent, *Acta Otol. Laryngol. Suppl*., **1987**, *442*, 7-16.
2. V. C. Hascall, *Glycoconj. J*., **2000**, *17*, 607-616.
3. A. Salustri, A. Camaioni, M. Di Giacomo, C. Fulop and V. C. Hascall, *Hum. Reprod. Update*, **1999**, *5*, 293-301.
4. R. Tammi and M. Tammi, "Science of Hyaluronan Today", V. Hascall and M. Yanagishita (Eds.), 2001, www. glycoforum.gr.jp./hyaluronan.
5. A.V. Noulas, S.S. Skandalis, E. Feretis, D.A. Theocharis and N.K. Karamanos, *Biomed. Chromatogr*., **2004**, *7*, 457-461.
6. G.D. Monheit, *Facial Plast. Surg. Clin. North Am.*, **2007**, *15*, 77-84.
7. N. Volpi, J. Schiller, R. Stern and L. Soltes**,** *Curr. Med. Chem*., **2009**, *16*, 1718-1745.
8. A.K. Yadav, P. Mishra and G.P. Agrawal, *J. Drug Target*, **2008**, *16*, 91- 98.
9. A.M. Croce, F. Boraldi, D. Quaglino, R. Tiozzo and I. Pasquali-Ronchetti**,** *Eur. J. Histochem.*, **2003**, *47*, 63-73.
10. B. P. Toole and V. C. Hascall, *Am. J. Path*., **2002**, *161*, 745-747.
11. V. Leroy, F. Monier, S. Bottari, S. Trocme, N. Sturn, M.N. Hilleret, F. Morel and J. P. Zarski, *Am. J. Gastroenterol*., **2004**, *2*, 271-279.
12. A. Asari and S. Miyauchi, *Science of Hyaluronan Today*, Ed. V. Hascall & Yanagishita/ www.glycoforum.gr.jp./ hyaluronan/ **2000**.
13. E. A. Balazs and J. L. Denlinger, *Ciba Foundation Symposium,* **1989**, *143*, 265-275.
14. E. Teodor, F. Cutaş, L. Moldovan, L. Tcacenco and M. Caloianu, *J. Biol. Sci*., **2003**, *I*, 35-46.
15. N. Volpi, F. Maccari and R.J. Linhardt, *Electrophoresis*, **2008**, *29,* 3095-3106.
16. A. Grimshaw, A. Kane, J. Trocha-Grimshaw, A. Douglas, U. Chakravarthy and D. Archer, *Electrophoresis,* **1994**, *15*, 936-940.
17. M. Plätzer, J.H. Ozegowski and R.H.H. Neubert, *J. Pharm. Biomed. Anal.*, **1999**, *21*, 491-496.
18. E. Teodor, V. Coroiu, M. Caloianu and T. Leau, *Rev. Roum. Biol.- Biol. Anim.,* **2004**, *49*, 113-118.
19. E. Teodor, A. Rugina and G. L. Radu, *Rev. Chim. (Bucharest)*, **2005**, *56,* 1211-1214.
20. J. Danishefsky, *J. Biol. Chem*., **1996**, *241,* 1-5.
21. C. Woodward and R. Weinberger, https://www.chem.agilent.com/Library/applications/5990-3403 EN.pdf. **1994**.
22. M.K. Cowman, C.C. Chen, M. Pandya, H. Yuan, D. Ramkishun, J. LoBello, S. Bhilocha, S. Russell-Puleri, E. Skendaj, J. Mijovic and W. Jing W, *Anal. Biochem.,* **2011**, *417*, 50-56.
23. S. Bhilocha, R. Amin, M. Pandya, H. Yuan, M. Tank, J. LoBello, A. Shytuhina, W. Wang, H.G. Wisniewski HG, C. de la Motte and M.K. Cowman, *Anal. Biochem*., **2011**, *417*, 41-49.

ACADEMIA ROMÂNĂ
Revue Roumaine de Chimie
http://web.icf.ro/rrch/

Rev. Roum. Chim.,
2012, *57*(3), 229-234

NEW DERIVATIVES OF 5-NITROINDAZOLE WITH POTENTIAL ANTITUMOR ACTIVITY

Corina CHEPTEA ,[a,b] Valeriu SUNEL,[a] Cristina STAN[c,*] and Dana Ortansa DOROHOI[d]

[a] "Al.I.Cuza" University, Department of Organic Chemistry, 11 Carol I Blv. RO-700506, Iaşi, Roumania
[b] "Gr.T. Popa" Medicine and Pharmacy University, Department of Biomedical Sciences, 9-13 Kogalniceanu Street, RO-700454, Iaşi, Roumania
[c] "Politehnica" University of Bucharest, Department of Physics, 313 Spl. Independentei, RO-060042, Bucharest, Roumania
[d] "Al.I. Cuza" University, Department of Optics and Spectroscopy, 11 Carol I Blv. RO-700506, Iaşi, Roumania

Received January 30, 2012

New 5-nitroindazole derivatives substituted in 1st position with radicals that contains the di-(β-chloroethyl)-amine group have been synthesized in order to obtain substances with enhanced antitumor activity. The structure of the new compounds has been confirmed by elemental and spectral analyses (^{1}H-NMR and FT-IR). The potential cytostatic action of the compounds studied on Guérin experimental tumors proves that new alkylating agents significantly suppress the proliferation of the neoplastic cells.

INTRODUCTION

The remarkable pharmacodynamics properties of many chemical compounds widely used in medicine are the result of interactions between certain groups of atoms within molecule and biological environment. The indazolic ring and di-(β-chloroethyl)-amine group are structures often considered as potential candidate for synthesis of substances for medical applications due to their notable biological activity. The substances containing indazolic ring have antiinflammatory, fungicidal, bactericidal, hepatoprotective, analgesic-antipyretic, antibacterial, antiangiogenic, antiprotozoal and cytostatic properties.[1-9] Di-(β-chloroethyl)-amine group is known as one of the most active alkylating agents, with antitumoral activity that can be explained by the capacity of alkylating a number of cellular components (amines, alcohols etc) through nucleophilic substitution. In order to eliminate the high toxicity of substances containing di-(β-chloroethyl)-amine group, methods of grafting di-(β-chloroethyl)-amine group on various organic substrates (both biologically active and with no toxicity) were proposed.[10-17]

Synthesis of organic compounds containing indazole ring and di-(β-chloroethyl)-amine group is very useful both for chemical and biological studies on the mechanisms of mutual influence within the molecule or of the global influence over the biological activity as well for the potential applications in medical treatments as new substances with high antitumor activity.

The present study continues the previous work related to the synthesis of the compounds containing di-(β-chloroethyl)-amine group and proposes new different ways of preparation of chemical complexes with di-(β-chloroethyl)-amine group grafted on the pyrazol ring of the substrate.[10-15]

RESULTS AND DISCUSSION

The procedure for the synthesis of the bioactive compounds studied in this work involves different stages, schematically shown in Figs.1-3. Sodium

* Corresponding author: cstan@physics. pub.ro

salt (I) was obtained by dissolving of 5-nitroindazole in hot alcoholic solution containing the sodium etoxid. The reaction between (I) and sodium monochloroacetate produces a sodium salt of acid 5-nitroindazole-1-yl-acetic (II) (see Fig. 1).

The reactions between sodium salts (I) or (II) and tris β-chloroethyl amine create new organic compounds with alkylating group grafted on indazolic substrate through an ethylene bridge: 1-[N-di-(β-chloroethyl)-aminoethyl]-5-nitroindazole (III) and ester form 1-[N-di-(β-chloroethyl)-aminoethyl)-carboxy-methyl]-5-nitroindazole (IV), respectively (see Fig. 2).

Quantitative chemical analysis and the spectral investigations using FT-IR and ^{1}H-NMR methods, as well as good yield obtained for pure products prove that the reactions occur at the nucleophile center in the molecule of sodium salt, which is negatively charged nitrogen-bearing for the compound (I) and oxygen derived from carboxyl group for the compound (II).

Attaching the group alkylated by ethylene and ester bridge is important because they ensure the split of the molecule *in vivo*, thus releasing the alkylating fragment.

The reaction of sodium salt of the 5-nitroindazole (I) with monochloroacetic acid chloride creates N-chloroacethyl-5-nitroindazole (V) which in reaction with di-(β-chloroethyl)-amine produces N-[di-(β-chloroethyl)-aminoacethyl]-5-nitroindazole (VI) (see Fig. 3).

The substituted acetyl group is also present in the biological substrate (proteins, etc.) so the compound (VI) having this common group with the substrate will be probably more easily accepted by this.

The compounds (I)-(VI) are new and unreported in the literature. The preparation steps are presented for each particular compound in the Experimental Part. The specific characteristics and chemical structures were established by chemical and spectral analysis (FT-IR and ^{1}H-NMR).

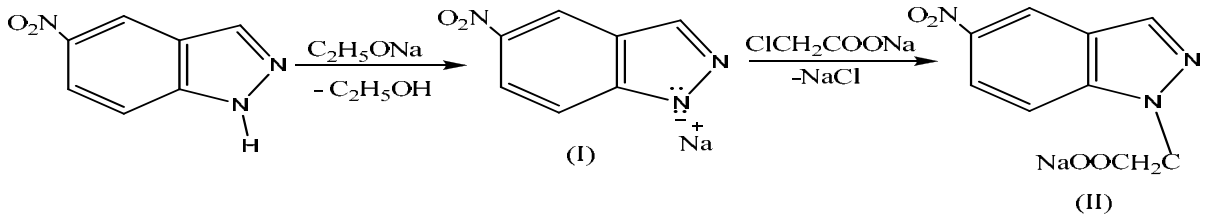

Fig. 1 – Synthesis steps for the compounds (I) and (II).

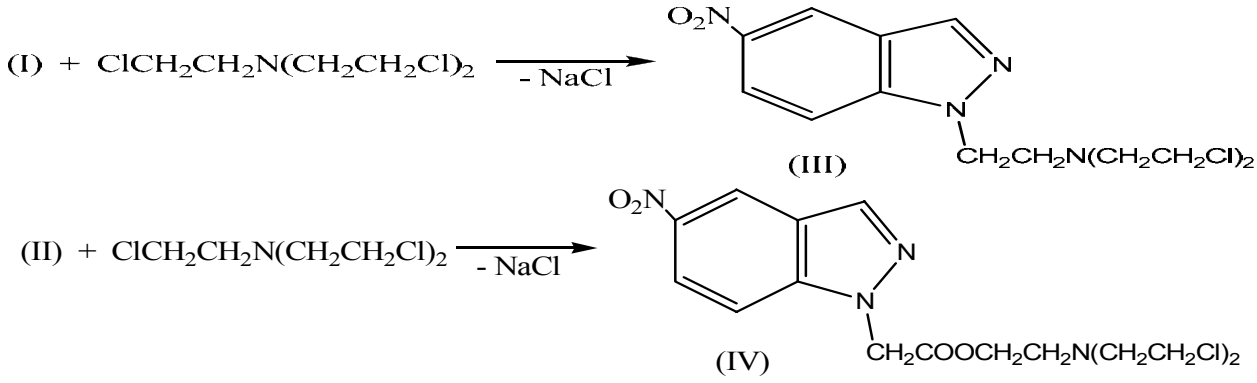

Fig. 2 – Synthesis steps for the compounds (III) and (IV).

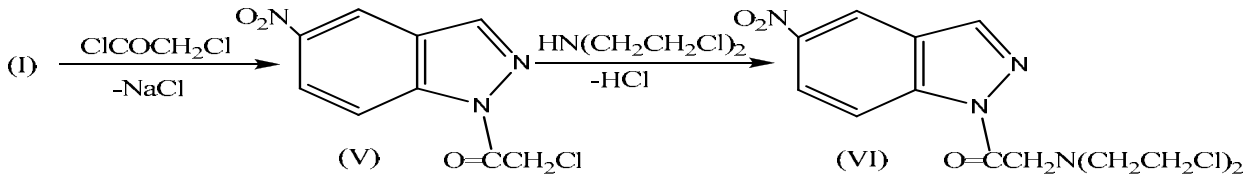

Fig. 3 – Synthesis steps for the compound V and VI.

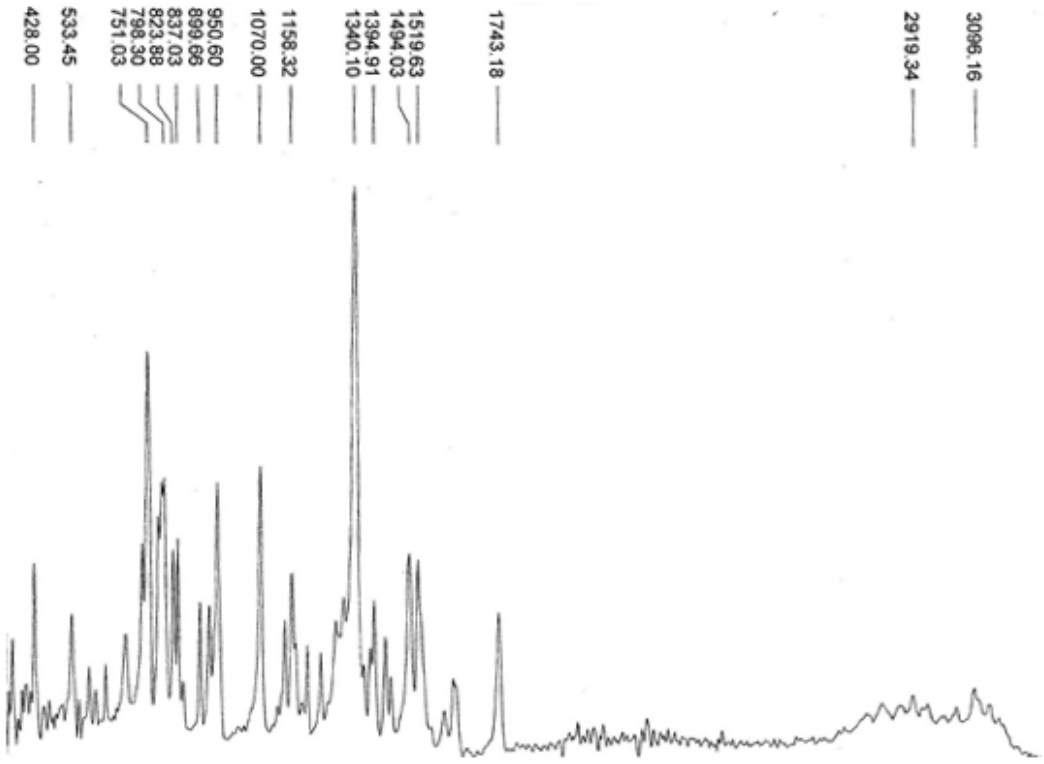

Fig. 4 – FT-IR spectrum for the compound (IV).

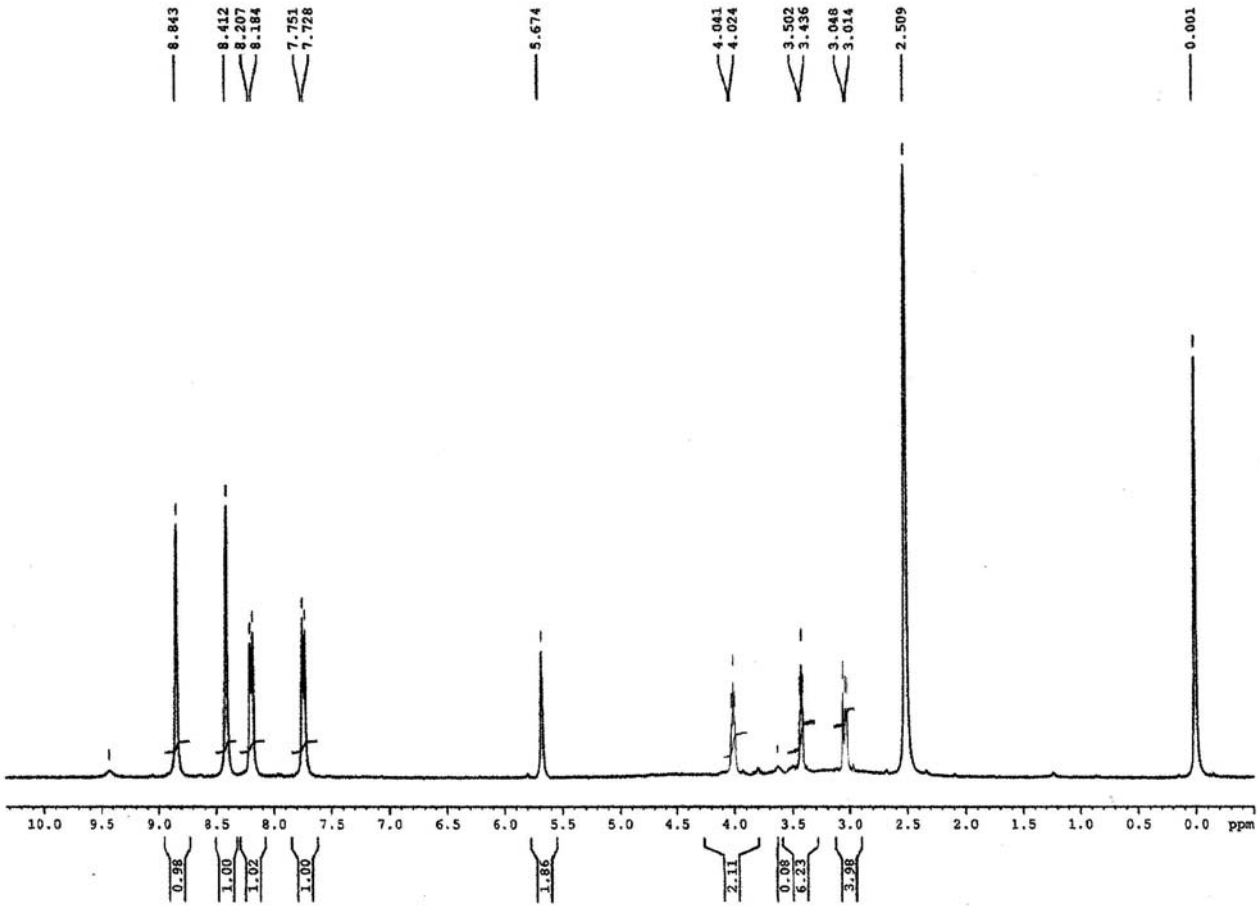

Fig. 5 – ^{1}H-NMR spectrum for the compound (IV).

As general remarks, in the FT-IR analysis, the frequencies for NO_2 group symmetric and asymmetric ranged between 1334-1340 cm^{-1} and 1519-1595 cm^{-1}. The carboxylate ion in compound (II) is identified by an absorption band at 1610 cm^{-1} and C-Cl bond from compound (V) is identified by a weak intensity band at 749 cm^{-1}. From the absorption spectra for N-mustards (III), (IV) and (VI), C-N stretching frequency was identified at 1305-1307 cm^{-1} while the C-Cl stretching frequency ranged between 747-789 cm^{-1}.

Fig. 4 illustrates a typical FT-IR spectrum, particularly for the compound (IV), showing the identification of the frequencies characteristic to the groups of interest (expressed in cm^{-1} and written upper to the spectrum).

The analysis of ^{1}H-NMR spectra adds new information on the properties of the chemical structures (I)-(VI). Thus, N-mustard protons present signals at δ=3.02-3.43 ppm and at 4.02-4.74 ppm. Fig. 5 shows a typical ^{1}H-NMR spectrum of the compound (IV).

Toxicity and potential antitumoral activity

The biomedical activity of the compounds (I)-(VI) was tested on mice lots.

a) Toxicity

The compounds (I)-(VI) may have antitumor activity functioning as antimetabolites (I), (II) and (V) or as alkylating agents (III), (IV) and (VI). The toxicity activity was evaluated using the lethal dose DL_{50}.

The results are presented in Table 1.

Grafting di-β-chloroethyl-amine through ethylene bridges, ester group or acetyl on the nucleus of indazole derivatives (I), (II), (V) led to mustards (III), (IV), (VI), which present a lower toxicity than free di-(β-chloroethyl)-amine and slightly up from the intermediaries support. This result is acceptable if taking into account data from literature, according to which the use of heterocyclic structures as transport agents have a positive influence on reducing the cytotoxic grouping. [2, 6, 9, 19-21]

b) Antitumoral activity

The antitumoral activity of N-mustards (III), (IV) and (VI) was established by the tumor evolution in the Guérin experimen.

We have found that for the untreated rats, tumors have greatly expanded, reaching 50-60 cm^3 and even more of a surveillance during 10-15 days, with clinical dissemination, macroscopic nodal in packages and multiple visceral dissemination. In contrast, for the group of treated animals, the tumor growth was slower. After a few days of treatment, ulceration occured only at a rate of 65-70% of tumors, dissemination was slower and at a lower percentage (30-35%). The administration of products to animals with induced tumors resulted in a prolongation of survival up to 40-45 days compared to untreated animals.

Table 2 present the results of the antitumor inhibition for the new N-mustards.

Table1

LD_{50} (mg/kg body) for indazole derivatives (I)-(VI)

Compound	LD_{50} (mg/kg body)			
	24 hours	48 hours	7 days	Average value
I	1675	1675	1640	1663
II	1775	1775	1730	1760
III	1580	1580	1550	1570
IV	1620	1620	1600	1613
V	1590	1590	1565	1581
VI	1555	1555	1535	1548
Di-β-chloroethyl-amine	378			

Table 2

Antitumor activity of N-mustards (III), (IV), (VI)

Compound	Route of administration	Experimental animals	Inhibition%, Guérin carcinom
III	p.o.	Rats	60
IV	p.o.	Rats	70
VI	p.o.	Rats	56
Endoxan			84

Experimental data show that the tested N-mustards present a remarkable antitumor activity. More selective is N-mustard (IV) which produces an inhibition of Guérin carcinoma close to that of endoxan (considered as a reference cytostatic). The probable explanation is that besides the alkylating effect, the compounds may have a specific antimetabolite effect.

EXPERIMENTAL

A. The experimental procedure and the main characteristics of the synthetized compounds (I)-(IV).

I) Sodium salt of the 5-nitroindazole (I). In a flask provided with ascendant condenser, ethyl alcohol (100 mL), sodium (0.1 mol) and 5-nitroindazole (0.1 mol) are added. The mixture of reaction, after 15-20 minutes of stirring, is heated under reflux on water bath, for 90 minutes. The ethanolic excess was removed by distillation under reduced pressure. The sodium salt of 5-nitroindazole was filtered under vacuum and then dried. The compound is slightly soluble in water.

Characteristics: Yellow solid, yield 82.5% (15.26 g) m.p.=250-253°C. Anal. calc. for $C_7H_4N_3O_2Na$: 45.40%C; 2.16%H; 22.70%N. Found: 45.77%C; 2.35%H; 23.11%N. IR(ν cm^{-1}): 3100 (CHAr); 1480 (C=N); 1335 (NO_2 sym); 1555 (NO_2 asym); ^{1}H-NMR (DMSO-d6, 400 MHz), δ (ppm): 7.70-7.74 (d, 1H, Ar); 8.17- 8.19 (d, 1H, Ar); 8.40 (s, 1H, Ar); 8.82 (s, 1H, Ar).

II) Sodium salt of the 5-nitroindazole-1-yl-acetic acid (II). In a flask the sodium salt (I) (0.02 mol) is dissolved in 100 mL anhydrous ethanol and then, under stirring 0.02 mol sodium salt of monochloroacetic acid in 40 mL anhydrous ethyl alcohol are added. The mixture of reaction is heated under reflux by stirring for 2 hours and then was filtered. The excess of ethyl alcohol was removed by distillation under reduced pressure to 40-45 mL. The crude solid (II) is filtered and dried under vacuum and then it is washed with anhydrous ethyl alcohol. The sodium salt (II) is slightly soluble in water.

Characteristics: White yellow solid; yield 87% (4.22 g); m.p.= 203-205°C. Anal. calc. for $C_9H_6N_3O_4Na$: 44.44%C; 2.47%H; 17.28%N. Found: 44.82%C; 2.76%H; 17.59%N. IR(ν cm^{-1}): 3096 (CHAr); 1491 (C=N); 1336 (NO_2 sym); 1595 (NO_2 asym); 1416 (CH_2). ^{1}H-NMR (DMSO-d6, 400 MHz), δ(ppm): 3.78 (s, 2H, CH_2); 7.72-7.75 (d, 1H, Ar); 8.18- 8.20 (d, 1H, Ar); 8.41 (s, 1H, Ar); 8.84 (s, 1H, Ar).

III) N-[di-(β-chloroethyl)-aminoethyl]-5-nitroindazole (III). The suspension of 0.01 mol, sodium salt (I) in 25 mL anhydrous dioxane is treated with 0.02 mol tris-(β-chloroethyl)-amine hydrochloride. The mixture of reaction is heated at 50-55ºC, for 45 minutes. The compound (III) is precipitated with anhydrous ethyl ether after filtering sodium chloride from dioxin solution and then is purified from anhydrous ethyl alcohol.

Characteristics: Cream-colored solid, yield 72% (2.38 g); m.p.=194-196°C. Anal. calc. for $C_{13}H_{16}Cl_2N_4O_2$: 47.12%C; 4.83%H; 21.45%Cl; 16.91%N. Found: 47.41%C; 5.24%H; 21.87%Cl; 17.27%N. IR(ν cm^{-1}): 3095 (CHAr); 1491 (C=N); 1305(C-N); 1336 (NO_2 sym); 1534 (NO_2 asym); 748, 789 (C-Cl). ^{1}H-NMR (DMSO-d6, 400 MHz), δ(ppm): 3.09-3.11 (m, 4H, $2CH_2$); 3.37-3.41(m, 6H, 3 CH_2) 4.62-4.74 (m, 2H, CH_2); 7.73-7.75 (d, 1H, Ar);); 8.18- 8.20 (d, 1H, Ar); 8.41 (s, 1H, Ar); 8.85 (s, 1H, Ar).

IV) N-[di-(β-chloroethyl)-aminoethyl-carboxy-methyl]-5-nitroindazole (IV) The same procedure for compound (III) was used, starting from 0.01 mol sodium salt (II), 30 mL anhydrous dioxane and 0.01 mol tris-(β-chloroethyl)-amine.

Characteristics: Yellow solid, yield 74% (2.87 g); m.p.=146-148°C. Anal. calc. for $C_{15}H_{18}Cl_2N_4O_4$: 46.27%C; 4.62%H; 18.25%Cl; 14.39%N. Found: 46.49%C; 4.96%H; 18.52%Cl; 14.67%N. IR(ν cm^{-1}): 3096 (CHAr); 1494 (C=N); 1743(C=O ester); 1158 (C-O-C); 1340 (NO_2 sym); 1519 (NO_2 asym); 751, 793 (C-Cl). ^{1}H-NMR (DMSO-d6, 400 MHz), δ(ppm): 3.01-3.04 (m, 4H, $2CH_2$); 3.43-3.50 (m, 6H, 3 CH_2) 4.02-4.04 (m, 2H, CH_2); 5.67 (s, 2H, CH_2) 7.72-7.75 (d, 1H, Ar); 8.18- 8.20 (d, 1H, Ar); 8.41 (s, 1H, Ar); 8.84 (s, 1H, Ar).

V) N-chloroacethyl-5-nitroindazole (V). The sodium salt (I) (0.01 mol) is dissolved in anhydrous dioxane (50 mL) and the monochloroacetic acid chloride (0.01 mol) is added. The mixture of reaction is heated under reflux on water bath for 120 minutes, by stirring under cooling. A sticky product is obtained and by repeated washing with anhydrous ethyl ether changes into a fine powder. By recristallization in acetone the pure product is obtained.

Characteristics: Yellowish white solid, yield 79% (1.88 g); m.p.=166-168°C. Anal. calc. for $C_9H_6ClN_3O_3$: 45.09%C; 2.50%H; 14.82%Cl; 17,53%N. Found: 45.51%C; 2.87%H; 15.04%Cl; 17.93%N. IR(ν cm^{-1}): 3097 (CHAr); 1493 (C=N); 1624(C=O amide); 1338 (NO_2 sym); 1535 (NO_2 asym); 749 (C-Cl). ^{1}H-NMR (DMSO-d6, 400 MHz), δ(ppm): 5.26 (s, 2H, CH_2), 8.45-8.47 (d, 1H, Ar); 8.50- 8.57 (d, 1H, Ar); 8.75 (s, 1H, Ar); 8.91 (s, 1H, Ar).

VI) N-[di-(β-chloroethyl)-aminoacethyl]-5-nitroindazole (VI). The suspension of 0.01 mol compound (V) in 100 mL anhydrous dioxane is treated with 0.012 mol di-(β-chloroethyl)-amine, free base in ether. The mixture of reaction is heated under reflux, for 4 hours. The excess of dioxane was removed by distillation under reduced pressure and the product is recrystallization from hot benzene.

Characteristics: Yellowish white solid, yield 65% (2.24 g); m.p.=181-183°C. Anal. calc. for $C_{13}H_{14}Cl_2N_4O_3$: 45.21%C; 4.05%H; 20.57%Cl; 16.23%N. Found: 45.37%C; 4.32%H; 20.92%Cl; 16.54%N. IR(ν cm^{-1}): 3094 (CHAr); 1490 (C=N); 1622 (C=O amide); 1334 (NO_2 sym); 1533 (NO_2 asym); 747, 788 (C-Cl). ^{1}H-NMR (DMSO-d6, 400 MHz), δ(ppm): 3.02-3.08 (m, 4H, $2CH_2$); 3.31-3.34 (m, 4H, $2CH_2$); 4.67 (s, 2H, CH_2); 7.74-7.76 (d, 1H, Ar); 8.17- 8.20 (d, 1H, Ar); 8.40 (s, 1H, Ar); 8.83 (s, 1H, Ar).

B. Evaluation of the toxicity and potential antitumoral activity

a) Toxicity

The lots were composed of 10 mice of either gender with a weight of 20±2 g and a safety limit of 90%. After intraperitoneal administration of drug suspensions in Tween80, the mortality was registered after 24 hrs, 48 hrs and 7 days.[18]

b) Potential antitumoral activity

We evaluated the cytostatic effect of the synthesized N-mustards (III), (IV), (VI), by transplanting subcutaneously the Guérin experimental tumors T8 to 15 males rats weighing 100-150 g (±15 g) each. The substance administration was started when tumor volume reached sizes of 5-6 cm^3 (product of three diameters larger tumors).

The inhibition of tumor growth was assessed by tumor weights from animals slaughtered at 24 hours after last administration and was calculated using the formula:

$$I(\%) = \frac{C - T}{C} \times 100 \quad (1)$$

where: C is the average weight of tumors in the control group and T the average weight of tumors in the treated group.

The compound was extemporaneously suspended in saline solution and esophageal probe was administered to 10 animals in daily dose of 20 mg/animal; 5 animals were treated as control group. The animals were monitored for 10-15 days, watching the effects on hematopoietic system and the variations in the peripheral blood cell count.

All experiments were organized in conformity with Ordinance for animal protection used for scientific or experimental purposes, no. 37/2002 from 30/01/2002 published in Monitorul Oficial, Part I, no. 95 from 02/02/2002.

CONCLUSIONS

Six new derivatives of 5-nitroindazole (I)-(VI) were synthesized, three of them (III), (IV), (VI) containing grafted di-(β-chloroethyl)-amine group. The structure of the new compounds was confirmed by elemental and spectral analysis (FT-IR and ^{1}H-NMR).

The toxicity activity evaluated using the lethal dose DL_{50} demonstrates that all compounds have low toxicity. The experimental study of the inhibition of the antitumor activity for N-mustards (III), (IV) and (VI) shows a significant regression on Guérin carcinoma, close to the reference cytostatic - endoxan.

REFERENCES

1. M. Ribeira, J. Cabral and A. Cimas, *J. Chem. Thermodynamics,* **2010**, *42*, 1240-1247.
2. V. Arán, C. Ochoa, L. Boiani, P. Buccino, H. Cerecetto, A. Gerpe, M. Gonzáles, D. Montero, J. Nogal, A. Barrio, A. Azqueta, A. Ceráin, O. Piro and E. Castellano, *Bioorg. Med. Chem.,* **2005**, *13*, 3197-3207.
3. C. Cano, C. O. Azar, V. Arán and C. D. Urrutia, *Spectrochimica Acta Part A,* **2010**, *75,* 375-380.
4. S. Berhe, A. Slupe, C. Luster, H. Charlier, D. Warner, L. Zalkow, E. Burgess, N. Enwerem and O. Bakare, *Bioorg. Med. Chem.,* **2010**, *18*, 134-141.
5. J. Rodriguez, A. Gerpe, G. Aguirre, U. Kemmerling, O. Piro, V. Arán, J. Maya, C. O. Azar, M. Gonzáles and H. Cerecetto, *Eur. J. Med. Chem.,* **2009**, *44*, 1545-1553.
6. L. Bouissoine, S. Kazzouli, L. Pfeiffer, E. M. Rakis, M. Khouili and G. Guillaumet, *Bioorg. Med. Chem.,* **2006***, 14,* 1078-1088.
7. L. Huang, M. L. Shih, S. H. Chen, L. S. Pan, M. C. Teng, F. Lee and S. Kuo, *Bioorg. Med. Chem.,* **2006**, *14*, 528-536.
8. A. Gerpe, G. Aguirre, L. Boiani, H. Cerecetto, M. Gonzáles, C. O. Azar, C. Riogol, J. Maya, A. Morello, O. Piro, V. Arán, A. Azqueta, A. Ceráin, A. Monge, A. M. Rojas and G. Yalluf, *Bioorg. Med. Chem.,* **2006**, *14*, 3467-3480.
9. T. Yakaiah, V. P. Lingaiah, B. Naraiah, B. Shireesha, B. Kumar, S. Gururaj, T. Parthasarathy and B. Sridhar, *Bioorg. Med. Chem. Lett,* **2007**, *17*, 3445-3453.
10. V. Sunel, A. Cecal, A. Soldea and N. Asandei, *Rev. Roumaine de Chimie,* **1995***, 40*, 763-768.
11. V. Sunel, M. Popa, A. Popa and C. Soldea, *Cellulose Chem. Technol.,* **2000**, *34*, 269-274.
12. M. Popa, L. Balaita and V. Sunel, *J. Biomaterials Applications,* **2003**, *18,* 83-94.
13. V. Sunel, C. Lionte, C. Basu and C. Cheptea, *Chem. Indian Journal,* **2005**, *2*, 1-6.
14. M. Popa, V. Sunel, N. Dulea, A. Popa, R. Ottenbrite and C. Uglea, *J. Bioactive Polymers*, **2007**, *22*, 651-666.
15. V. Sunel, M. Popa, J. Desbrieres, L. Profire, O. Pintilie and C. Lionte, *Molecules*, **2008**, *13*, 177-189.
16. H.C. Lee, C.T. Chou, L.T. Su, J. Yu, E.L. Shao and L.A. Yu, *Cancer Lett.*, **2009**, *276*, 204-211.
17. N. Kapuriya, R. Kakadiya, H. Dong, A. Kumar, C.P. Lee, X. Zhang, T. Chou, C.T. Lee, H.C. Chen, K. Lam and B. Marvania, *Bioorg. Med. Chem.,* **2011**, *19*, 471-485.
18. S. Kärber, *Envir. Sci. Technol.,* **1978**, *12*, 417.
19. G. Gravatt, B. Baquley, W. Wilson and W. Denny, *J. Med. Chem.,* **1994**, *37*, 4338.
20. R. Bartzatt, *Preclinica,* **2003**, *1*, 127.
21. V. Sunel, S. Ciovica, N. Asandei and C. Soldea, *Cellulose Chem. Technol.,* **1995**, *29*, 11.